Spatio-temporal analysis of HadCM3 GCM Climate projections using Parameterized MiSTIC framework - study of Elevation Dependent Warming across Peninsular India

Thesis submitted in partial fulfilment
of the requirements for the degree of

Master of Science in
Computer science and Engineering
by Research

by

Ankitha Eravelli
2019900009
ankitha.eravelli@research.iiit.ac.in

International Institute of Information Technology
Hyderabad - 500 032, INDIA

April 2024

International Institute of Information Technology
Hyderabad, India

CERTIFICATE

It is certified that the work contained in this thesis, titled "Spatio-temporal analysis of HadCM3 GCM Climate projections using Parameterized MiSTIC framework - study of Elevation Dependent Warming across Peninsular India" by Ankitha Eravelli, has been carried out under my supervision and is not submitted elsewhere for a degree.

Date	Adviser: Prof. K. S. Rajan

Acknowledgments

I would like to express my deepest gratitude and appreciation to my advisor, Prof. K. S. Rajan, for his unwavering guidance, invaluable support, and constant encouragement throughout the entire duration of this research thesis. His profound knowledge, insightful suggestions, and dedication to my academic growth have been instrumental in shaping this work. I am truly fortunate to have had the opportunity to learn from him and be a part of his mentorship.

I extend my heartfelt thanks to the Laboratory for Lab for Spatial Informatics (LSI), where this research was conducted. I am indebted to the previous research students of the lab whose contributions paved the way for this work.

I would also like to extend my sincere appreciation to my colleagues and friends who have been an integral part of this research journey. Their intellectual discussions, valuable feedback, and camaraderie have been instrumental in shaping the direction and quality of this work. Their support and collaboration have made this experience rewarding and enjoyable.

Lastly, but most importantly, I am deeply grateful to my family for their encouragement and understanding throughout this entire endeavour. Their constant support and belief in my abilities have been the pillars of strength that have propelled me forward. Their unwavering faith in me has been my motivation during challenging times, and for that, I am forever grateful.

I extend my heartfelt thanks to all those mentioned above and to anyone who has contributed in any form to the completion of this research.

Abstract

General Circulation Models (GCMs) aid in developing climate-resilient policies, preparing for extreme events and implementing governance and disaster management mitigation strategies. Thus, assessing GCMs' climate forecasting capabilities is crucial to establishing the credibility and reliability of climate projections, facilitating well-informed decision-making and climate change readiness. The UK Met Office Hadley Centre Coupled Model, version 3 (HadCM3), is extensively evaluated in this study. HadCM3 is used to simulate global and regional climate patterns and has been crucial to climate change assessments. This thesis explores the spatio-temporal dynamics of temperature in contiguous Peninsular India by identifying regions of high & low variability, with an emphasis on Elevation-Dependent Warming (EDW).

The central objective of this study is to improve our understanding of the attributes, patterns, trends, and fundamental factors that affect temperature variations across diverse spatial and temporal dimensions and the HadCM3 model's ability to accurately represent this phenomenon. Through a 30-year analysis of observed and modelled minimum (Tmin) and maximum temperature (Tmax) data (1991-2020 and 1990-2019, respectively) over the study region, this study explores the relationship between elevation and warming trends.

The observed and modelled Tmin and Tmax have been increasing at a rate of +0.13°C/decade and +0.17°C/decade for observed data & +0.43°C/decade and +0.45°C/decade for modelled data, whereas the observed and modelled diurnal temperature range (DTR) increased at +0.03°C /decade & +0.02°C/decade. The lapse rates of observed and modelled minimum and maximum temperatures are found to be positive, but the DTR lapse rate is found to be negative, indicating increasing DTR with elevation. Modelled data shows more pronounced trends (+6.344°C/km for Tmin, +5.954°C/km for Tmax, and -0.39°C/km for DTR) than observed temperature (+2.376°C/km for Tmin, +2.341°C/km for Tmax, and -0.193°C/km for DTR). This discrepancy suggests that the global average lapse rate (+6.5°C/km) underlines the modelled data, resulting in much higher lapse rates in the study region, which implies that the model uses

a uniform lapse rate to model temperature and fails to account for the study region's unique topographic temperature relationships.

The study proposes the P-MiSTIC method, a multivariate extension of MiSTIC, to identify zones with spatio-temporal consistency and investigate these inconsistencies. This study uses Tmin and Tmax as P-MiSTIC inputs with weights of -1 and 1. Using MiSTIC, the study finds 12, 9, 8, and 4 spatio-temporally invariant zones for observed and modelled Tmin and Tmax, respectively. Importantly, the elevation-based change rates of variables for these zones (-2.57°C/km and -2.19°C/km for observed Tmin and Tmax, and -7.48°C/km and -6.67°C/km for modelled Tmin and Tmax) closely match the data-derived lapse rates. Using the P-MiSTIC method, 11 and 1 zones are identified for observed and modelled data, respectively, indicating that modelled data is consistent over the Peninsular region. DTR change rates for zones within observed temperature data increase with elevation, indicating elevation-dependent warming in specific study regions. In particular, the Western Himalayan region and the Karakoram region, with the highest elevations, drive the phenomenon in the study region with the Western Himalayan and Karakoram DTRs increasing at 0.19°C/decade and +0.28°C/decade over the study period. The GCM model's DTR data shows a much slower increase of +0.02°C/decade in the study region.

Using the P-MiSTIC method on three decade-wise subsets, only one zone is identified in modelled data across all decades, while observed data identifies 12, 11, and 9 zones for decades 1, 2, and 3. The elevation-based DTR change rates for the observed temperature zones are estimated at -0.03°C/km, -0.028°C/km, and +0.533°C/km for decades 1, 2, and 3. DTR trends change from decreasing to increasing as the study progresses from decades 1 and 2 to decade 3, suggesting elevation-dependent warming in the study region is accelerating. The Western Himalayas and the Karakoram experience considerable variations of DTR. In the Western Himalayas, the DTR decreases at -0.14°C/decade, -0.29°C/decade, and -0.41°C/decade for decades 1, 2, and 3, while in the Karakoram, it increases at +0.11°C/decade, +0.13°C/decade, and +2.46°C/decade. However, the model's DTR data shows a uniform increase of +0.02°C/decade across all decades, indicating the model's uniform rate.

By dividing the datasets into DJF, MAM, JJA, and SON seasons, the study examined seasonal spatio-temporal variations. Seasonal observations identified 11, 10, 7, and 8 zones where the diurnal temperature range (DTR) changed with elevation at -0.518°C/km, -0.089°C/km, 0.668°C/km, and 0.453°C/km for the four seasons. Western Himalayan and Karakoram regions continue to be identified by P-MiSTIC in all the seasons, indicating their distinct trends. In these zones, DTR values were lowest in JJA and highest in MAM. The DTR has been increasing in the Western Himalayan (0.28°C/decade, 0.34°C/decade, 0.22°C/decade, and 0.21°C/

decade) and Karakoram (0.26°C/decade for all seasons) over the study period. The Western Himalayas showed seasonal variations while the Karakoram region showed a relatively uniform trend. However, the modelled data yielded DJF, MAM, JJA, and SON zones of 3, 3, 3, and 2 with DTR trends of -0.539°C/km, 0.451°C/km, 4.689°C/km, and 1.737°C/km. This reinforces weak spatial variability but strong seasonal variability. Most zone-wise temporal DTR trends in the modelled data were insignificant, ranging from -0.07°C/decade to 0.05°C/decade except during SON, the Himalayan zone exhibited a 0.14°C/decade increase. Both datasets exhibited a seasonal cycle of DTR with minimum DTR values in JJA, followed by a gradual increase in SON. The elevation-based DTR trends showed the greatest increase in summer and a decrease in winter.

Data-driven zoning analysis illustrates how zonal boundaries and temperatures vary through time. These zones allow researchers to examine contrasting trends in a study region that are challenging to extrapolate over large areas. The modelled data has been identified as a single zone in the entire study region, highlighting the lack of spatio-temporal variability in the modelled data for the region. The decrease in zonal variability over the past three decades is evident in the observed data zones, suggesting that this trend may be occurring in regions outside of the study area also. With a single zone throughout the study and decade-wise datasets, the modelled data indicated low spatio-temporal heterogeneity. The diagonal zone separation in the seasonal analysis reveals the model's inherent discrepancies, which may be due to parameterizations and systematic errors.

Despite its data-driven approach, the study's identified zones correlate with natural patterns, indicating specific environmental and ecological conditions governing climate behaviour across the study region. P-MiSTIC consistently identified the Western Himalayan and Karakoram regions, confirming that elevation influences temperature patterns and also demonstrating that it is capable of identifying zones with unique spatio-temporal characteristics. The study shows that Elevation-Dependent Warming occurs in higher-elevation zones. JJA, where DTR values are low, has seen a faster warming rate in the past decade than in previous decades. The study illustrates how high-elevation Himalayan zones drive temperature variations. It stresses the importance of accounting for spatio-temporal variations when studying climate in complex topographies and the model's inability to accurately capture these patterns. GCMs modelling the Indian subcontinent as a whole presents a challenge in enhancing climate patterns and comprehending its impacts.

Table of Contents

List of Figures

Figure Page

List of Tables

Chapter 1

Introduction

The Earth is a multifaceted and ever-changing entity, shaped by a multitude of interconnected phenomena across its diverse spheres. The Earth's climate is one such important phenomenon. Essential Climate Variables (ECVs) are the numerous surface, atmospheric, and atmospheric composition variables used to analyze the climate of the Earth. A physical, chemical, or biological variable, or a collection of related variables that significantly influences how the climate on Earth is characterized, is known as an Essential Climate Variable (ECV). ECV datasets provide the empirical evidence needed to learn and predict climate evolution, guide mitigation and adaptation measures, evaluate risks, enable attribution of climate events to underlying causes, and underpin climate services [1]. The surface temperature is a component of the surface ECVs and a crucial element of the Earth's climate.

Climate change and its associated impacts are among the most critical challenges facing our planet today. Global warming is the gradual increase in the global average temperature. This warming trend has existed for a very long time, but its rate has accelerated substantially over the past century as a result of human activities such as the combustion of fossil fuels [1]. Earth's global average surface temperature in 2020 statistically tied with 2016 as the hottest year on record, continuing a long-term warming trend due to human activities [2].

In India, there is a notable warming trend beginning in the 1970s and accelerating in the 2000s and 2010s [3]. Annual mean, maximum and minimum temperatures averaged over India during 1986–2015 show a significant warming trend of 0.15 °C, 0.15 °C and 0.13 °C per decade, respectively [4]. India will likely face irreversible impacts of climate change, with increasing heat waves, droughts and erratic rainfall events in the coming years if no mitigation measures are put in place [1].

Modelling a phenomenon plays a crucial role in the understanding and predictability of the phenomena. Environmental, climate and hydrological modelling require spatially continuous and temporally consistent gridded datasets. The key sources for climate data sets are meteorological station records, satellite observations, and estimates from weather radar [5]. Records from near-surface weather stations are the foundation of climate research. They are essential because of their high reliability and accuracy. They are the only available records of spatial and temporal variation of climatic variables before the first satellite-based observations became available in the 1960s [6]. However, the spatial locations of weather stations could be more sparse and irregularly distributed over a region of interest. In addition, the temporal consistency of data for a given parameter over long periods is not guaranteed.

In the face of these challenges, accurate predictions of future climate patterns are essential for informed decision-making and policy formulation. General Circulation Models (GCMs) have emerged as indispensable tools in understanding the complex interactions of the Earth's climate system. These models simulate the behavior of the atmosphere, oceans, land surfaces, and ice on a global scale, enabling scientists to project future climatic conditions under different scenarios. In the context of regional climate assessment, evaluating the performance of GCMs becomes paramount, particularly in areas of diverse topographies and climate characteristics.

The Earth's climate system exhibits remarkable variability across both space and time. Regional climate features, such as those observed in the contiguous Peninsular India, are influenced by a multitude of factors, including latitude, altitude, proximity to oceans, and complex topographical features [7]. GCMs are computational models designed to simulate the Earth's climate by incorporating physical principles governing atmospheric, oceanic, and terrestrial processes [7]. One such GCM is the Hadley Centre Coupled Model, version 3 (HadCM3), developed by the UK Met Office Hadley Centre. HadCM3 has been widely employed to simulate global and regional climate patterns and has played a crucial role in climate change assessments [8] [9].

Elevation-dependent warming (EDW) is a phenomenon that underscores the varying rates of temperature increase across different altitudes. This means high-elevation regions, such as mountain ranges, are experiencing more rapid warming than lower-elevation regions. EDW is a significant component of global warming because it has significant effects on mountain ecosystems. Mountain regions are home to unique ecosystems and provide critical ecosystem services such as water supply, biodiversity, and carbon storage. Changes in temperature can have cascading effects on these ecosystems, affecting the plants, animals, and people that depend on them [11]. The influence of elevation on temperature patterns is attributed to various factors, including changes in atmospheric pressure, lapse rates, and land-atmosphere interactions. Understanding EDW is essential for predicting local climate impacts, such as shifts in ecological zones, glacial retreat, and water resource availability. Studying EDW can also help improve our understanding of the Earth's climate system and the factors that influence it. This includes understanding the natural variability of the climate system, as well as the human activities that are driving changes in the climate [12]

Detecting EDW can be challenging due to the complexity and heterogeneity inherent in mountain environments and in mountain climates, which would require a dense and homogeneous network of ground stations up to the highest elevations, which are generally not available for most mountain areas [13]. One way to detect EDW is through the analysis of temperature data from meteorological stations at different elevations. However, long-term meteorological stations (with more than 20 years of records) are extremely sparse at high elevations. Another way to detect EDW is through the use of satellite-based remote sensing and model simulations [11].

Several mechanisms contribute towards EDW, including snow albedo and surface-based feedbacks; water vapour changes and latent heat release; surface water vapour and radiative flux changes; surface heat loss and temperature change; and aerosols [11]. All these mechanisms lead to enhanced warming with elevation (or at a critical elevation), and it is believed that combinations of these mechanisms may account for contrasting regional patterns of EDW [11]. In India, an elevation-dependent warming trend is mostly perceived in the northwest Himalayan region [15]. In this study, we aim to investigate Elevation-Dependent Warming in India using Spatio-Temporal Cluster Analysis of Observed and Modelled Temperature Data.

.

Analyzing and exploring the enormous amounts of observed and modelled climate data over many decades poses a data mining challenge. Previous research in data mining for geospatial data has focused mainly on capturing only the spatial aspect of phenomena, neglecting the temporal dimension. However, since real-world phenomena constantly evolve, understanding spatial and temporal aspects is crucial for comprehending geographic processes and events. Furthermore, extracting knowledge from spatio-temporal data can lead to more accurate predictions of spatial processes or events. As a result, conducting research on data mining in spatio-temporal datasets has become increasingly important.

In the assessment of GCMs like HadCM3, it is imperative to employ methodologies that capture the intricacies of temperature patterns in regions with varying elevations. The spatio-temporal analysis provides a comprehensive approach to examining how temperature trends evolve across space and time [17]. Spatio-temporal clustering is the clustering of objects according to their spatial and temporal similarity. In the context of temperature data, spatio-temporal clustering can be used to group temperature measurements based on their localized characteristics. Spatio-temporal clustering can be useful for analyzing temperature data and identifying patterns and trends. For example, it can be used to identify regions that are experiencing similar temperature changes over time or to identify periods of time when temperature changes are more pronounced in certain regions [18]. Various methods of spatio-temporal clustering exist, each with its own strengths and limitations. Some common methods include hierarchical clustering, k-means clustering, and density-based clustering [18]. These methods can be applied to temperature data to identify clusters of similar temperature measurements in space and time [18].

There are many techniques used in spatiotemporal cluster analysis, such as k-means clustering, density-based clustering, hierarchical clustering, and grid-based clustering [19]. Density-based clustering is a popular technique that groups together points that are close to each other in space and time [20]. Hierarchical clustering is another popular technique that groups together points based on their similarity [20]. Grid-based clustering divides the space into a grid and then groups together points that fall within the same grid cell [20]. The selection of an appropriate clustering method depends on the nature of the data and the specific research objectives.

Spatio-temporal clustering is used in many applications, such as climate modelling and environmental monitoring, to identify zones that are similar in both their temporal and spatial characteristics. This can be useful in identifying areas that are experiencing similar weather patterns or environmental conditions. India is particularly vulnerable to climate change and has been experiencing its impacts like increased extreme precipitation and decreased normal precipitation [21]. Regions that are experiencing similar weather patterns in India are important for climate studies because they can help us understand how climate change is affecting different parts of the country. For example, the Himalayan mountains play a crucial role in shaping India's climate by blocking cold winds from the north and creating a barrier for monsoon winds from the south [4]. Understanding how these factors interact with each other can help us develop more accurate models of how climate change will affect India in the future.

According to the Intergovernmental Panel on Climate Change (IPCC), India is likely to face irreversible impacts of climate change, including increasing heat waves, droughts, and erratic rainfall events in the coming years if no mitigation measures are put in place [4]. Identifying the spatio-temporal characteristics of climate variables can help identify areas that are at risk of these impacts.

Spatio-temporal data mining involves the analysis of data that changes over space and time. This data type can be particularly challenging to analyze due to its high dimensionality, complexity, and the need to account for spatial and temporal dependencies. In addition, the data may be noisy, incomplete, or contain missing values, making it difficult to draw accurate conclusions. Spatio-temporal data mining techniques are designed to overcome these challenges and extract meaningful patterns and relationships from the data.

Phenomena are often observed at discrete times, resulting in snapshots of data representing the phenomenon's state at that specific moment. Comparing pairs of snapshots taken at subsequent time intervals can provide insight into how the phenomenon has changed in both space and time, and attribute values to help answer questions about where, what, and when changes occurred. However, understanding how a phenomenon evolves is of great interest to both scientists and decision-makers. Even if snapshots are taken at suitable intervals to capture significant changes as a geographic event unfolds, comparing pairs of snapshots only addresses changes between two instances in time and does not capture the entire life-cycle of the event. An exhaustive search is required to determine the extent of change over a specified period, making it difficult to identify patterns of change that span multiple snapshots. [24].

Numerous studies have been conducted in the area of spatio-temporal change analysis, such as detecting changes in land use [25][26][27]. However, in identifying significant changes, there has been a tendency to overlook areas with minimal changes, which may provide valuable insights into the process under investigation. In this research, we focus on identifying regions with localized behaviour for dynamic phenomena, referred to as "invariant/consistent zones," rather than solely focusing on change detection. These regions can be represented by a single point or a set of points with defined properties. Given the dynamic nature of the phenomenon, this information can be highly informative in understanding the phenomenon and serve as a reference point for sampling and interpolation. For example, the localized behaviour of temperature in climate studies has been extensively investigated in recent years [28][29] to understand its dynamics, with varying outcomes. Detecting patterns of events through the identification of invariant regions can aid in defining the associative process or in defining measures to manage it, as well as in explaining the controlling and regulating factors.

Identifying consistent patterns and deviations using spatio-temporal analyses allows for a more nuanced understanding of how GCMs perform in simulating EDW. The Parametric Mining of Spatio-Temporally Invariant Cores (P-MiSTIC) method, introduced in this research, is one such powerful tool for spatio-temporal analysis, which takes into account both minimum and maximum temperatures and their associated weights to reveal regions with coherent spatio-temporal patterns over the study duration.

1.1 Motivation and Summary of Work Done

Climate change is an existential challenge that poses significant threats to our planet and its inhabitants, with far-reaching consequences. The scientific community has long recognized the importance of understanding the complex dynamics of temperature patterns, especially in regions susceptible to climate variability, for effective adaptation and mitigation strategies. In this context, the assessment of General Circulation Models (GCMs) holds paramount importance, as these models provide insights into future climate trends and guide policy decisions. The region of study i.e., the contiguous Peninsular India, characterized by vast geographical expanse and diverse topographies and climate patterns, presents a unique opportunity to explore the accuracy of GCMs in simulating regional climate changes.

The motivation for this research stems from several key factors:

Climate Resilience and Adaptation: Accurate regional climate projections are pivotal for formulating adaptive strategies to minimize the impacts of climate change. This research seeks to contribute valuable insights that can inform policymakers, planners, and stakeholders in Peninsular India about potential changes in temperature patterns, aiding in the development of context-specific adaptation measures.

GCM Performance Assessment: GCMs are fundamental tools for projecting future climate scenarios. However, their accuracy on regional scales, especially in complex terrains, requires rigorous examination. This research seeks to fill the gap by scrutinizing the performance of the widely used HadCM3 GCM in simulating temperature patterns over the Peninsular India region.

Regional Climate Variability: The Peninsular India region is marked by its intricate blend of coastal, mountainous, and plateau areas. These diverse landscapes result in varying climate patterns, making it an ideal testbed for evaluating GCMs' ability to capture localized climatic intricacies.

Elevation-Dependent Warming (EDW): Elevation plays a crucial role in shaping local climate patterns, and the phenomenon of EDW highlights the disproportionate warming experienced by different elevation zones. The impacts of EDW are multifaceted, affecting ecosystems, water resources, and agriculture. Evaluating GCMs' accuracy in predicting EDW trends is vital for understanding regional vulnerabilities.

Spatio-Temporal Analysis Techniques: The integration of advanced spatio-temporal analysis techniques, such as the Pattern Mining and Spatio-Temporal Information Clustering (P-MiSTIC) method, presents a novel approach to assessing GCM performance. By applying these techniques to model outputs and observational data, this research aims to identify spatio-temporally consistent zones (sub-regions) and uncover spatio-temporal patterns and deviations, enhancing our understanding of GCM strengths and weaknesses.

Scientific Advancement: The outcomes of this research hold significance beyond regional boundaries. Methodologies employed in evaluating GCMs' performance and exploring spatio-temporal patterns can be adapted and applied to other regions, further enhancing the scientific community's understanding of climate dynamics and model capabilities.

By addressing these motivations, this research endeavours to enhance our understanding of how well GCMs represent elevation-dependent warming patterns in regions with diverse topographies. The insights gained from this study can contribute to informed decision-making, sustainable development, and effective climate change mitigation efforts, ultimately working towards a more resilient and prepared future in the face of a changing climate.

1.2 Objectives of this research

The research objectives are structured as follows:

1. Development of P-MiSTIC as a Parametric Method:

   The first objective is to enhance the existing spatio-temporal analysis framework by transforming the Mining Spatio-Temporally Invariant Cores (MiSTIC) method into a parametric variant (P-MiSTIC). This involves modifying MiSTIC to integrate parametric components, allowing for more precise quantification and comparison of spatio-temporal temperature patterns using user-assigned weights for all the components. The development of P-MiSTIC will facilitate a more robust analysis of observed and simulated temperature data.

2. Understanding Spatio-Temporal Patterns in Observed Temperature:

   The second objective involves the application of the newly developed P-MiSTIC method to observed temperature datasets over the contiguous Peninsular India. By analyzing these datasets, the research seeks to identify and characterize consistent spatio-temporal patterns of temperature variation. This objective aims to provide an empirical baseline for temperature trends over the study region.

3. Spatio-Temporal Patterns of Temperature Captured by Climatic Models:

   The third objective focuses on evaluating the performance of the HadCM3 GCM in simulating spatio-temporal temperature patterns over the contiguous Peninsular India region. By subjecting HadCM3 model outputs to the P-MiSTIC method, the research aims to quantify the extent to which the model captures temperature patterns. This objective will provide insights into the GCM's ability to reproduce the intricate spatio-temporal variations observed in real-world temperature datasets.

4. Assessment of Deviant Behavior of Climatic Changes and Elevation-Dependent Warming:

   The fourth objective involves a comprehensive assessment of the deviations between the simulated temperature patterns by HadCM3 and observed temperature patterns over a span of three decades. Specifically, the research will examine the model's performance in simulating elevation-dependent warming (EDW) and identify regions where the model deviates significantly from the observed trends. This objective seeks to uncover areas of model weakness, highlighting potential biases and discrepancies in the GCM's representation of regional climate dynamics.

By achieving these four interconnected objectives, this research aims to contribute to a holistic understanding of GCM performance in capturing elevation-dependent warming patterns over the contiguous Peninsular India. The insights gained from this study will enhance our comprehension of regional climate modelling, assist in climate change adaptation strategies, and lay the foundation for more accurate projections of future temperature trends in complex topographical regions.

1.3 Thesis Organization

The remaining thesis content is structured as follows:

- Prior Work on Spatial, Temporal, and Spatio-Temporal Data Mining: Review of existing literature and studies related to spatial, temporal, and spatio-temporal data mining in the context of climate science and temperature analysis.
- Data and Preliminary Analysis: Description of the data sources and preliminary exploratory analysis of the temperature data to identify trends and patterns.
- Methodology: Detailed explanation of the P-MiSTIC methodology, its extensions from MiSTIC, and its application to elevation-dependent warming analysis in contiguous Peninsular India.
- Study of Gridded Temperature Patterns in contiguous Peninsular India using MiSTIC and P-MiSTIC: Investigation of gridded temperature patterns across contiguous Peninsular India using MiSTIC and application of P-MiSTIC to detect and analyze elevation-dependent warming clusters within the study area.
- Decadal Analysis using P-MiSTIC: Examination of decadal temperature trends using P-MiSTIC and identification of long-term patterns and changes in elevation-dependent warming across different time periods.
- Seasonal Analysis using P-MiSTIC: Analysis of seasonal temperature variations using P-MiSTIC and exploration of how elevation-dependent warming manifests during different seasons and its implications for climate dynamics.
- Discussions: Comparison and evaluation of observed temperature data with modelled data, insights gained from the modelled data and its relevance in understanding elevation-dependent warming, utilization of spatio-temporal analysis to comprehend the regulating behaviour of different zones concerning temperature variations, elevation-dependent warming.
- Conclusions of the Study: Key findings and insights derived from the study, contributions, limitations, and implications of the research, and recommendations for future research and potential applications of the study's outcomes.

Chapter 2

Literature Review

2.1 Data Mining & Analysis

Data mining is the process of applying computational methods to massive quantities of data to unearth new, non-trivial, and pertinent information. It is a process of discovering patterns and extracting useful information from large datasets. It involves the use of computational techniques, statistical algorithms, and machine learning methods to analyze data and uncover hidden relationships, trends, and patterns that may be useful for decision-making or prediction. It is used for finding interesting patterns from the data and exploring large data sets, building models that describe the relevant properties of data, and making predictions based on the data [32]. Data mining can be applied to a wide range of data types, including structured and unstructured data, text data, and multimedia data. Data mining has a number of applications, and these applications have enhanced various fields of human life, including business, education, social media, medicine, scientific etc. [33]. The ultimate goal of data mining is to extract meaningful and actionable insights from data to support decision-making processes.

The data mining process typically involves several steps, including [34]

- Knowledge of application domain
- Data acquisition
- Data cleaning & preprocessing
- Data reduction
- Selection of data mining category (classification/regression/clustering)

- Selection of data mining technique
- Implementation of data mining algorithm
- Interpretation of the results

In climate studies, data mining is used to extract useful information from large datasets. The exponential growth of climate data combined with Knowledge-Discovery through Data-mining promises an unparalleled level of understanding of how the climate system responds to anthropogenic forcing [35]. Weather forecasting analyzes troves of historical data to identify patterns and predict future weather conditions based on time of year, climate, and other variables. Data mining in climate studies involves extracting information in both space and time. Data mining in space and time involves the analysis and extraction of knowledge from data that is both spatially and temporally referenced. This type of data mining is used in many fields, including environmental science, astronomy, geology, and urban planning, among others.

Spatial data mining involves the analysis of data that has a spatial component, such as geographic location, and typically involves techniques such as spatial clustering, spatial regression, and spatial interpolation. Time-series data mining, on the other hand, involves the analysis of data that is collected over time, such as temperature or rainfall measurements. Techniques used in time-series data mining include trend analysis, forecasting, and anomaly detection. When these two types of data are combined, it is possible to analyze and understand phenomena that evolve over space and time, such as weather patterns or land use changes. This type of analysis can reveal complex relationships and patterns that might not be apparent when considering spatial or temporal data separately. To extract novel, useful, and understandable patterns from spatial and spatio-temporal data, complex data preprocessing, transformation, data mining, and post-processing techniques are required [36].

A unique quality of Spatio-Temporal data that differentiates is the presence of dependencies among measurements induced by the spatial and temporal dimensions. Many of the widely used data-mining methods are founded on the assumption that data instances are independent and identically distributed. This assumption is violated, however, when dealing with spatial-temporal data, whereby instances are structurally related in the context of space and time and reflect distinct characteristics across various spatial regions and time periods [37]. Data mining in space and time is becoming increasingly important as the amount of data being collected in these fields continues to grow. There is an active research field that focuses on developing novel algorithms and techniques capable of effectively managing the complexity associated with this type of data.

2.1.1 Spatial Data Mining & Analysis

Spatial data mining is an interdisciplinary field that combines concepts from geography, data mining, and spatial analysis to extract valuable insights from spatially referenced datasets. It involves the application of various techniques and algorithms to uncover hidden patterns, relationships, and trends in spatial data. Conventional data mining techniques are limited in their ability to derive spatial patterns due to the complexity of spatial data and inherent spatial relationships. Spatial data mining has evolved from data mining fields in statistics and computer science, such as clustering, classification, and visualizing information. The most broadly utilized spatial data mining methods are decision trees, neural networks, Support Vector Machines, rule-based classification, and machine learning [38]. Extracting interesting and useful patterns from spatial datasets is more difficult than extracting the corresponding patterns from traditional numeric and categorical data due to the complexity of spatial data types, spatial relationships, and spatial auto-correlation [39].

2.1.1.1 Spatial Pattern

A spatial pattern pertains to how objects, phenomena, or features are positioned, dispersed, or organized in space. It reveals the spatial connections between entities or events and offers valuable insights into the fundamental structure and arrangement of spatial data. Spatial patterns can manifest in diverse forms, including clustering, dispersion, regularity, randomness, or spatial dependence, each carrying its own distinct characteristics and implications.

The following questions arise while attempting to recognize and understand spatial patterns: [40]

- Are there any clusters or concentrations of objects or phenomena on the map? Where are they located?
- Do you observe any patterns of dispersion or scattering of objects or phenomena across the map? Are there areas with low or high density?
- Are there any distinct patterns of arrangement or regularity in the distribution of objects or phenomena?

- Do you notice any spatial dependencies or correlations between neighbouring locations? Are similar values or characteristics clustered together?
- Are there any gradients or gradual changes in the spatial patterns? Are there areas of transition or abrupt shifts?
- How does the spatial pattern compare to the underlying geography, terrain, or environmental factors?
- Are there any spatial patterns that align with known or expected patterns based on prior knowledge or hypotheses?

2.1.1.2 Spatial Data & Format

The two primary formats of spatial data are vector and raster.

- Vector Format: Vector data represents spatial information using points, lines, and polygons. It describes the geometry and attributes of geographic features.
- Raster Format: Raster data represents spatial information as a grid of cells or pixels, where each cell has a value. It is commonly used for continuous phenomena like satellite imagery or elevation models.

These two formats, as depicted in Figure 2.1, have different characteristics and are used for different types of spatial data. The choice of format depends on factors such as the nature of the data, the desired analysis or visualization, and the software or systems being used.

2.1.1.3 Spatial neighbourhood Relations

There are three fundamental categories of spatial relationships: topological relationships, distance relationships, and direction relationships [41].

- Topological Spatial Relations: The topological spatial relations of objects are characterized by their connectivity and containment. These relations are concerned with the arrangement and connectivity of objects, regardless of their specific distances or directions. Examples of topological relations include ”inside,” ”touching,” ”overlap,” and ”adjacency.” (Figure 2.1(a))

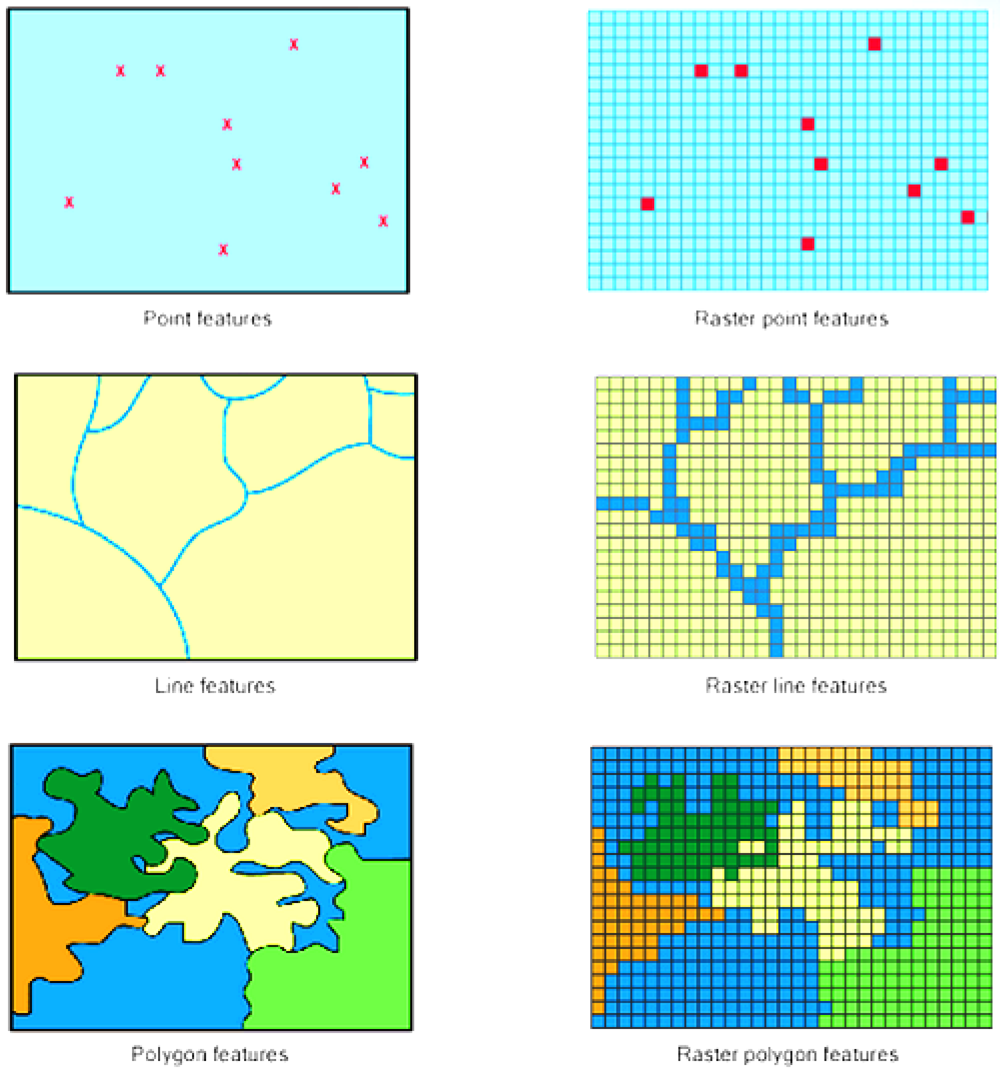

Figure 2.1: Vector and Raster data format representation

- Distance Spatial Relations: Distance spatial relations quantify the proximity or separation between objects in space. They are based on the measurement of distances using various distance metrics, such as Euclidean distance, Manhattan distance, or Minkowski distance. These relations provide information about the spatial arrangement and relative distances between objects.

- Directional Spatial Relations: Directional spatial relations describe the orientation or direction between objects or points in space. They capture the angular relationship or bearing between objects, indicating the direction in which one object is located with respect to another. Examples of directional relations include ”north,” ”south,” ”left,” and ”right.” (Figure 2.1(b))

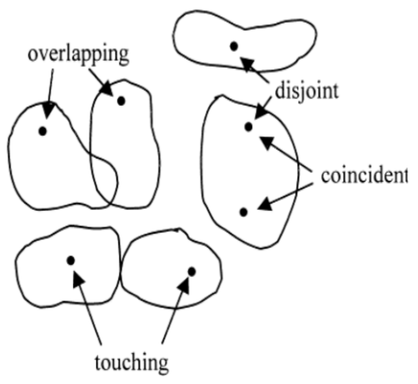

(a) Topological relations

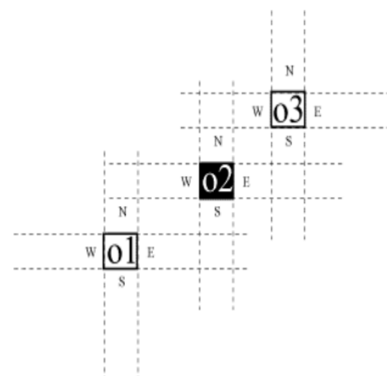

(b) Directional relations

Figure 2.2: Spatial Neighbourhood Relations

2.1.1.4 Spatial Analysis

Spatial analysis encompasses a range of formal techniques that examine entities based on their topological, geometric, or geographic characteristics. It involves the application of various analytic approaches, with a particular emphasis on spatial statistics, to study and understand spatial patterns and relationships, predicting values, modelling patterns, and exploring interactions.

Here are various types of spatial analysis: [42]

- Autocorrelation: Autocorrelation refers to the degree of similarity or correlation between spatially adjacent observations. It measures the extent to which a variable’s value at one location is related to its value at neighbouring locations. It measures the spatial pattern of dependence or similarity in the data.

- Interpolation: Interpolation is the process of estimating values at unobserved locations within a study area based on observed data from surrounding locations. It is commonly used in spatial analysis to fill in the gaps between data points and create continuous surfaces or maps from sparse and irregularly distributed data points.

- Regression: Regression analysis in spatial analysis involves modelling the relationship between a dependent variable and one or more independent variables, taking into account spatial dependencies in the data. Spatial regression methods account for the spatial structure and spatial dependence among observations, enabling the identification of spatially varying relationships.

- Interaction: Interaction analysis in spatial analysis refers to the influence or effect of one variable on another. It involves examining how the relationships between variables change across space and identifying areas where interactions have significant effects.

2.1.1.5 Fundamental Issues

Spatial analysis encounters various key issues, including the characterization of spatial phenomena, spatial dependency or autocorrelation, scaling, sampling, spatial data integration, computational complexity and common errors that can occur in spatial analysis [43].

- Spatial characterization: Spatial characterization involves representing and describing spatial patterns and structures in the data to understand their characteristics and properties. It includes techniques for summarizing spatial attributes, identifying spatial patterns, and extracting meaningful features.

- Autocorrelation: Autocorrelation refers to the spatial dependence or similarity between neighbouring or nearby spatial observations. It measures the degree to which the values of a variable at one location are correlated with the values at surrounding locations. Methods to detect and account for autocorrelation include spatial autocorrelation indices and spatial regression models.

- Scaling issues: Scaling issues arise when spatial data mining techniques need to handle data at different spatial scales or resolutions. Spatial data may be available at various levels of detail, from fine-grained to coarse-grained representations. Scaling issues can arise when integrating data from multiple sources or analyzing data at different resolutions. Inconsistencies in scale can lead to biased interpretations and incorrect conclusions.

- Sampling: Sampling involves selecting a subset of spatial data for analysis to infer properties of the entire dataset. Spatial data sampling presents unique challenges due to the spatial dependencies and spatial heterogeneity in the data. Issues such as biased sampling, inadequate sample size, and sampling design can affect the representativeness and generalizability of results. Proper sampling strategies, such as random or stratified sampling, are essential to minimize sampling bias.

- Data integration: Data integration refers to combining and integrating multiple sources or types of spatial data for analysis. It involves addressing issues related to data heterogeneity, interoperability, and semantic consistency. Data integration techniques, such as data fusion, spatial data matching, and harmonization, are crucial for combining diverse datasets into a consistent and usable form.

- Computational complexity: Spatial data mining often involves computationally intensive algorithms and techniques due to the large size and complexity of spatial datasets. The various computational challenges in spatial data mining include efficient indexing, retrieval, and processing of spatial data.

2.1.2 Temporal Data Mining & Analysis

2.1.2.1 Temporal Data Mining

Temporal data mining involves the investigation of chronologically ordered events. It has two primary directions: one focuses on identifying connections among temporally-oriented events, and the other, time series analysis, focuses on detecting similar patterns within a single sequence of time or across multiple time sequences. Sequence mining occurs when events are organized in sequences and data mining techniques are applied to these sequences [44].

2.1.2.2 Temporal Analysis

Time series data refers to a sequence of data points recorded over time, typically at regular intervals. Time series analysis involves studying and modelling these data points to uncover patterns, trends, and relationships within the data. There are various techniques and methods used in time series analysis to extract meaningful insights. Following are some types of time series analysis [45]:

- Time Series Forecasting: Time series forecasting aims to predict future values based on historical data patterns. It involves analyzing the temporal dependencies and trends within the data to make accurate predictions.

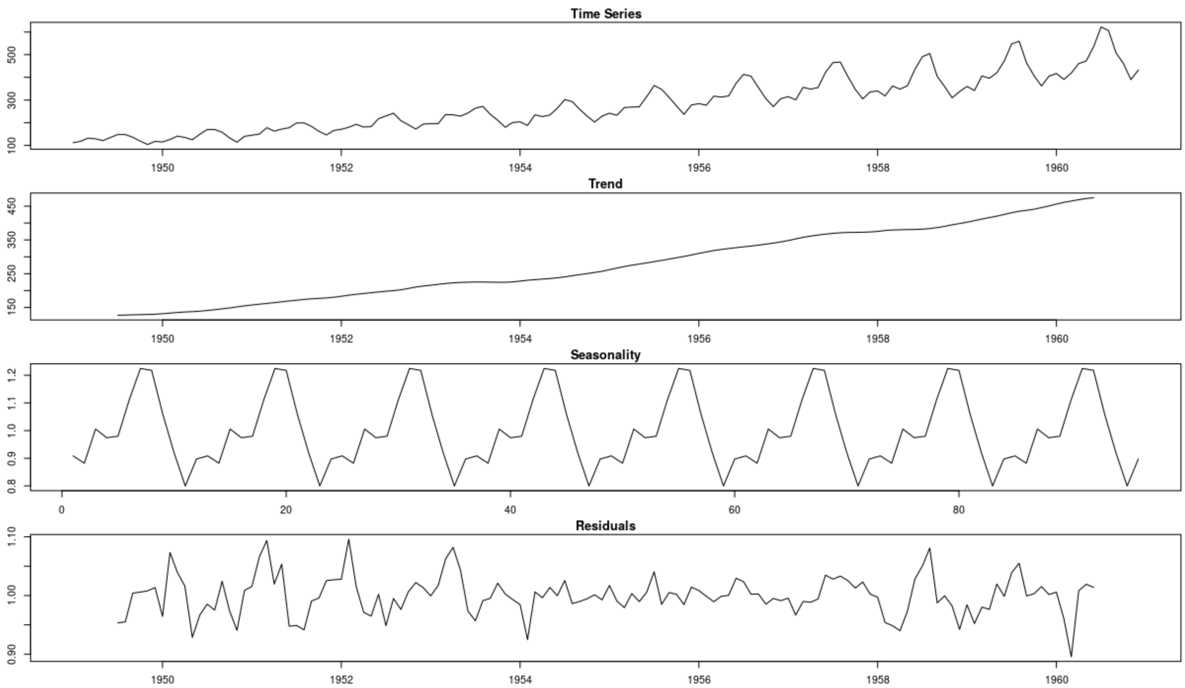

Figure 2.3: Decomposition of Time-series

- Seasonal Patterns and Decomposition: Many time series exhibit seasonal patterns, where certain patterns repeat at regular intervals. Decomposition methods help separate these patterns from the overall trend and irregular components. (Figure 2.3)

- Time Series Classification: Time series classification involves assigning a label or category to a given time series based on its patterns, characteristics, or behaviour.

- Time Series Clustering: Time series clustering involves grouping similar time series together based on their patterns, shapes, or other features.

- Anomaly Detection in Time Series: Anomaly detection in time series aims to identify unusual or abnormal patterns or events that deviate from the expected behaviour.

2.1.2.3 Fundamental Issues

Various key problems and obstacles arise in the context of time series analysis, including data quality, data sparsity, model selection and complexity, forecast uncertainty, interpretability, causality and other factors that can impact the analysis.

2.1.3 Spatio-Temporal Data Mining & Analysis

Spatio-Temporal Data Mining (STDM) is a multidisciplinary field that focuses on discovering patterns, relationships, and knowledge from data that vary in space and time. It combines techniques from spatial analysis, time series analysis, and data mining to handle the complexities of data that exhibit both spatial and temporal dimensions. It is important to consider both the spatial and temporal dimensions in data analysis, as they provide valuable context and enable the discovery of complex patterns that may not be apparent when analyzing spatial or temporal data separately. Spatio-temporal data mining has gained significant attention due to the increasing availability of data that includes both spatial and temporal aspects. Examples of such data include GPS trajectories, climate data, social media check-ins, transportation data, and surveillance data.

The objective of spatio-temporal data mining is to discover interesting and useful patterns, relationships, and trends within these datasets. The patterns can be used to understand the underlying processes, make predictions, support decision-making, and develop effective strategies in various domains such as transportation planning, urban development, environmental monitoring, crime analysis, and epidemic outbreak detection.

The features of spatio-temporal data mining can be summarized as follows: [44]

- Integration of Spatial and Temporal Dimensions: Spatio-temporal data mining allows for the integration of spatial and temporal dimensions in a unified framework. This integration helps capture the dependencies and interactions that exist between space and time, leading to a more comprehensive analysis.

- Improved Predictive Power: By considering both spatial and temporal factors simultaneously, spatio-temporal data mining models can provide more accurate predictions and forecasts. Spatial patterns and temporal trends are jointly incorporated, resulting in enhanced predictive power compared to standalone spatial or time series analysis.

- Unveiling Dynamic Patterns and Processes: Spatio-temporal data mining facilitates the exploration of dynamic patterns and processes that unfold over time and space. It enables the identification of evolving trends, periodic patterns, and cyclic behaviour, which may not be evident when analyzing spatial or time series data separately.

- Identification of Spatio-Temporal Clusters: Spatio-temporal data mining techniques enable the discovery of clusters that exhibit both spatial proximity and temporal similarity.

These clusters can reveal significant patterns or events that occur in specific locations during particular time periods, contributing to a deeper understanding of spatio-temporal phenomena.

- Handling Non-Stationarity: Many real-world spatio-temporal processes exhibit non-stationarity, where the statistical properties change over time or space. Spatio-temporal data mining offers methods to model and account for non-stationarity, allowing for more accurate analysis and prediction of evolving spatial and temporal phenomena.

Spatio-Temporal Data Mining has multiple challenges caused by the following factors: [37]

- Relationships between spatiotemporal objects are complex and implicit.
- STDM necessitates multidisciplinary effort and the incorporation of multiple heterogeneous datasets and data mining algorithms.
- The effects of magnitude and zoning on the results of data mining create a spatio-temporal region discretisation issue.
- Data characteristics including heterogeneity and variability.
- Data representations, advanced modelling, visualization, and comprehensiveness require additional work in STDM

Following are the key steps involved in spatio-temporal data mining:

- Data Collection: The first step is to collect the spatio-temporal data from relevant sources. This data can come from various sources at various spatial and temporal resolutions. The data should include spatial coordinates (latitude and longitude) and temporal information (timestamps or time intervals).
- Data Preprocessing: Once collected, data must be preprocessed to ensure its quality, usability, and consistency across datasets. This phase involves removing inconsistencies, errors, and absent values from the data. This step involves cleaning the data by removing any inconsistencies, errors, or missing values. It may also involve transforming the data into a suitable format for analysis, such as converting time formatting or aggregating data at different spatial or temporal resolutions.
- Spatial Data Analysis: The next step is to perform spatial analysis on the data. This can involve tasks such as spatial clustering, spatial interpolation, spatial autocorrelation, or

spatial pattern detection. Spatial clustering techniques can group similar data points together based on their spatial proximity, while interpolation methods can estimate values at unobserved locations based on the values of nearby locations. Spatial autocorrelation measures the degree of similarity between neighbouring data points, and spatial pattern detection identifies significant spatial patterns or hotspots.

- Temporal Data Analysis: In addition to the spatial analysis, the temporal aspect of the data needs to be explored. This can involve tasks such as temporal aggregation, time series analysis, temporal pattern detection, or change detection. Temporal aggregation techniques can summarize data at different time intervals

2.2 Assessment of GCMs

General Circulation Models (GCMs) are essential tools in climate science, providing projections of future climate conditions based on complex simulations of the Earth's climate system. These models play a pivotal role in informing policy decisions, designing adaptation strategies, and understanding the potential impacts of climate change. However, the accuracy of GCMs' predictions is subject to various uncertainties arising from the intricate nature of Earth's climate system, model parameterizations, and computational limitations. This underscores the critical need to rigorously assess and evaluate GCMs to ensure their reliability and relevance in shaping climate-related policies.

1. Ensuring Credible Climate Projections:

   GCMs are central to generating climate projections that underpin crucial decisions related to resource management, urban planning, agriculture, and disaster preparedness. Reliable projections are essential for minimizing risks and optimizing responses to changing climatic conditions. Therefore, assessing GCMs for their prediction accuracy becomes paramount to instill confidence in the credibility of the projected climate scenarios [46].

2. Refining Climate Change Adaptation Strategies:

   Effective climate change adaptation strategies require accurate information about future climate conditions. Decision-makers rely on GCM projections to anticipate changes in temperature, precipitation, sea level rise, and other critical variables. Ensuring the predictive ability of GCMs is vital for tailoring adaptive measures that can withstand the challenges posed by a changing climate [47].

3. Identifying Model Biases and Improving Parameterization:

   Assessment of GCMs often reveals biases in their simulations, where model outputs deviate from observed climate data. Understanding these biases is crucial for refining model parameterizations, addressing structural limitations, and improving the overall representation of physical processes. Effective evaluation contributes to the iterative process of model development and enhancement [48].

4. Enhancing Scientific Understanding of Climate Processes:

   GCMs provide insights into the complex interactions within the climate system. Through rigorous evaluation, scientists can identify areas where models excel and areas where they fall short. This process enhances our understanding of climate processes, refines hypotheses, and guides further research to bridge gaps in our knowledge [49].

The need to assess and evaluate GCMs for their prediction accuracy arises from their central role in shaping climate-related decisions and policies. Rigorous evaluation helps establish the credibility of climate projections, supports effective adaptation strategies, refines model parameterizations, and enhances our scientific understanding of the climate system. As climate change continues to impact societies and ecosystems, the reliability of GCMs becomes crucial in guiding actions towards a sustainable future.

2.3 Elevation-Dependent Warming (EDW)

Elevation-dependent warming (EDW) is a climate phenomenon that refers to the uneven distribution of temperature changes across different elevations within a geographic region. In a warming climate, areas at higher elevations experience more significant increases in temperature compared to lower-elevation regions. Several factors drive this phenomenon:

1. Lapse Rate: Normally, temperatures decrease with increasing elevation due to the lapse rate, which describes how temperature decreases as you ascend in the atmosphere. In a warming climate, this lapse rate can change, leading to amplified warming at higher elevations [11].

2. Snow-Albedo Feedback: As temperatures rise, higher elevation areas may experience earlier snowmelt. Snow has a high albedo, meaning it reflects sunlight, whereas the ground absorbs it. When snow melts, the ground is exposed, and it absorbs more heat, leading to further warming [50].

3. Atmospheric Changes: Changes in atmospheric circulation patterns can affect temperature distribution. In a warming climate, alterations in circulation can influence temperature variations at different elevations [51].

Understanding EDW is essential for understanding the multifaceted impacts on ecosystems, water resources, glacial retreat, agriculture (particularly in mountainous regions), increased frequency of floods & landslides, and communities in mountainous regions.

2.4 Related Work

Spatio-Temporal Data Mining is an emerging discipline of study that incorporates both spatial and temporal data mining. The existing research can be identified in two directions. The first is the incorporation of a temporal consciousness into spatial systems, and the second is the incorporation of space into temporal data mining systems [44]. This means that either spatial analysis is done and then observed over time or time-series/temporal mining is done first, followed by mapping results over the space. In any instance, space and time are utilized simultaneously.

Gowtham Atluri. et al.[37] describes the challenges and techniques involved in mining spatio-temporal data. The authors note that spatio-temporal data, which is characterized by both spatial and temporal aspects, is being increasingly collected and analyzed in numerous disciplines, including climate science, social sciences, and Earth sciences. This presents unique challenges distinct from traditional relational data mining techniques. The article provides a thorough overview of the field of spatio-temporal data mining, covering the various categories of spatio-temporal data and its associated mining concerns. The authors divide the literature on spatio-temporal data mining into six categories: clustering, predictive learning, change detection, frequent pattern mining, anomaly detection, and relationship mining. The paper discusses the numerous types of spatio-temporal data mining challenges within each category.

K. Sravanthi. et al.[31] evaluate and comprehend natural and anthropogenic events in particular regions. The authors propose the method MiSTIC, which integrates watershed delineation, neighbourhood analysis, and frequent item mining to identify regions affected by events over a given period. The method uses spatial analysis to determine focal points and spatio-temporal analysis to determine core regions. The core regions are categorized according to the type of neighbourhood (contiguous points or a defined radius) and the frequency of occurrences (highly dominating points, less dominating points, or no dominating points). The frequent focal points capture the localized event behaviour, whereas the neighbourhood constraints reflect the event's dynamic or non-dynamic nature. In the case of monsoon rainfall in Central and Peninsular India over a 56-year period (1951-2006), the study identifies primary regions. Due to the dynamic character of rainfall, it has been observed that core regions with a defined radius (CR) perform better than those with contiguous points (CC).

The Mountain Research Initiative EDW Working Group in the paper 'Elevation-dependent warming in mountain regions of the world' [11] provides a comprehensive analysis of temperature trends in mountain regions globally. It highlights the phenomenon of EDW and its potential consequences for these regions. The study uses a wide range of climate data and models to quantify temperature changes at different elevations and discusses the implications for ecosystems, water resources, and human societies.

Cai et al. [51] takes a broader perspective by investigating temperature trends across different elevations and latitudes. It explores the relationship between elevation, latitude, and temperature changes. The research discusses the implications of EDW for climate change adaptation and highlights the need for region-specific assessments. The analysis of the TP temperature trends shows continuing warming for higher elevations and a positive warming–elevation correlation from 1961 to 2014.

Qinglong You et al.[52] summarize elevation-dependent warming (EDW) on the Tibetan Plateau. Since the TP is called the "Third Pole," the authors contend that understanding the EDW is crucial to estimating warming rates and their effects in this region. EDW over the TP is studied using observed datasets and model-based simulations. EDW's spatial expression and explanatory mechanisms are poorly understood due to data scarcity. Their research examines snow/ice-albedo feedback, cloud feedback, atmospheric water vapour feedback, aerosol feedback, land use changes, ozone, and vegetation. However, EDW's primary mechanisms are uncertain. New perspectives and unresolved issues include quantifying EDW in climate model simulations, understanding the long-term EDW reconstructed from substitutes, the interaction between the Asian summer monsoon and EDW, the importance of EDW for future environmental and water resource changes, and the lack of understanding of EDW at extremely high elevations. The authors recommend a comprehensive ground observation network, increased remote sensing data use, and high-resolution climate modelling that accurately represents atmospheric and cryospheric processes to advance the field. These actions, according to the authors, will aid in understanding EDW on the Tibetan Plateau.

Chapter 3

Data

3.1 Region of Study

India presents an ideal study area for investigating elevation-dependent warming, a phenomenon where temperature changes vary based on the altitude of a region. India's diverse topography, ranging from the mighty Himalayan mountain range in the north to the coastal plains in the south, offers a unique opportunity to explore the impacts of elevation on temperature patterns and climate dynamics. In this study, we will focus on understanding how temperature trends vary across different clustered zones in India, providing valuable insights into the effects of altitude on climate change.

India's geography plays a crucial role in shaping its climate and temperature patterns. The Himalayan range, stretching across the northern border, not only provides a majestic backdrop but also acts as a barrier, impacting weather systems and influencing temperature gradients. As we move southward, the elevation decreases, leading to diverse landscapes such as plateaus, river plains, and coastal regions. This variation in topography creates distinct micro-climates across different elevations, making India an ideal region to investigate elevation-dependent warming.

The study region and agro-ecological zones of India are depicted in Figure 3.1(a & b). To ensure the continuity of data, the North-Eastern part of India is excluded from the study due to the spatial disconnectivity and distinct agro-ecological conditions of the region compared to the contiguous Peninsular India. The contiguous Peninsular India, with 307 grid points, as depicted in Figure 3.1(a), has been chosen as the region for this study. The agro-ecological zones are used as a reference to understand the results of this research and understand if the patterns of temperature align with these zones.

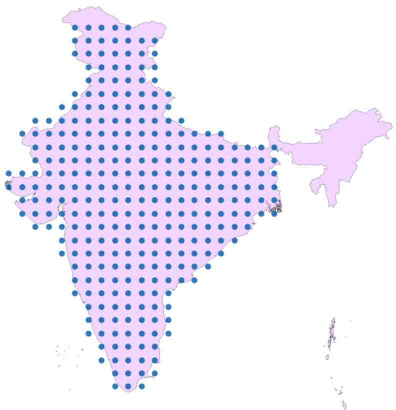

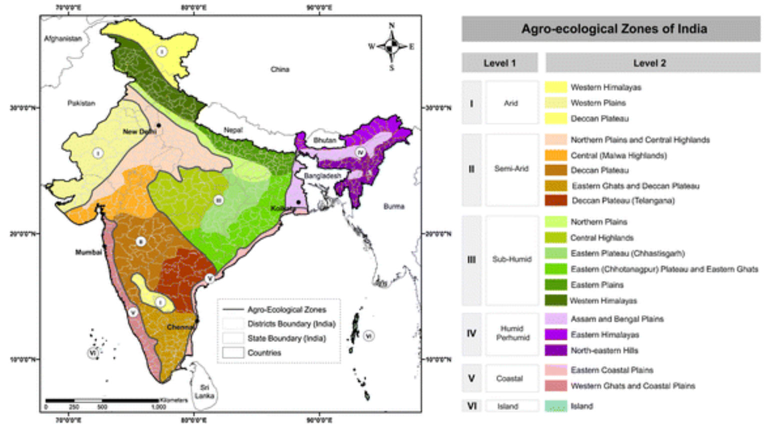

(a) Study Region

(b) Agro Ecological Zones of India [53]

Figure 3.1: Study Region & Agro Ecological Zones of India

3.2 Observed Data - IMD Gridded daily Temperature data

The IMD high-resolution $1^o \times 1^o$ gridded daily temperature dataset for the Indian region was developed using temperature data from 395* quality-controlled stations from 1969. A modified version of Shepard's angular distance weighting algorithm was used for interpolating the station temperature data into 1^o latitude $\times$ 1^o longitude grids. The cross-validation estimated error is less than 0.5°C. This data is arranged into 31x31 grid points. For leap years, data for 366 days is included.
* Gridded data for 2008 and on-wards is based on relatively fewer stations (around 180) for which data is received operationally on a real-time basis. [54]
The data for minimum and maximum temperatures for the years 1990 to 2020 has been used in this study. The temperature is expressed in degree Celsius.

3.3 Modelled Data - IPCC CMIP5 HadCM3 Gridded daily Temperature data

The Hadley Centre in the United Kingdom developed HadCM3, a coupled atmosphere-ocean general circulation model (AOGCM). It was one of the principal models utilized in the 2001 IPCC Third Assessment Report (AR3) [8]. HadCM3 is a GCM that has played a crucial role in IPCC assessment reports, contributes to models like PRECIS, is also one of the models used to generate WorldClim Global Climate data [9] and has been used, evaluated and validated in various climate studies in the last 2 decades [10]. This research utilized temperature data from the HadAM3 component of the HadCM3 model. HadAM3 is a grid point model with a horizontal resolution of $3.75^o \times 2.5^o$ in longitude and latitude and 96×73 grid points on the scalar grid (pressure, temperature, and humidity) [8].

The data for minimum and maximum temperatures for the years 1989 to 2019 has been used [9]. In order to achieve a uniform resolution for each input dataset, the gridded temperature data from HadCM3 from 1989 to 2019 have been resampled to 1^o x 1^o spatial resolution. The temperature is expressed in degrees Kelvin.

HadCM3, like many General Circulation Models (GCMs), can exhibit regular disparities or biases in its simulations compared to observed climate data. These disparities arise due to various factors related to the model's complexity, simplifications, and limitations. Factors like model parameterization, representation of land surface processes, initialization and boundary conditions, numerical methods implemented, structural bias, incomplete representation of Climate Forcing and model calibration can contribute to there disparities [46] [55]. Bias correction has not been applied to HadCM3 data in this study for the following reasons: (1) By applying bias correction, the quantification of deviant behavior of the simulated temperature patterns cannot be achieved & (2) The derivations of the analysis of HadCM3 temperatures from this study are not being used for further predictions or applications.

Regular disparities in GCMs are a recognized challenge in climate modelling. Researchers work to understand and reduce these biases through model improvements, enhanced observations, and statistical techniques. Evaluating these disparities is crucial for using GCMs effectively in climate research and for providing reliable climate projections for policy and planning purposes.

3.4 Preliminary Analysis of Observed & Modelled data

A preliminary analysis of data with time and elevation has been carried out to characterize the data trends of minimum, maximum and Diurnal Temperatures. The temporal trends depict the fluctuations in min, max and diurnal temperatures with year. The temporal change rates and lapse rates of temperatures are evaluated by fitting a regression line and estimating the slope of the line.

For observed IMD data, the temporal trends of minimum and maximum Temperatures are evaluated as 0.13°/decade & 0.17°/decade. With maximum Temperatures increasing at a higher rate, the difference between minimum and maximum Temperatures is bound to increase. The increase rate with the observed Diurnal Temperatures is evaluated as 0.03°/decade.

For modelled HadCM data, the temporal change rates of minimum and maximum Temperatures are evaluated as 0.43°/decade & 0.45°/decade. With the minimum Temperatures increasing at a slower rate, the difference between minimum and maximum Temperatures is bound to increase. The rate of increase is estimated as 0.02°/decade for the modelled Diurnal Temperatures. The discrepancy between the considerably higher rate of increase for minimum and maximum temperatures in modelled data and the observed trend suggests that the model incorporates a warming trend that surpasses the actual observations.

The lapse rate of minimum and maximum observed Temperatures is evaluated to be positive at 2.376°/decade & 2.341°/km. The lapse rate with the observed Diurnal Temperatures is evaluated at a negative rate of 0.193°/km, suggesting increased warming in higher elevations.

The lapse rate of minimum and maximum modelled Temperatures is evaluated to be positive at 6.344°/decade & 5.954°/km. The lapse rate with the observed Diurnal Temperatures is evaluated at a negative rate of 0.39°/km. The comparison between observed and modelled data reveals that the lapse rates in the modelled data indicate the utilization of a uniform & elevated lapse rate, which is close to the global average lapse rate of 6.5°/km in addition to other model parameterizations.

	Lapse rate (°/km)	**RMSE (°)**
IMD Tmin	2.376	1.87
IMD Tmax	2.341	1.57
IMD DTR	-0.193	1.56

Table 3.1: Lapse Rate and RMSE of Observed data trends

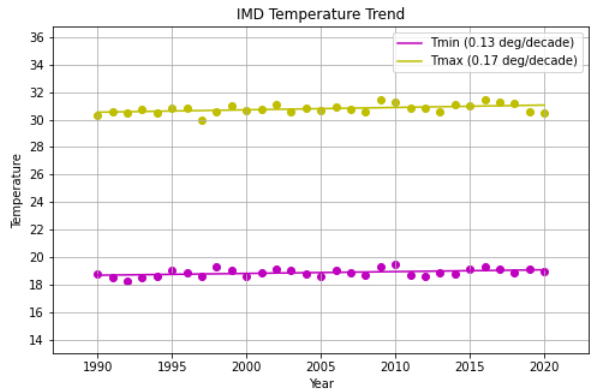

(a) IMD min, max Temperatures vs. Year

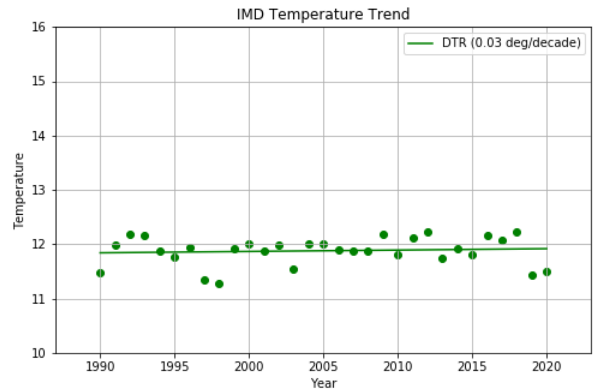

(b) IMD Diurnal Temperatures vs. Year

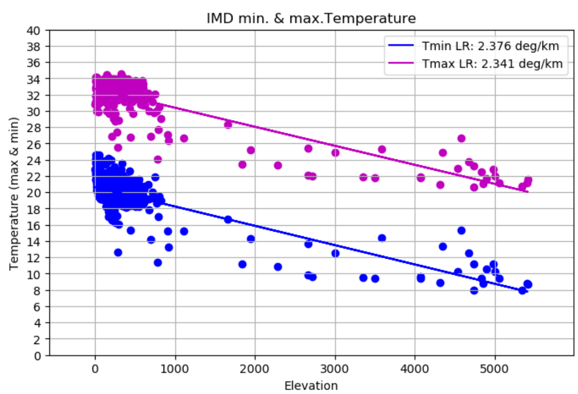

(c) IMD min, max Temperatures vs. Elevation

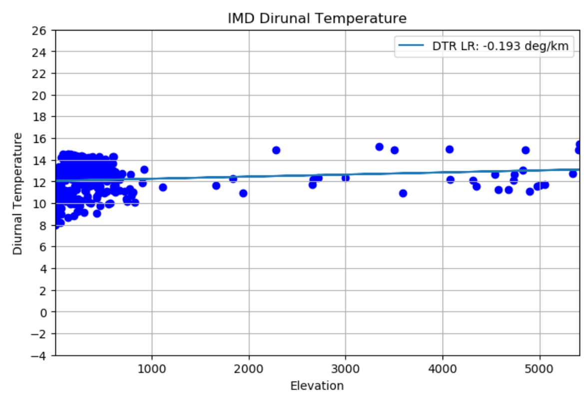

(d) IMD Diurnal Temperatures vs. Elevation

Figure 3.2: Data Trends of Observed (IMD) Data over the study region over the entire study period

	Lapse rate (°/km)	**RMSE (°)**
HadCM Tmin	6.344	4.6
HadCM Tmax	5.954	3.36
HadCM DTR	-0.39	4.23

Table 3.2: Lapse Rate and RMSE of Modelled data trends

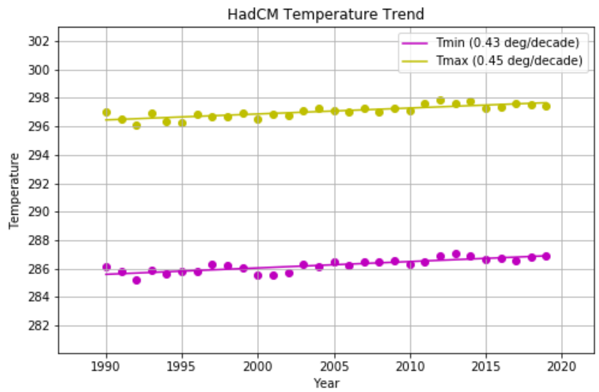

(a) HadCM min, max Temperatures vs. Year

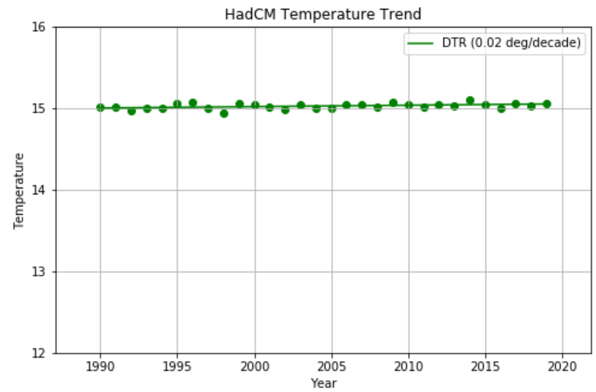

(b) HadCM Diurnal Temperatures vs. Year

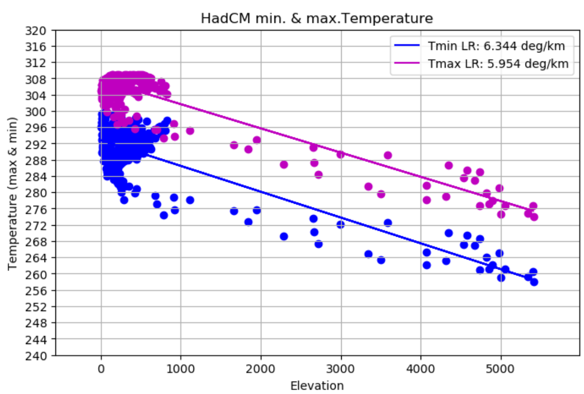

(c) HadCM min, max Temperatures vs. Elevation

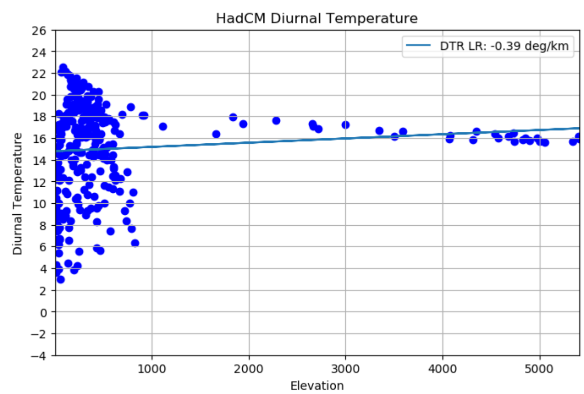

(d) HadCM Diurnal Temperatures vs. Elevation

Figure 3.3: Data Trends of Modelled (HadCM) Data over the study region over the entire study period

Source	**Temporal Change rate (°/decade)**
IMD Tmin	0.13
IMD Tmax	0.17
IMD DTR	0.03
HadCM Tmin	0.43
HadCM Tmax	0.45
HadCM DTR	0.02

Table 3.3: Temporal change rates of observed and modelled Temperature data

3.5 Digital Elevation Model

Viewfinder Panoramas (VFP) 3 arc-second (DEM) is a Digital Elevation Model (DEM) primarily derived from data acquired by the 2000 Shuttle Radar Topography Mission (SRTM) [56]. It offers global coverage with 1^o X 1^o tiles at a spatial resolution of 3 arc-second or 90 m. The term ”arc-second” refers to a unit of angular measurement used to express the resolution of a DEM, where one arc-second represents approximately 30 meters on the Earth’s surface [56].

SRTM voids are common in the Himalayan region. The VFP DEM is a global coverage DEM with SRTM voids filled using alternative sources like Topographic Maps, ASTER GDEM, Russian 200k and 100k, Nepal 50k and others [56]. The dataset offers high-resolution and detailed information about the Earth’s topography.

Chapter 4

Methodology

4.1 MiSTIC - Mining Spatio-Temporally Invariant Cores

MiSTIC is a versatile method for analysing data that aims to identify regions that are significantly affected by a phenomenon across different time periods, regardless of their geographical location. The approach relies on the identification of watershed boundaries, analysis of neighbouring areas, and extraction of common patterns. The process starts by conducting spatial analysis to identify focal points, which are representative points. Next, a comprehensive analysis is conducted on the data over the entire duration to identify central regions, commonly known as cores. The flowchart in Figure 4.6(a) illustrates the process of identifying core areas for a given dataset throughout the entire time period (T). For each time step from 1 to T, the initial stages involve identifying focal points and creating corresponding zones. To complete this process, it is necessary to identify the specific locations of the focal points. In continuation, the results of the spatial analysis steps are observed over a specific time period referred to as T (temporal analysis) to detect the central points. [58]

This process consists of two components of analysis: a spatial analysis conducted at time step t and a spatio-temporal analysis which involves the spatial analysis conducted at step A within period T.

4.1.1 Spatial Analysis

4.1.1.1 Detection of Focal Points

The focal point in a given area with connected components is determined by the component that has the highest/lowest value for the studied attribute among its connected components. Every individual cell within the grid has eight neighbouring cells that are connected to it. The value of each cell in the data grid is preprocessed and transformed into an integer. Similar to the D8 Pour Point Model [26], the initial step involves assigning a value between 0 and 8 to each cell. Each integer represents the direction of the highest increase in a specific attribute from that cell. Grids that have a missing value are assigned a negative integer. The assigned values for directions are as follows: if the maximum increase is towards the east, a value of 1 is assigned to the respective cell. In the same way, cells that are adjacent to each other are represented by values 2 through 8, as shown in Figure 4.3.

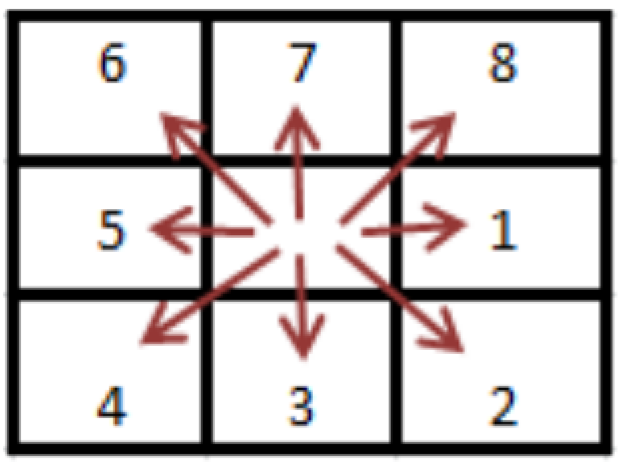

Figure 4.1: Direction Values [58]

4.1.1.2 Delineation of Zones

After identifying the focal points, it is necessary to divide the area into zones or segments, ensuring that each focal point is surrounded by its own designated zone. Every zone is given a distinct identifier (zone ID) that matches the ID of the focal point. The analysis cannot include zones that only consist of the focal point due to their lack of validity. After delineation, each grid cell or polygon is assigned a zone ID value to indicate its corresponding zone. This

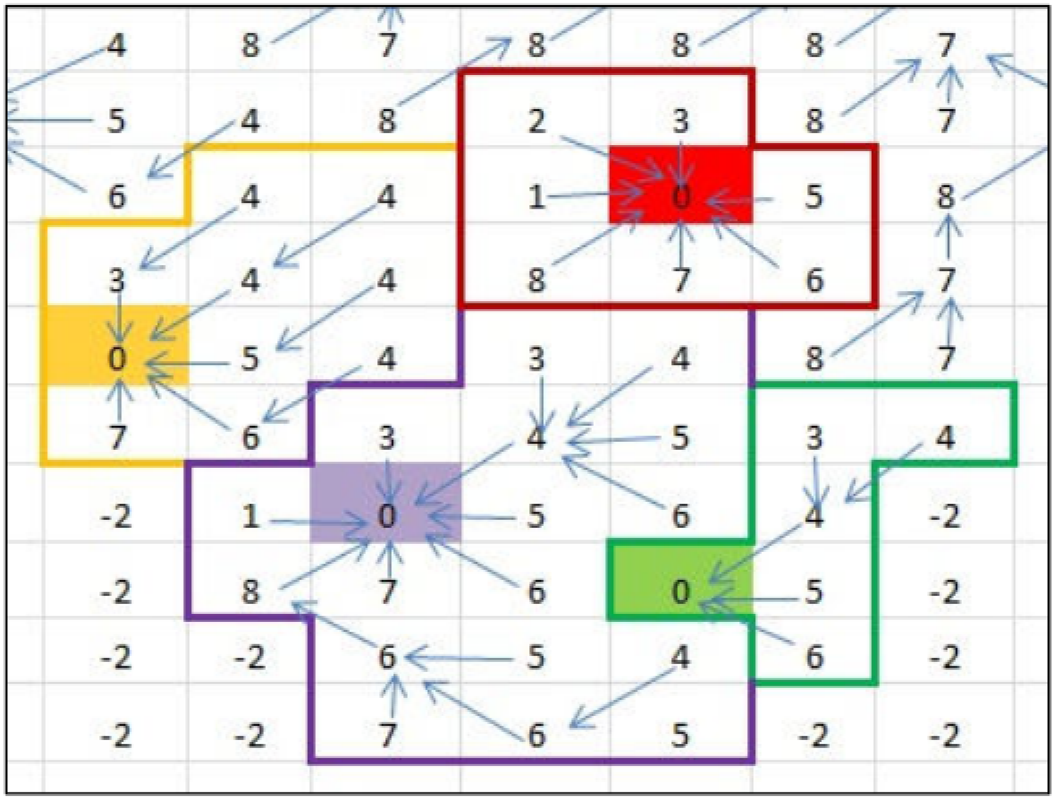

Figure 4.2: Four focal points detected [58]

method is similar to the process of delineating watersheds [27].

Delineation is achieved by creating a boundary between two neighbouring grid points using a direction that does not converge (separating areas with a high value of the variable from areas with a low value). To put it differently, the trajectory of a point is traced until it reaches a focal point, and subsequently, it is included in the corresponding zone.

Four focal points can be found in Figure 4.2, along with the directional values of cells. By examining the trajectory of any of the four focal points, valuable insights can be gained regarding the underlying process. Let's focus on the focal point highlighted in red, say P. Out of the eight cells surrounding P, seven of them have flow in the direction of P and are located in the surrounding region. These seven cells exhibit the lowest magnitude when compared to their neighbouring cells. As a result, there are no extra grid points within the zone. The outcome of the delineation phase is illustrated in Figure 4.3, which displays the zone IDs in a clear and direct manner. The cells with the value -2 represent no data units.

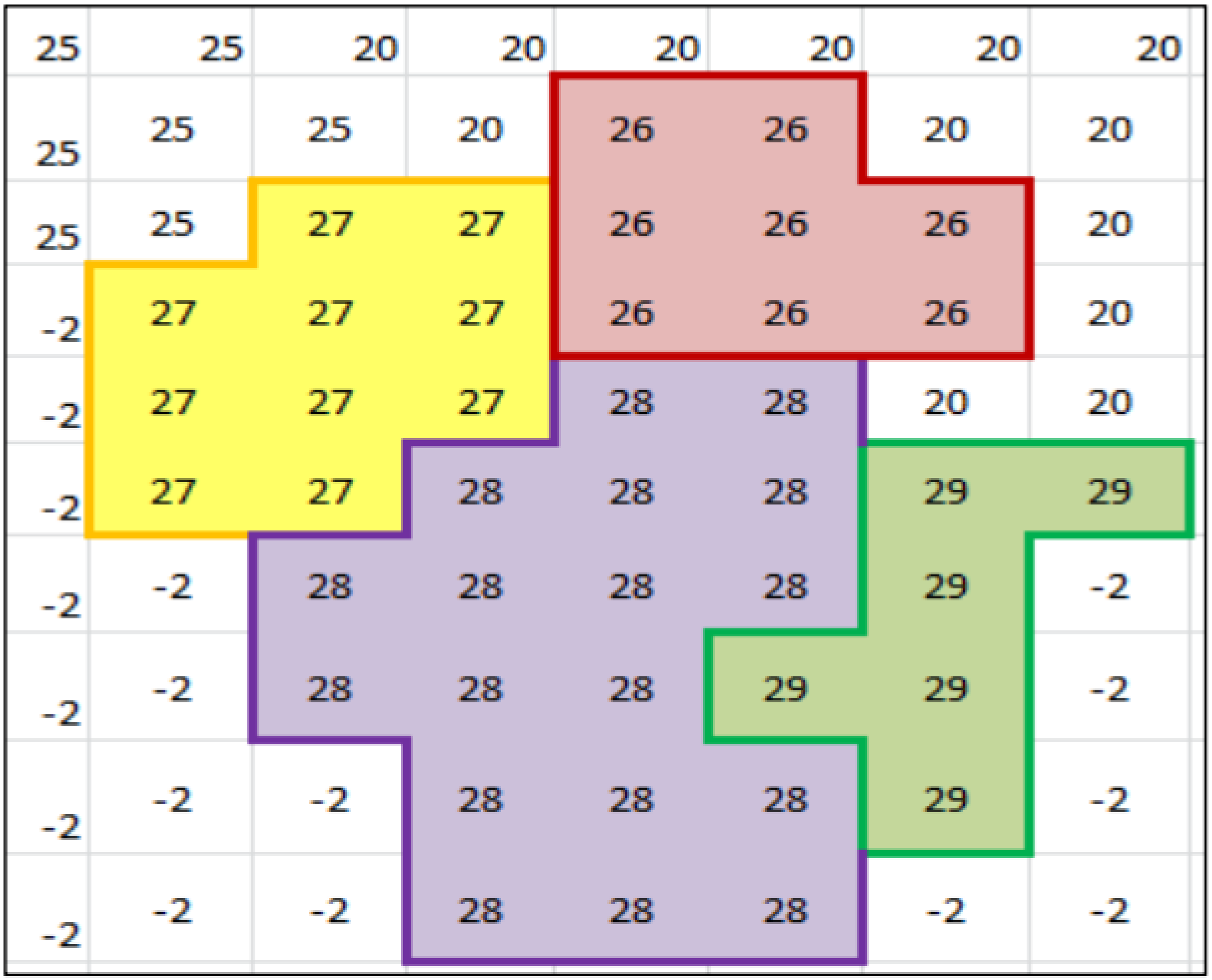

Figure 4.3: Zones created for each of the four Focal Points (corresponding to those locations shown in Figure 4-2) [58]

4.1.2 Spatio-Temporal Analysis

Core regions, referred to as Cores, are identified by examining the complete collection of focal points and their corresponding zones in space (the result of spatial analysis at each time step t) during the time period T (temporal analysis) [58].

A core region, also known as a core, refers to a group of focal points that are frequently found within a particular neighbourhood. The collection of points on a complete time period is created by selecting a maximum of one point from each time interval.

4.1.2.1 Neighbourhood Analysis

The number of focal points and the shape and size of the zones surrounding them can change with each time step t. Cores are categorised into two types based on the neighbourhood constraints they meet in order to understand the spatial event behaviour over a given time period T and the range of dynamic behaviours.

1. Core with Contiguous points (CC) : [58]
This particular core pertains to a set of focal points that are adjacent to each other in both space and time. In other words, it is a sequence of focal points arranged in chronological order, where each consecutive focal point is connected in terms of physical proximity. To illustrate, if there is a focal point i at time step t and cell ci, and the focal point j at time step t+1 and cell cj is located in any of the eight adjacent cells of ci, then both i and j will belong to the same core. Likewise, if the focal point k is present in time step t+2 and cell ck is found in any of the eight neighbouring cells of cj, ck will be included in that core. The core is made up of a series of consecutive points that are contiguous. If a focal point is not within the specified neighbourhood, it can be excluded at time step t. In Figure 4.4, there is a depiction of a core that consists of seven consecutive points across ten different time steps. A dashed arrow is used to represent instances where there are gaps in the timeline, such as one-time occurrences, extremes, or deviations. The time step (or year) t4 is not close to the time step (or year) t3, which means it is excluded and labelled as Not Satisfactory (NS) time step. In the same manner, the sequence removes t9 and labels it as NS. The focal point in two-time steps (t1 and t7) is represented by a central point.

The CC core type is suitable for datasets with limited progression or spread of phenomena or event occurrences. These phenomena demonstrate a predictable spillover effect [58]. However, certain phenomena demonstrate widespread distribution in all directions, regardless of whether they have a changing nature or not. Examples of such phenomena include epidemics, crime rates, and various others, where the central point of occurrence can vary across different locations. The next section, Cores with desired Radius (CR), discusses the most optimal core for these types of datasets [58].

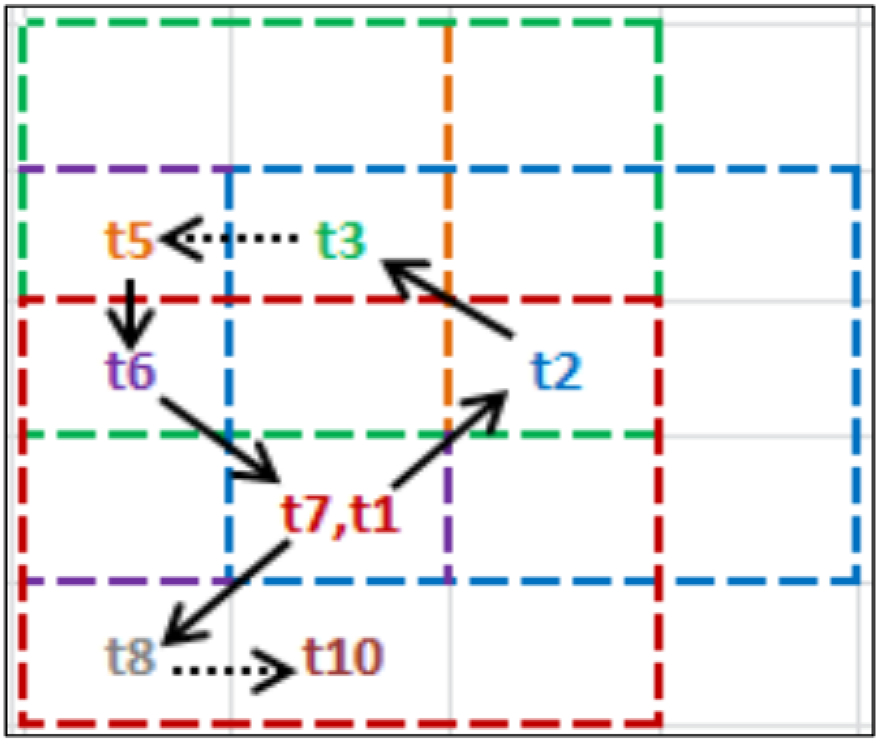

Figure 4.4: Core with Contiguous Points. t1 to t10 represent consecutive time steps. Dotted boundary lines define the neighbourhood for a given point (eight adjacent cells) [58]

2. Core with defined Radius (CR) : [58]

Spatial contiguity is unnecessary for the focal points in consecutive time steps in this core type. As shown in Figure 4.5, a radius is established around a reference focal point P (which can be at the initial step, t=1), and all subsequent focal points must be located within this radius r. As a result, the core is made up of a group of focal points in space that are not connected, and they are enclosed within a region with a radius r around the main focal point. The user determines the value of r, which varies depending on the study domain. In the event that there are multiple points located within the specified radius during a given time step, the point that is nearest to P is selected. If several points are equidistant from P, any of them can be chosen.

Points or time steps that do not meet the constraints of the neighbourhood are labelled as Not Satisfactory (NS) points or time steps. NS points are also referred to as Outliers.

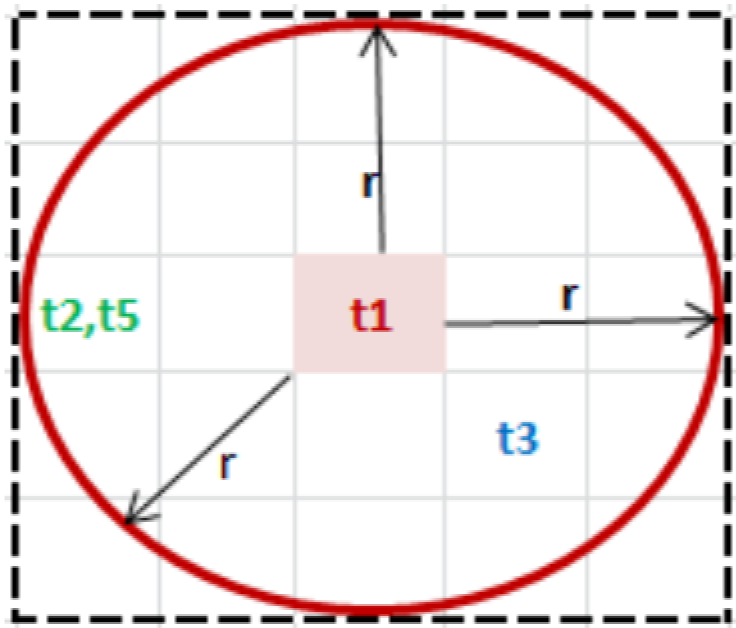

Figure 4.5: Core with defined Radius. Neighbourhood with radius r defined around a focal point in time step t1. The focal point in t4 is missing as it is outside the defined area. [58]

4.2 Parametric MiSTIC

This study introduces and describes P-MiSTIC (P-MiSTIC), a modified variant of the MiSTIC method. P-MiSTIC is specifically designed to detect focal points and identify invariant cores using multiple inputs. Based on earlier work, the thesis focuses on the extension of the original MiSTIC algorithm, which primarily mines invariant cores in spatio-temporal data of a single variable. The proposed P-MiSTIC algorithm enhances this capability by incorporating multiple input variables or parameters.

The flowchart depicting the MiSTIC algorithm for a single variable is illustrated in Figure 4.6. The primary modification in the transformation from MiSTIC to P-MiSTIC occurs in the *Mark Directions* step. The MiSTIC algorithm utilizes the variable value as the basis to assess and mark the direction of flow. Conversely, in the P-MiSTIC algorithm, a weighted average of the inputs is computed using user-defined weights for each input. The weighted average is subsequently employed to determine the direction of flow at each spatial unit.

The main objective of P-MiSTIC is to effectively capture the spatial and temporal dependencies of multiple variables concurrently, enabling a comprehensive analysis of intricate spatio-temporal patterns. P-MISTIC aims to identify invariant cores that exhibit consistent behaviours across different variables by considering multiple input variables, such as temperature, humidity, precipitation, wind speed, or any other relevant data. P-MiSTIC utilizes user-specified weights assigned to input variables analysis. By evaluating the weighted average at each point in space and time, the identifies directions that can be used to extract the unified focal points.

The thesis explores the potential of P-MiSTIC in uncovering hidden relationships and dependencies within spatio-temporal data by simultaneously considering multiple dimensions and their dependencies. The analysis of various variables and their interactions can yield significant insights into the mining of invariant cores.

The benefits of P-MiSTIC include:

- Comprehensive Analysis: Since P-MISTIC considers a number of different input variables, it can provide a more comprehensive analysis of spatio-temporal patterns, which in turn enables a deeper understanding of the processes at play.
- Increased Comprehension of the Context: The use of P-MiSTIC makes it possible to investigate how the various variables interact within the spatio-temporal context. This aids in the identification of intricate relationships and dependencies.
- Application in a wide range of fields and datasets: Because of its adaptable nature, the P-MiSTIC model can be used in a wide variety of fields and datasets, particularly those in which the interaction of multiple variables is critical to the comprehension of spatio-temporal phenomena.

By incorporating multiple input variables, P-MiSTIC offers an improved method over the original MiSTIC method. This results in an analysis of spatio-temporal patterns that is more thorough and accurate. Its potential lies in the fact that it has the ability to provide valuable insights and a more in-depth understanding of complex spatio-temporal dynamics in a variety of domains.

For the purpose of this study, the neighbourhood analysis in MiSTIC & P-MiSTIC evaluates Cores with Contiguous points (CC) for identifying core regions because temperature is a contiguous phenomenon.

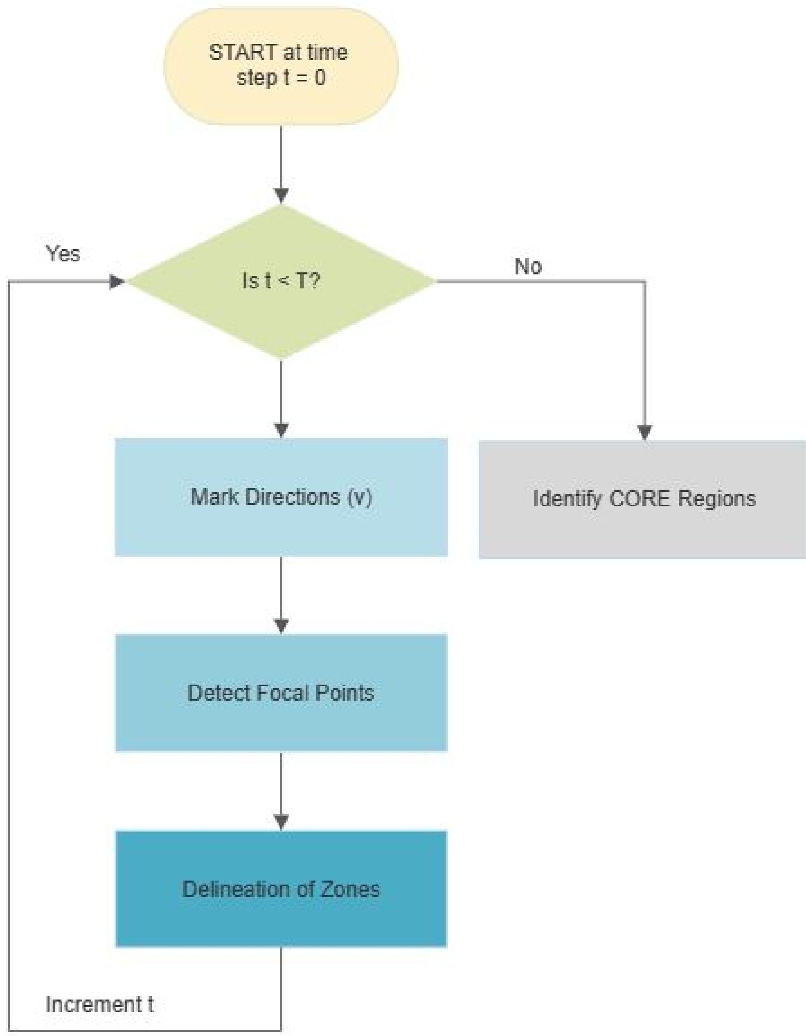

Figure 4.6: Flowchart of MiSTIC

Chapter 5

Study of Gridded Temperature Patterns in contiguous Peninsular India using MiSTIC & P-MiSTIC

The preliminary analysis for minimum, maximum and Diurnal Temperatures of observed and modelled data have been presented in section 3.4. A remarkable difference between the trends of observed and modelled data has been observed. In this chapter, the authors further explore the data & its patterns by employing the Spatio-Temporal methods - MiSTIC & P-MiSTIC.

5.1 MiSTIC on Observed and Modelled Data

The study utilizes the MiSTIC method to investigate the observed and modelled annual minimum and maximum temperatures separately. The identified zones for each dataset are illustrated in Figure 5.1, providing a visual representation of the spatial distribution of these zones.

The results of implementing the MiSTIC method on IMD and HadCM minimum and maximum temperature datasets have revealed interesting patterns and variations in the identified zones. IMD Tmin dataset has shown the maximum variation and resulted in the highest number of zones (12), indicating diverse temperature patterns across different regions. On the other hand, IMD Tmin and Tmax zones have partial overlaps, suggesting a relationship between minimum and maximum temperatures in certain areas.

However, the HadCM zones for Tmin and Tmax are predominantly divided diagonally. The diagonal division of HadCM zones can be attributed to several factors. One possible expla-

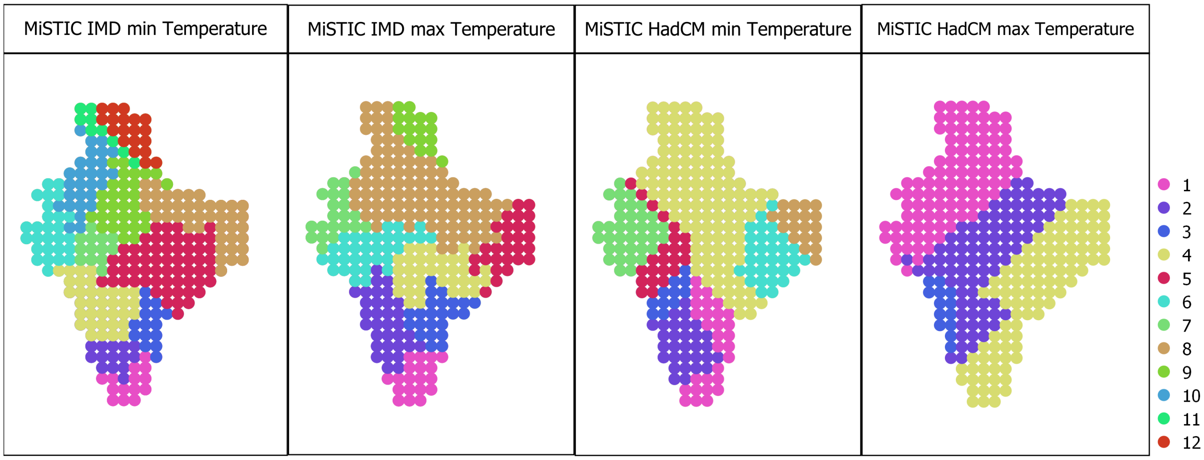

Figure 5.1: Zones identified for a) IMD Tmin b) IMD Tmax c) HadCM Tmin d) HadCM Tmax

nation is the nature of climate models like HadCM, which simulate climate patterns based on complex mathematical equations and physical processes. These models may exhibit inherent biases or limitations that affect their representation of spatial and temporal variability. The diagonal division might arise due to specific model characteristics or calibration processes. The diagonal division of zones might also reflect the inherent spatial and elevational gradients present in the modelled data.

It is essential to consider these factors when interpreting the results of spatio-temporal analysis in India. The resultant zones are further analyzed to evaluate the zone-wise mean variable vs. mean elevation trends and determine the lapse rates for each dataset using linear regression. The calculated positive lapse rates (negative rate of change) (presented in Figure 5.2) are as follows: 2.57^o/km for IMD Tmin, 2.19^o/km for IMD Tmax, 7.48^o/km for HadCM Tmin, and 6.67^o/km for HadCM Tmax. The corresponding root mean square errors (RMSE) are 1.74^o, 0.74^o, 3.06^o, and 0.81^o, respectively. The number of zones, lapse rate & RMSE for each output are presented in Table 5.2. The steep slopes in Figure 5.2 (a and b) are driven by the high elevation Himalayan zones identified in IMD data through MiSTIC. The relatively lower temperatures of the regions have resulted in steep slopes.

Comparing the modelled lapse rates to the observed data, it is noticed that the modelled lapse rates are relatively higher. This suggests that the model might be overestimating the rate of temperature decrease with increasing elevation compared to the actual observed data. The magnitude of lapse rates of modelled temperatures is in close proximity to the global average

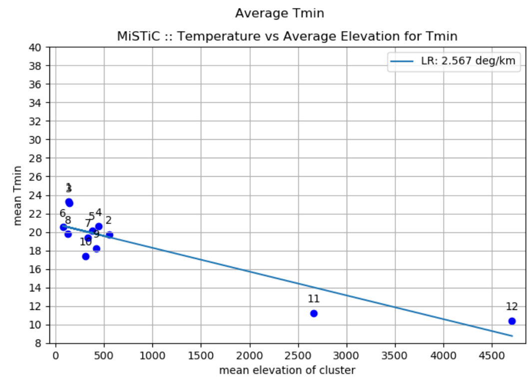

(a) IMD Tmin

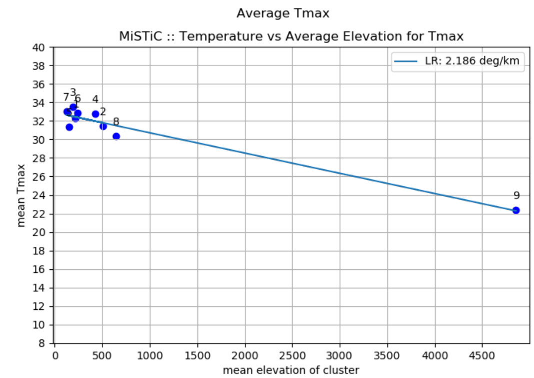

(b) IMD Tmax

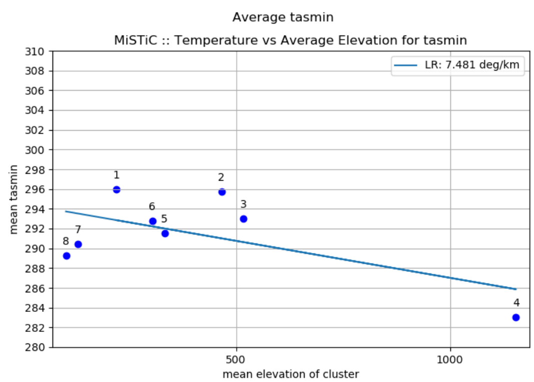

(c) HadCM Tmin

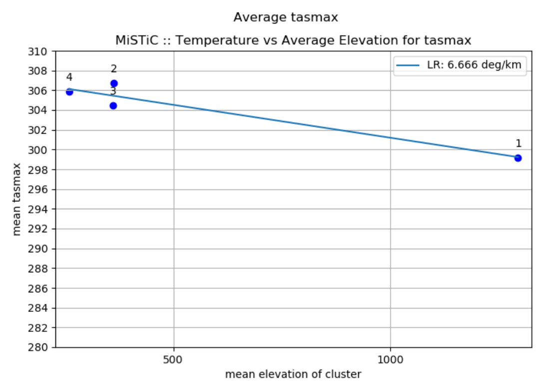

(d) HadCM Tmax

Figure 5.2: MiSTIC Zone-wise mean DTR vs mean elevation trends

environmental lapse rate of 6.5^{o}/km [60]

However, it's worth noting that the zone-wise lapse rates for each dataset closely align with the actual lapse rates presented in Section 3.4 of this study. The close agreement between the zone-wise lapse rates and the actual lapse rates from Section 3.4 indicates that the zonal trends are consistent with the overall patterns observed. This reinforces the notion that temperature changes with elevation vary across different regions, with each zone exhibiting its unique lapse rate. This consistency between the estimated change rates and the actual lapse rates adds confidence to the analysis's accuracy and validates the results' reliability.

	Num. Zones	Change rate (º/km)	RMSE (º)
IMD Tmin	12	-2.57	1.74
IMD Tmax	9	-2.19	0.74
HadCM Tmin	8	-7.48	3.06
HadCM Tmax	4	-6.68	0.81

Table 5.1: MiSTIC Number of zones, rate of change & RMSE for observed and modelled minimum and maximum Temperatures

5.2 P-MiSTIC on Observed and Modelled Data

To investigate the spatio-temporal variation and relationship between minimum and maximum temperatures in the study region, this study employs the P-MiSTIC method introduced in this research. This method is applied to the observed and modelled data to capture these temperature dynamics.

In the current P-MiSTIC analysis, the minimum and maximum temperatures are considered variables of interest, with specific weights assigned to each variable. To achieve an analysis equivalent to Diurnal Temperature Ranges (DTR), the minimum temperature is assigned a weight of -1, while the maximum temperature is assigned a weight of 1.

By incorporating the weighted minimum and maximum temperatures, the P-MiSTIC method conducts spatio-temporal analysis taking into consideration the interaction between them. This analysis enables the identification of spatio-temporal zones across the study area, providing insights into the patterns and variations in temperature dynamics over time and space.

It's important to note that this implementation of P-MiSTIC with the assigned weights allows for a comprehensive exploration of the relationship between minimum and maximum temperatures, mimicking the concept of Diurnal Temperature Ranges. This approach enhances the understanding of the temperature variations and their spatio-temporal characteristics within the study region.

The study further examines the potential influence of the agro-ecological regions of India, depicted in Figure 3.1(b), on variations in temperature through a comparison with the 11 core

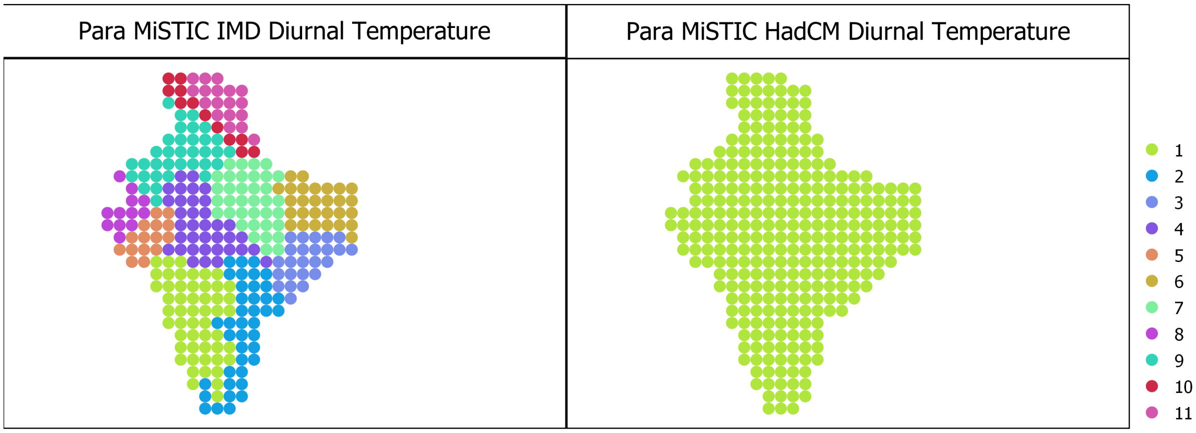

Figure 5.3: P-MiSTIC Zones identified for a) Observed (IMD) & b) Modelled (HadCM) Temperatures

regions identified from IMD data. Certain zones exhibit significant overlap with geophysical and agro-ecological zones. For instance, zone 1 predominantly encompasses the arid and semi-arid areas of the Eastern Ghats and Deccan plateau. Zone 3 includes the sub-humid Eastern Ghats, while zones 4 and 5 comprise the Central Highlands. Zone 7 covers the Northern Plains, while zones 8 and 9 span the arid Western Plains. Lastly, zones 10 and 11 cover the sub-humid and arid Western Himalayas. It is noteworthy that despite the non-inclusion of topography and agro-ecological zone knowledge for the identification of core regions, the P-MiSTIC algorithm identifies similar zones, demonstrating a proficient ability to identify spatio-temporally consistent zones. This observation illustrates the extent of temperature fluctuations within the study region.

The resultant zones for observed and modelled Temperatures are presented in Figure 5.3. The significant difference in the number of zones identified by P-MiSTIC between the observed and modelled data, with 11 zones for the observed data and only one zone with a mean diurnal temperature of 15° for the modelled data, suggests a potential discrepancy or limitation in the model's representation of the temperature patterns. This discrepancy indicates that the model might not accurately capture the spatial and temporal variability of the observed data.

Analyzing the resultant zones of the observed data further, the evaluation of zone-wise mean Diurnal Temperature Range (DTR) vs. mean elevation trends using linear regression reveals an increasing rate of 0.133°/km. The change rate and RMSE are presented in Table 5.4. This implies that the difference between daily maximum and minimum temperatures tends to widen

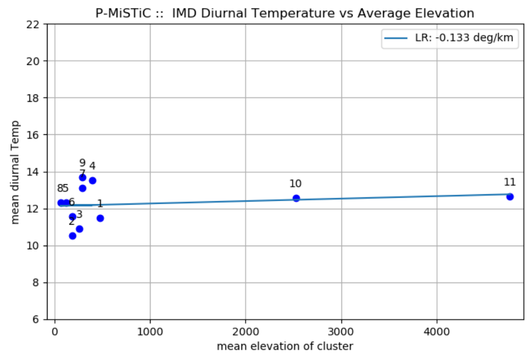

Figure 5.4: P-MiSTIC Zone-wise mean DTR vs mean elevation trends for observed Temperature

	IMD	HadCM)
Num. zones	11	1
Change Rate (°/km)	0.133	-
RMSE (°)	0.96	-

Table 5.2: P-MiSTIC Number of zones, rate of change & RMSE for observed and modelled

as elevation increases.

An increasing trend of DTR with elevation can signify important climatic and geographical characteristics in the study region. It suggests that higher elevations experience more significant temperature fluctuations between daytime and nighttime, potentially due to variations in factors such as solar radiation, cloud cover, and atmospheric stability. This finding highlights the influence of elevation on temperature dynamics and emphasizes the importance of considering elevation-dependent effects in climate studies and assessments of the study region.

These results emphasize the potential of the P-MiSTIC method, as it enables a comprehensive analysis of the observed data by identifying multiple zones with distinct temperature patterns. This highlights the capability of P-MiSTIC to capture the complexity and heterogeneity of temperature variations across the study region, which is valuable for understanding local climate dynamics.

To better understand the temporal trends exhibited by each zone, a zone-wise temporal analysis was conducted. This analysis involved estimating the change rate for the 11 zones in the observed data and the single zone in the modelled data. The temporal trends for each zone are visually represented in Figure 5.5, providing insights into the variation of temperature over time.

Additionally, the change rate statistics for each zone are presented in Table 5.5, offering quantitative information about the rate of change observed in each zone.

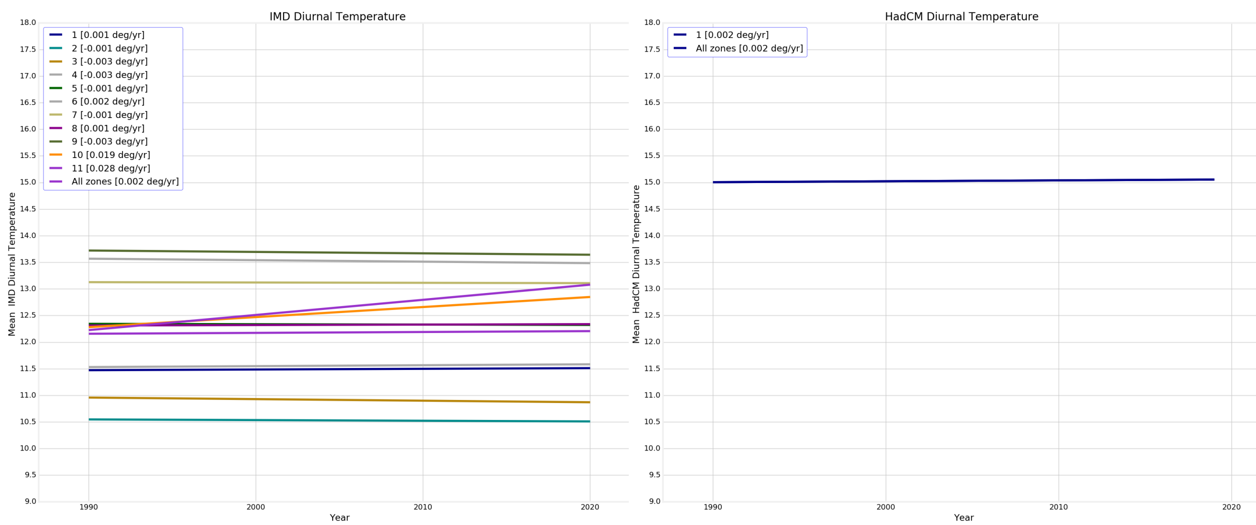

(a) IMD Temperature

(b) HadCM Temperature

Figure 5.5: P-MiSTIC Zone-wise Temporal Trends

The overall change rate of diurnal temperatures with time, calculated as 0.02°/decade, remains consistent for both the observed and modelled data. This indicates a relatively small but consistent increase in diurnal temperatures over the studied period.

The similarity in the change rates between the observed and modelled data suggests that the model captures the overall temporal trend reasonably well. The estimated change rate of 0.02°/decade signifies a gradual warming trend in diurnal temperatures over time. However, it is important to note that the specific zone-wise variations and trends, as mentioned earlier, might deviate from this overall change rate. These variations highlight the significance of considering localized factors and elevation-dependent effects on temperature patterns.

Zone	Change rate (°/decade)	RMSE (°)
Zone 1	0.01	0.056
Zone 2	-0.01	0.07
Zone 3	-0.03	0.101
Zone 4	-0.03	0.097
Zone 5	-0.01	0.097
Zone 6	0.02	0.094
Zone 7	-0.01	0.095
Zone 8	0.01	0.129
Zone 9	-0.03	0.092
Zone 10	0.19	2.606
Zone 11	0.28	1.848
All Zones	0.02	0.19

Table 5.3: P-MiSTIC Zone-wise change rate of DTR per decade for observed Temperature

Zone	Change rate (°/decade)	RMSE (°)
Zone 1	0.02	0.03

Table 5.4: P-MiSTIC Change rate of DTR per decade for modelled Temperature

The zone-wise change rates analysis reveals that for the majority of the identified zones over the 30-decade period, the change rates are statistically insignificant, indicating minimal temperature variations over time. However, two specific zones stand out: Zone 10, which corresponds to the Western Himalayan region, and Zone 11, which represents the Karakoram region.

In Zone 10 (the Western Himalayan region), a change rate of 0.19^{o}/decade is observed, indicating a noticeable increasing trend in diurnal temperatures over time. Similarly, Zone 11 (the Karakoram region) exhibits an even higher change rate of 0.28^{o}/decade. This suggests a significant warming trend in these high-elevation Himalayan zones.

The fact that the Karakoram region demonstrates a higher increase rate compared to the Western Himalayan region implies that the warming trend becomes more pronounced at higher elevations. In other words, as elevation increases, the diurnal temperatures experience a greater rate of increase.

These findings highlight the importance of considering the specific characteristics of high-elevation regions, elevation-dependent effects and the role of high-altitude regions in climate change studies. The higher warming trends observed in the Karakoram region and the Western Himalayan region suggest that these high-elevation areas are particularly vulnerable to the impacts of global warming.

Further analysis is required to gain a deeper understanding of the observed and modelled Temperature trends. By conducting decadal and seasonal analyses on both the observed and modelled data, the study aims to extract meaningful insights into the temperature trends.

Decadal analysis allows for the examination of temperature trends over each decade, providing insights into potential shifts in patterns. By analyzing the data decade by decade, it becomes possible to detect any significant trends, variations, or anomalies that may have occurred from decade to decade.

Seasonal analysis, on the other hand, focuses on understanding temperature patterns within different seasons throughout the study period. This analysis helps uncover the season-specific variations in temperature and reveals any recurring patterns or anomalies that may exist within particular seasons.

The decadal and seasonal analyses can provide a comprehensive view of temperature variations and help identify any underlying patterns or trends that may not be evident in a broader analysis. By examining temperature data at finer temporal scales, the study aims to unravel additional insights and enhance our understanding of the complex dynamics and underlying mechanisms driving temperature fluctuations. The outcomes of the decadal and seasonal analysis are presented in Chapters 6 & 7, respectively.

Chapter 6

Decadal Analysis

Decadal analysis is an approach that allows for a detailed examination of temperature trends by dividing the study period into discrete decades using P-MiSTIC. By analyzing the observed and modelled data decade-wise, it becomes possible to explore the variations, patterns, and changes in temperature over time in a more granular manner.

Through decadal analysis, the study can assess the change rates of temperature with elevation for each decade individually. This analysis provides insights into how temperature patterns have evolved at different elevations over time. By calculating the change rate of temperature with elevation for each decade, the study can identify whether there are significant variations or trends in the relationship between temperature and elevation within each decade and from decade to decade.

To enhance clarity, the dataset covering the 30-year study period will be referred to as the ”30-year dataset” in this chapter.

6.1 Decadal Analysis of Observed Data using P-MiSTIC

The decade-wise zones generated for observed (IMD) Temperature data are presented alongside the 30-year zones in Figure 6.1. Decades 1, 2, and 3 result in 12, 11, and 9 zones, respectively, indicating some variation in the identified zones over time. A significant overlap was observed in the zones identified for all four datasets, highlighting the presence of consistent regional and localized behaviour in the study region. This means that certain areas consistently exhibit similar temperature patterns across the different datasets and time periods analyzed.

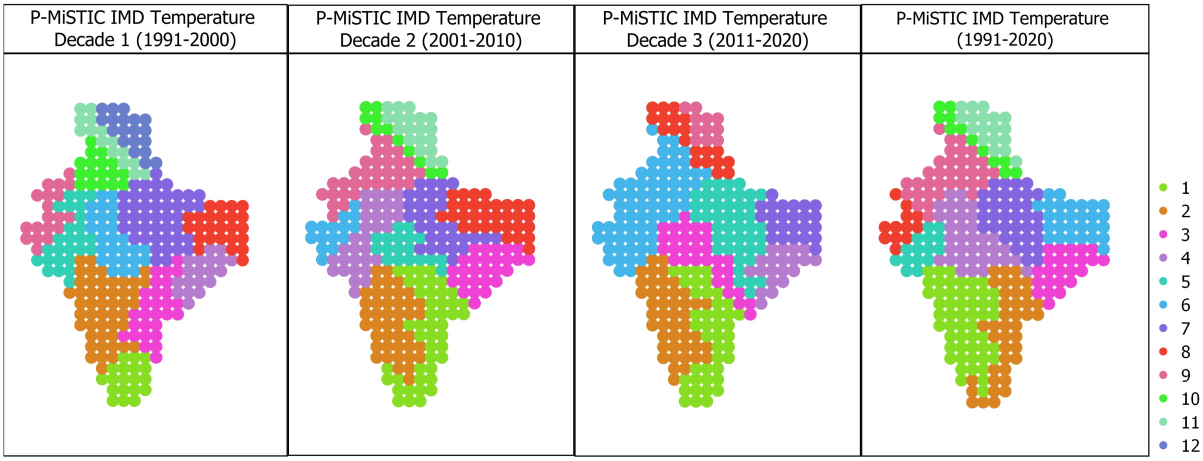

Figure 6.1: Zones identified for a) Decade-1 b) Decade-2 c) Decade-3 & d) 30-year Observed Temperature dataset

The overlap suggests that these regions have distinct characteristics that contribute to their consistent behaviour. It could be attributed to various factors such as geographical features, land use patterns, local climate dynamics, or specific micro-climatic conditions. These factors may create a unique environment that influences the temperature patterns and results in the observed overlap in the identified zones. The consistent regional behaviour suggests the presence of localized climate regimes or specific factors that influence temperature variations and contribute to the observed overlap. By studying these consistently behaving zones, this study aims to gain further insights into the localized behaviour of temperature patterns within the study region.

This study examines and compares the identified zones of the three decades with the agro-ecological zones of India. Zones identified in the decade-2 dataset are significantly similar to zones identified in the 30-year dataset compared to decades 1 and 3.

In the first decade, certain zones are found to align with the divisions of agro-ecological zones. Specifically, zone 1 overlaps with the semi-arid eastern ghats and Deccan plateau. Zone 2 encompasses portions of the western ghats and Deccan plateau. Zone 3 encompasses the Telangana Deccan plateau. Zone 4 includes the sub-humid eastern ghats and coastal plains. Central highlands are covered by zones 5 and 6. Zone 7 encompasses the sub-humid regions of the northern plains and central highlands. Sub-humid and humid areas of the northern plains, eastern plains, and eastern ghats fall within zone 8. Zone 9 covers the arid western plains. Zone 10 spans the sub-humid regions of the northern plains and parts of the western Himalayas. Zones 11 and 12 encompass the sub-humid and arid Western Himalayas, respectively.

During the third decade, zones 1 and 2 exhibit similarities to those observed in the second decade, encompassing the regions of the western coastal plains and ghats, the Deccan plateau, as well as the eastern ghats and coastal plains. Zone 3 covers the central highlands, while Zone 4 comprises the sub-humid eastern ghats and coastal plains. Zone 5 encompasses the sub-humid regions of the northern plains, central highlands, and eastern plateau. Zone 6 extends across the arid western plains, as well as portions of the semi-arid central highlands and northern plains. Zone 7 spans both sub-humid and humid areas of the northern plains, eastern plains, and eastern ghats. Lastly, Zones 8 and 9 pertain to the sub-humid and arid regions of the Western Himalayas.

A notable disparity is evident when comparing these regions to the other datasets. Zone 6 in the third decade encompasses a composite zone that includes the arid western plains, parts of the semi-arid central highlands, and the northern plains. This observation suggests that during the third decade, this zone experiences a reduction in temperature variability and exhibits a similar climate pattern. This observation is consistent with the findings of a research study on the effects of climate change on the deserts of India [62] The study highlights that the Thar desert, which constitutes the arid western plains of India, is currently witnessing a rise in precipitation. Furthermore, it is anticipated that this increase in precipitation will continue under moderate greenhouse gas (GHG) scenarios. This serves as an illustrative instance of how significant insights can be derived when the influence of preconceived zones is not incorporated as an input. Such reduction in zonal variability of temperature & the formation of larger clusters indicates homogenization of temperature over time in the zones. Furthermore, this study showcases the efficacy of P-MiSTIC in extracting impartial information while avoiding errors in the input data by employing zone delineation through neighbourhood analysis.

It is important to note that all four datasets highlight the presence of two zones within the high-elevation Himalayan region. These findings align with the findings presented in Chapter-5, which indicate that the high-elevation Himalayan zones are experiencing pronounced warming effects.

To gain a deeper understanding of the decade-wise zones and their Temperature trends, the study further evaluates the change rate of zone-wise mean Diurnal Temperature Range (DTR) with zone-wise mean elevation for each dataset. The results of this analysis are presented in Figure 6.2 & Table 6.1.

Notably, there is a shift observed from decades 1 and 2 to decade 3 in terms of the change rate of the Diurnal Temperature Range (DTR) with respect to elevation. Decades 1 and 2 exhibit negative change rates of -0.03°/km and -0.028°/km of diurnal temperature with elevation,

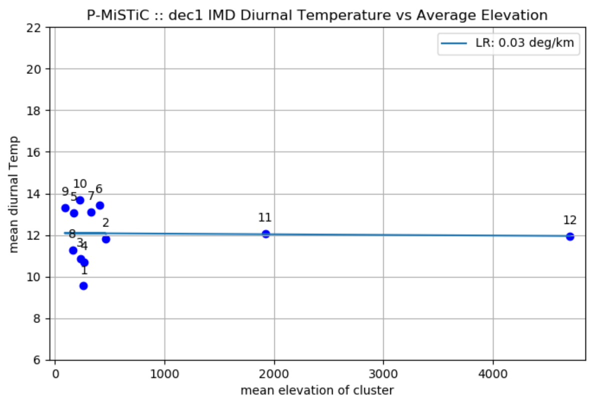

(a) Decade 1

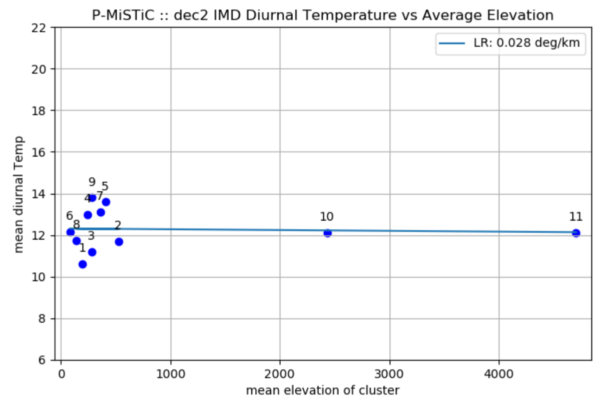

(b) Decade 2

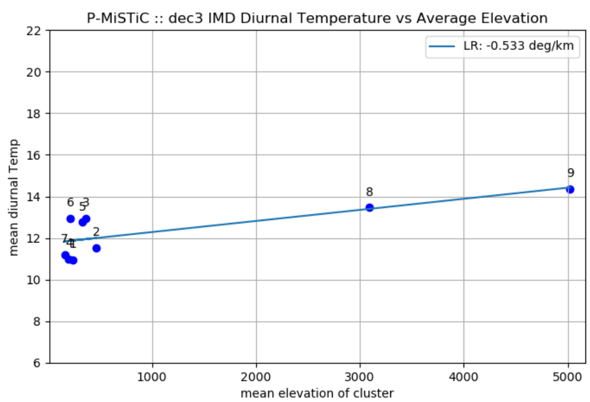

(c) Decade 3

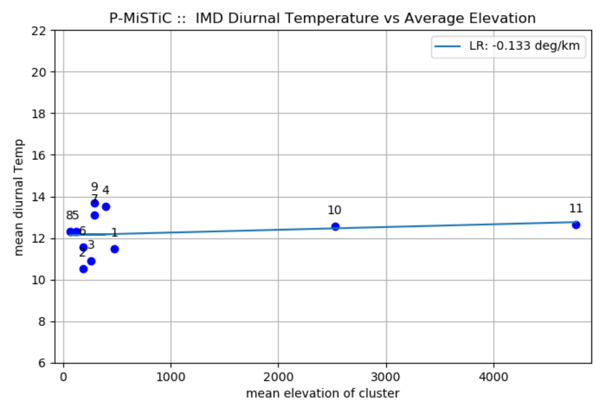

(d) 30 years

Figure 6.2: P-MiSTIC Decadal zone-wise mean DTR vs mean elevation trends for Observed data

respectively. This indicates a decreasing trend in DTR with increasing elevation during these periods. However, Decade 3 shows a significantly increasing rate of 0.533°/km of DTR with elevation. This suggests an increasing trend of DTR with elevation during this particular decade. The sudden shift in the change rate from negative values in decades 1 and 2 to a positive value in decade 3 signifies a notable change in temperature patterns. It indicates an accelerated rate of warming in the study region during the third decade.

The accelerated rate of warming indicated by the change rate in Decade 3 suggests that temperature variations become more pronounced with increasing elevation. This implies that higher elevations experienced a much larger DTR increase than lower elevations during that

	Num. Zones	Change Rate (°/km)	RMSE (°)
IMD Decade-1	12	-0.03	1.24
IMD Decade-2	11	-0.028	0.95
IMD Decade-3	9	0.533	0.75
IMD 30-year	11	0.133	0.96

Table 6.1: P-MiSTIC Decadal Zone-wise mean DTR vs mean elevation trends for Observed Temperature

particular decade. The elevated change rate may be attributed to various factors, such as changes in atmospheric circulation patterns, local climatic conditions, or interactions between climate systems.

The analysis of Figure 6.2 (c), which presents the trend for decade 3, reveals that zones 8 and 9 within this dataset are primarily driving the increasing trend of diurnal temperature with elevation. These zones correspond to the Western Himalayan region and the Karakoram region. This finding is noteworthy as it indicates that the trends observed in the high-elevation zones exert a stronger influence on the overall temperature patterns compared to the trends in other zones within the dataset. The fact that the trends in these high-elevation zones outweigh the trends in other zones within the dataset highlights the critical impact of elevation on warming trends. It indicates that the temperature variations and changes observed in the high-elevation Himalayan zones are more pronounced and influential compared to other regions.

This finding underscores the significance of elevation as a key factor contributing to temperature dynamics in the study region. Higher elevations are more exposed to factors such as changes in solar radiation, cloud cover, snow albedo, and topographic features, all of which can influence temperature patterns. The amplified warming trends in these high-elevation zones suggest that they are particularly sensitive to the effects of climate change. Quantifying the temporal rate of change for the identified zones enables the identification of zones with the highest rates of warming, which can aid in prioritizing areas for targeted climate change interventions or adaptation strategies.

The quantitative analysis of the temporal rate of change for the identified zones for each dataset is depicted in Figure 6.3 & Table 6.2.

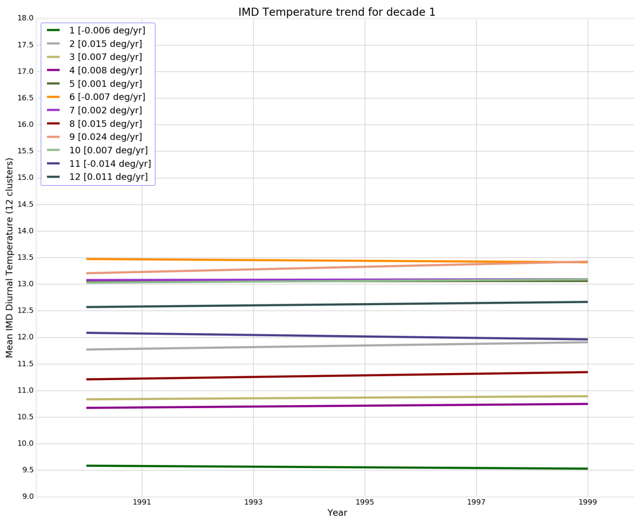

(a) Decade 1

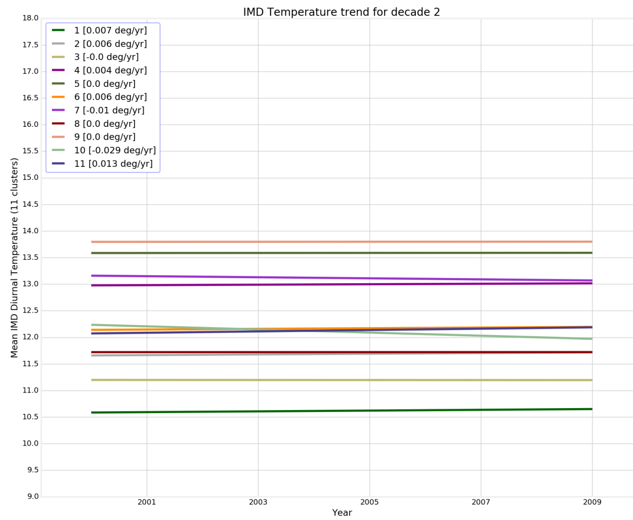

(b) Decade 2

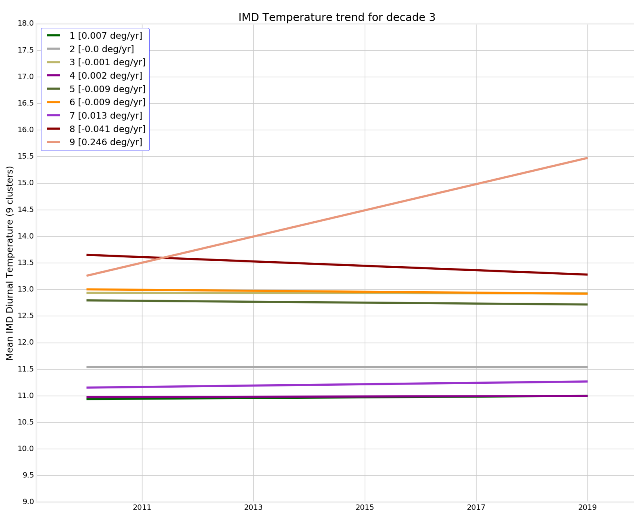

(c) Decade 3

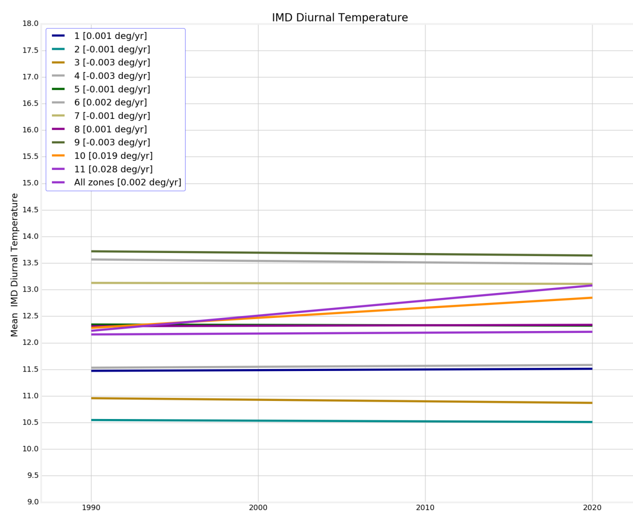

(d) 30 years

Figure 6.3: P-MiSTIC Decadal zone-wise Temporal Trends for Observed data

The observed variations in the identified zones and their change rates over the decades highlight the complex nature of temperature patterns in the high-elevation Himalayan region. The presence of distinct zones within the high-elevation Himalayas suggests that different regions

	Decade-1		Decade-2		Decade-3		30-years	
	Change rate (^{o}/decade)	RMSE (^{o})	Change rate (^{o}/decade)	RMSE (^{o})	Change rate (^{o}/decade)	RMSE (^{o})	Change rate (^{o}/decade)	RMSE (^{o})
Zone 1	-0.06	0.077	0.07	0.024	0.07	0.063	0.01	0.056
Zone 2	0.15	0.04	0.06	0.049	0	0.054	-0.01	0.07
Zone 3	0.07	0.085	0	0.099	-0.01	0.097	-0.03	0.101
Zone 4	0.08	0.056	0.04	0.057	0.02	0.095	-0.003	0.097
Zone 5	0.01	0.074	0	0.094	-0.09	0.082	-0.001	0.097
Zone 6	-0.07	0.06	0.06	0.083	-0.09	0.027	0.002	0.094
Zone 7	0.02	0.106	-0.1	0.057	0.13	0.087	-0.001	0.095
Zone 8	0.15	0.089	0	0.047	-0.41	2.562	0.001	0.129
Zone 9	0.24	0.106	0	0.07	2.46	3.17	-0.003	0.092
Zone 10	0.07	0.139	-0.29	0.192	-	-	0.019	2.606
Zone 11	-0.14	0.092	0.13	0.116	-	-	0.028	1.848
Zone 12	0.11	0.114	-	-	-	-	-	-

Table 6.2: P-MiSTIC Decadal zone-wise change rate of DTR per decade for observed Temperature

within this area exhibit unique characteristics and temperature trends.

The decreasing trends observed in the Western Himalayan region over the three decades (-0.14^o/decade, -0.29^o/decade, and -0.41^o/decade for decades 1, 2, and 3) indicate a cooling trend in this specific zone. In contrast, the Karakoram region shows increasing trends in all three decades (0.11^o/decade, 0.13^o/decade, and 2.46^o/decade). This indicates a warming trend in this zone over time. The significant increase in the third decade aligns with the sharp shift observed in Figure 6.2 and Table 6.1. The higher rate of warming in the Karakoram region compared to other zones suggests that this region is experiencing more pronounced temperature changes.

The presence of two additional zones (zone 2 and zone 8 of decade 1) displaying increasing trends of 0.15^o/decade through decade 1 (1991-2000) indicates localized variations within the study region. However, it is noteworthy that these rates of increase are not observed in the later decades. Various factors, including natural climate variability, local-scale effects, pacific decadal oscillations, or uncertainties, may be attributed to this trend.

6.2 Decadal Analysis of Modelled Data using P-MiSTIC

The decade-wise zones generated for modelled (HadCM) Temperature data are presented alongside the 30-year zones in Figure 6.4.

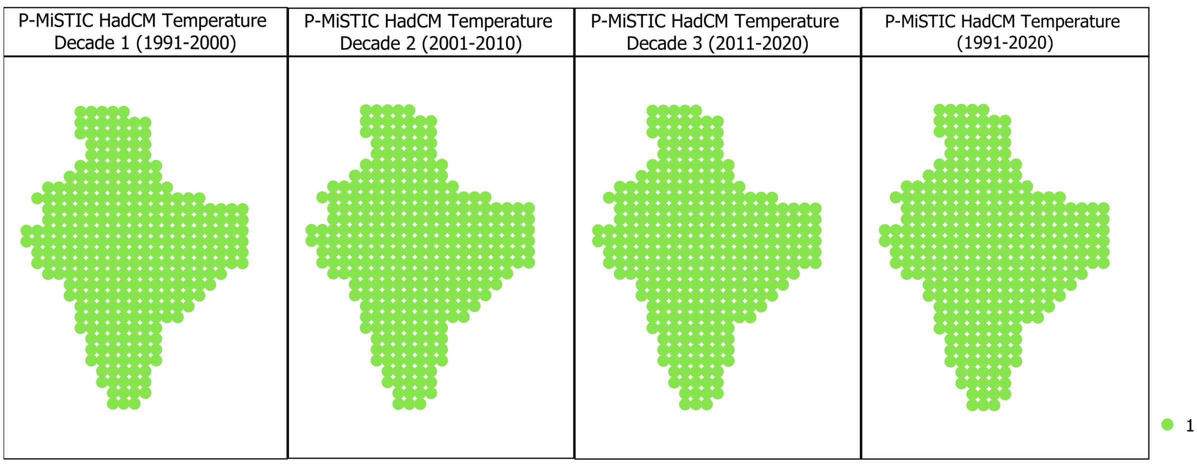

Figure 6.4: Zones identified for a) Decade-1 b) Decade-2 c) Decade-3 & d) 30-year Modelled Temperature dataset

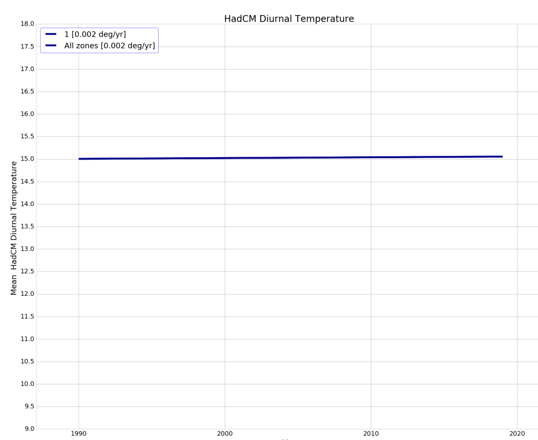

Figure 6.5: P-MiSTIC Decadal zone-wise Temporal Trends for Modelled data

The decadal analysis carried out on the modelled data using P-MiSTIC has resulted in only one zone for all the datasets, which denotes a significant difference compared to the observed data. This finding suggests that the diurnal temperature from modelled data, as represented by P-MiSTIC, exhibits a relatively uniform diurnal temperature pattern across the study region

	Deacde 1		Decade 2		Decade 3		30-years	
	Change rate (^{o}/decade)	**RMSE (^{o})**	**Change rate (^{o}/decade)**	**RMSE (^{o})**	**Change rate (^{o}/decade)**	**RMSE (^{o})**	**Change rate (^{o}/decade)**	**RMSE (^{o})**
Zone 1	0.02	0.022	0.02	0.037	0.02	0.054	0.02	0.03

Table 6.3: P-MiSTIC Change rate of DTR per decade for modelled Temperature

throughout the decades.

The presence of only one zone implies that the model employs uniform spatial variability to both minimum and maximum temperatures at the decade level. This could be attributed to various factors, such as the limitations of the model in representing the complex interactions between various climatic processes or the coarse spatial resolution of the model itself.

In Chapter 5, Section 1 of the study, the analysis of the modelled data for minimum and maximum temperatures using MiSTIC reveals some spatio-temporal variability within these datasets. This suggests that the model captures specific patterns and variations in temperature for these variables. However, when using P-MiSTIC to analyze the modelled data specifically for diurnal temperatures, minimal to negligible variability is observed.

To further explore the characteristics of diurnal temperatures, the authors conducted an investigation into seasonal variability to uncover potential fluctuations in diurnal temperature patterns throughout different seasons. The results are presented in Chapter 7, section 2 of this study.

Chapter 7

Seasonal Analysis

Seasonal analysis allows for a detailed examination of temperature patterns and variations within different seasons throughout the study period. By analyzing observed and modelled data season-wise, it becomes possible to explore the distinct characteristics and changes in temperature within seasons. This provides a more nuanced understanding of how temperature changes within the study region are influenced by seasonal factors.

The seasonal analysis also enables the assessment of the change rate of temperature with elevation for each season individually & helps quantify the rate at which temperature changes with increasing elevation within specific seasons. By examining how temperatures change within each zone across different seasons, the analysis can identify any season-specific patterns, trends, or variations in temperature within the identified zones.

By conducting seasonal analysis on observed and modelled data, it is possible to compare the temperature patterns and variations between the two datasets for each season. The authors believe that this comparison helps assess the model's ability to capture the seasonal dynamics of temperature and provides insights into the reliability and accuracy of the model's outputs.

The seasons are divided as DJF (December-January-February), MAM (March-April-May), JJA (June-July-August) & SON (September-October-November) for the analysis presented in this chapter.

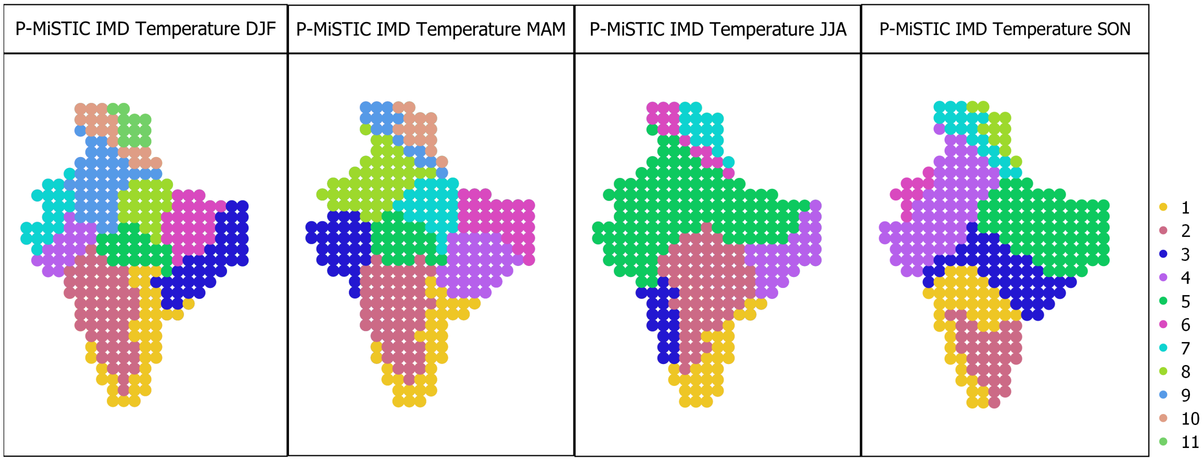

Figure 7.1: P-MiSTIC Zones identified for seasons a) DJF b) MAM c) JJA & d) SON of Observed Temperature dataset

7.1 Seasonal Analysis of Observed Data using P-MiSTIC

The analysis of the observed data for seasons DJF, MAM, JJA, and SON has resulted in different numbers of zones for each season. Specifically, there are 11 zones identified for DJF, 10 zones for MAM, 7 zones for JJA, and 8 zones for SON.

This varied number of zones across seasons suggests variations in temperature patterns and spatial characteristics during different seasons of the year. Each season exhibits its own distinct zones, indicating unique temperature dynamics within those periods.

The differences in the number of zones among seasons may be attributed to various factors. Seasonal variations in weather patterns, atmospheric conditions, and regional climatic influences can contribute to the emergence of distinct temperature patterns within each season. Additionally, factors such as local topography, vegetation cover, and land use may also influence the formation of specific temperature zones during different seasons.

This study examines the identified zones of the four seasons and compares them to the agro-ecological zones of India. The presence of distinct regional climates in the study region during various seasons is apparent. During the DJF season, Zone 1 encompasses the semi-arid Eastern Ghats and coastal plains. Zone 2 overlaps with the semi-arid Western Ghats and Deccan Plateau. Zone 3 corresponds to the sub-humid Eastern Plateau and Ghats. Zone 5 aligns with the Central Highlands. Zones 10 and 11 cover the sub-humid and arid Western Himalayas. In

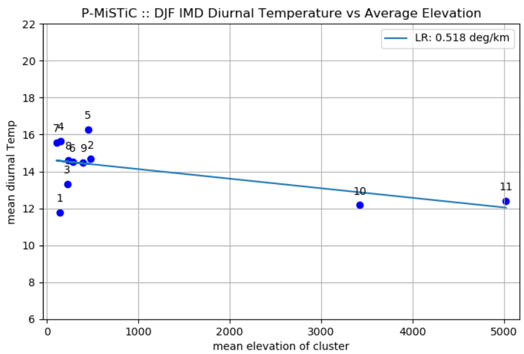

(a) DJF

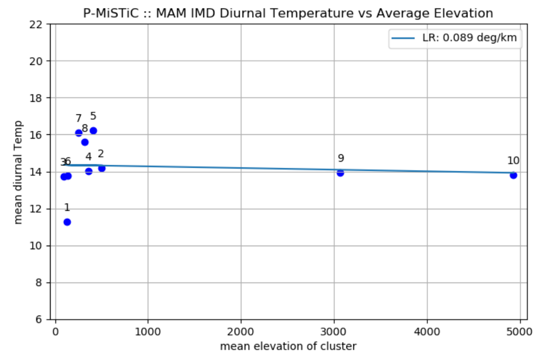

(b) MAM

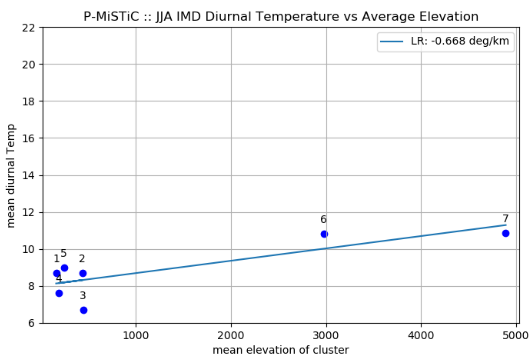

(c) JJA

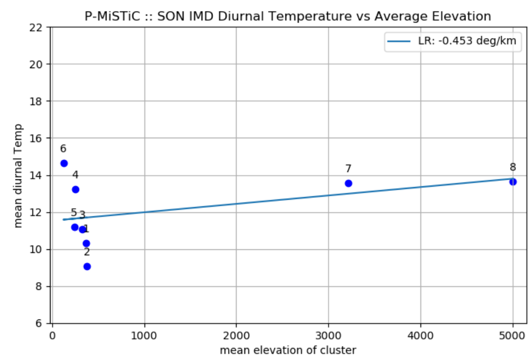

(d) SON

Figure 7.2: P-MiSTIC Seasonal zone-wise DTR trends with Elevation for Observed Data

the MAM season, Zone 1 encompasses the semi-arid Eastern Ghats and coastal plains. Zone 2, on the other hand, coincides with the semi-arid Western Ghats and Deccan Plateau. Zones 9 and 10 seem to be defined by the sub-humid and arid the Western Himalayas. The remaining zones demonstrate minimal overlap with any individual or combined agro-ecological zones. In the JJA season, Zone 1 consists of the semi-arid Eastern Ghats and coastal plains. Zone 2 overlaps with the Deccan Plateau. Zone 3 encompasses the Western Ghats and coastal plains. Zone 5 is a substantial region that spans across arid, semi-arid, and sub-humid areas in northern India. Zones 6 and 7 represent the sub-humid and arid Western Himalayas. In the season SON, the geographical distribution of zones is as follows: zone 1 encompasses the agro-ecological zone of semi-arid eastern ghats and Deccan plateau; Zone 2 primarily encompasses the central Deccan plateau, as well as the western ghats and coastal plains; zone 4 covers the semi-arid regions of western and northern India; zone 5 encompasses the sub-humid areas of northern India; and zone 6 represents a portion of the arid western plains. This suggests that within the arid western plains, there may be distinct variations in patterns between the western and eastern parts during this season. The western Himalayas are encompassed by zones 7 and 8.

It is important to note that all four datasets highlight the presence of two zones within the high-elevation Himalayan region. These findings re-iterate & align with the findings presented in Chapters 5 & 6, which indicate that the high-elevation Himalayan zones are experiencing pronounced warming effects.

The study delves deeper into the season-wise zones and their associated temperature trends by examining the change rate of the zone-wise mean Diurnal Temperature Range (DTR) with the zone-wise mean elevation for each dataset. This analysis provides insights into how the DTR varies with changes in elevation within specific zones over various seasons over the study period.

Figure 7.2 visually represents the trends of the zone-wise mean DTR with respect to the zone-wise mean elevation for each dataset. And Table 7.1 presents the numerical values of the change rates, providing quantitative information on how the DTR changes with elevation for the respective seasons.

	Num. zones	**Change rate (°/km)**	**RMSE**
IMD DJF	11	-0.518	1.19
IMD MAM	10	-0.089	1.36
IMD JJA	7	0.668	0.83
IMD SON	8	0.453	1.65

Table 7.1: P-MiSTIC Seasonal Zone-wise mean DTR vs mean elevation trends for observed Temperature

The analysis of the observed diurnal temperature trends with elevation has revealed a cyclic pattern. In particular, the seasonal breakdown shows distinct trends for each season. During the DJF season, a strong decreasing trend of -0.518°/km is observed, indicating a decrease in the diurnal temperature range with increasing elevation. In contrast, the MAM season exhibits a comparatively insignificant decreasing trend at -0.089°/km. However, during the JJA season, the most robust increasing trend of 0.668°/km is observed, indicating an increase in the diurnal temperature range with elevation. Further, in the SON season, the rate of increase is significant at 0.453°/km but is lower than that of JJA.

These findings provide additional insights into the spatio-temporal dynamics of diurnal temperature patterns across different seasons. The cyclic nature of the observed trends suggests that the relationship between diurnal temperature range and elevation is not constant throughout the year. Instead, it varies seasonally, indicating the influence of season-specific climatic processes and atmospheric conditions on localized temperature patterns.

By analyzing the temporal trends within each zone, the study aims to delve deeper into the underlying mechanisms that drive the observed cyclic patterns in diurnal temperature variations with elevation. It allows for the identification of zone-specific temperature dynamics, such as areas experiencing amplified temperature changes with increasing elevation during specific seasons, providing valuable insights into the micro-scale temperature patterns and their relationship with elevation.

By conducting further zone-wise temporal trend analysis, the study can uncover additional patterns and variations that may not be apparent in the overall trends. The zone-wise temporal trends for four seasons have been depicted in Figure 7.3 & Table 7.2.

The analysis of the season-wide mean Diurnal Temperature Range (DTR) trends with elevation, as depicted in Figure 7.2, reveals interesting patterns for the JJA and SON seasons. Specifically, a sharp fall in the mean diurnal temperatures is observed in the identified zones during the JJA (summer) season. This suggests a decrease in the temperature difference between day and night during the JJA season within these zones. On the other hand, a gradual increase in the mean diurnal temperature is observed in the identified zones during the SON (autumn) season. This indicates an increase in the temperature difference between day and night during the SON season within these zones.

This finding suggests that the diurnal temperatures within the identified zones reach their minimum levels during the summer season (JJA). This phenomenon contradicts the common expectation of higher temperatures during the summer months. The sharp fall in diurnal temperatures during JJA indicates a specific climatic behaviour within the study region.

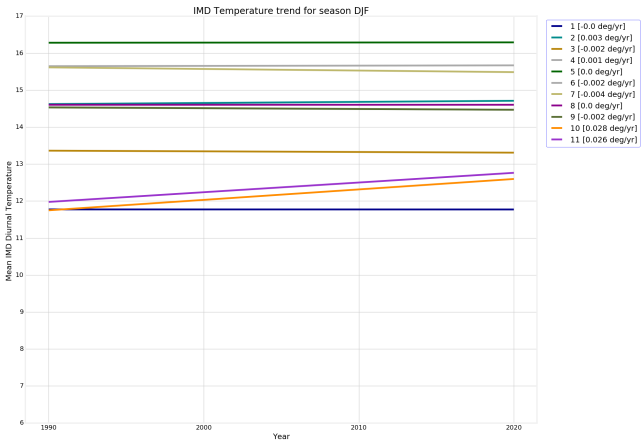

(a) DJF

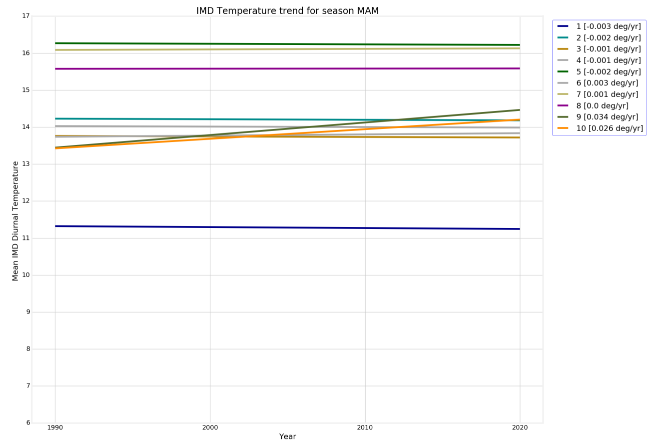

(b) MAM

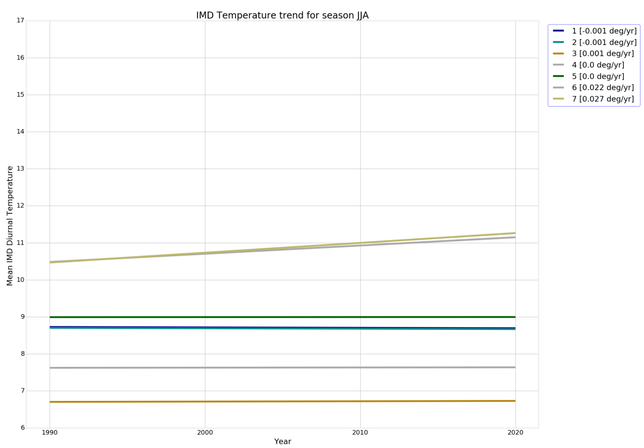

(c) JJA

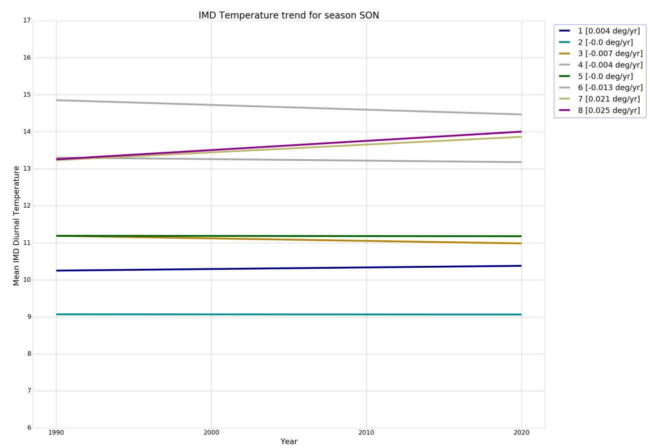

(d) SON

Figure 7.3: P-MiSTIC Seasonal zone-wise Temporal Trends for Observed Data

The observed trend of decreasing diurnal temperatures during the summer season could be attributed to several factors. One possible explanation is the influence of local climatic processes, such as the presence of cloud cover, increased rainfall, or specific atmospheric conditions that result in a cooling effect during JJA. Additionally, other factors like elevation, vegetation cover, or topography within the identified zones may contribute to this temperature behaviour.

On the other hand, the gradual increase in diurnal temperatures during the SON season suggests a transition towards higher temperatures after the summer months. This shift in temperature patterns aligns with the changing seasons and highlights the dynamic nature of temperature

	DJF		MAM		JJA		SON	
	Change rate (º/decade)	**RMSE (º)**	**Change rate (º/decade)**	**RMSE (º)**	**Change rate (º/decade)**	**RMSE (º)**	**Change rate (º/decade)**	**RMSE (º)**
Zone 1	0	0.106	-0.03	0.082	-0.01	0.058	0.04	0.101
Zone 2	0.03	0.118	-0.02	0.061	-0.01	0.087	0	0.091
Zone 3	-0.02	0.128	-0.01	0.083	0.01	0.12	-0.07	0.15
Zone 4	0.01	0.12	-0.01	0.087	0	0.089	-0.04	0.093
Zone 5	0	0.174	-0.02	0.112	0	0.055	0	0.086
Zone 6	-0.02	0.183	0.03	0.129	0.22	2.607	-0.13	0.454
Zone 7	-0.04	0.123	0.01	0.137	0.27	1.403	0.21	2.062
Zone 8	0	0.199	0	0.091	-	-	0.25	2.048
Zone 9	-0.02	0.14	0.34	2.63	-	-	-	-
Zone 10	0.28	2.652	0.26	1.668	-	-	-	-
Zone 11	0.26	2.383	-	-	-	-	-	-

Table 7.2: P-MiSTIC Seasonal zone-wise change rate of DTR per decade for observed Temperature

variations within the study region.

The analysis reveals interesting patterns in the diurnal temperature trends, particularly of the Himalayan zones, particularly in the JJA and MAM seasons. It is observed that the diurnal temperatures in the Himalayan zones reach their minimum levels during the JJA season and their maximum levels during the MAM season. However, the diurnal temperatures exhibit the most significant rate of increase in the JJA season.

The Western Himalayan region exhibits an increasing trend in diurnal temperatures for all seasons, with rates of 0.28, 0.34, 0.22, and 0.21 for DJF, MAM, JJA, and SON, respectively. This suggests a cyclic trend in which the maximum increase occurs during the MAM season, while the minimum increase occurs during the SON season. On the other hand, the Karakoram region shows a uniform increasing trend in diurnal temperatures across all seasons, with rates of 0.26, 0.26, 0.27, and 0.25 for seasons DJF, MAM, JJA, and SON, respectively.

These findings align with the earlier results presented in Chapter 5, section 2, where an increase rate of 0.28 was estimated for the Karakoram region using P-MiSTIC for the entire study period. The consistent and uniform rate of increase in diurnal temperatures in the Karakoram region, as well as the cyclic trend observed in the Western Himalayan region, may be underlying factors contributing to the consistent identification of these zones across various datasets using P-MiSTIC.

This demonstrates the capability of P-MiSTIC to identify and capture such spatio-temporal characteristics, highlighting its effectiveness in detecting and characterizing temperature patterns within specific zones.

7.2 Seasonal Analysis of Modelled Data using P-MiSTIC

The season-wise zones generated for modelled (HadCM) Temperature data are presented in Figure 7.4

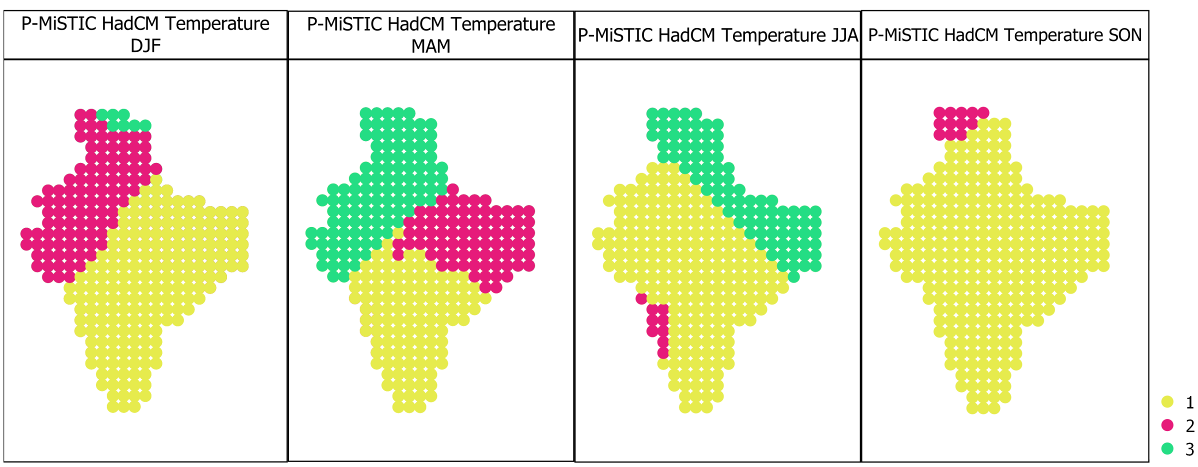

Figure 7.4: P-MiSTIC Zones identified for seasons a) DJF b) MAM c) JJA & d) SON of Modelled Temperature dataset

The implementation of P-MiSTIC on seasonal datasets has resulted in the identification of multiple zones, unlike the single zone observed in the decadal and 30-year datasets. Specifically, three zones were identified for the DJF, MAM, and JJA seasons, while two zones were identified for the SON season. This suggests that there is some level of spatial variability at the seasonal scale within the modelled data.

Interestingly, despite the spatial variability observed at the seasonal scale, the analysis of all seasons combined neutralizes this variability, resulting in the identification of a single zone. This implies that when the data from different seasons are analyzed collectively, the spatial differences between the zones become less pronounced or are averaged out.

Furthermore, the observation of diagonal separation in the identified zones aligns with the diagonal separation of zones observed in Chapter 5, section 1, where the zones identified for minimum and maximum modelled temperatures using MiSTIC were presented in Figure 5.1. This similarity in the diagonal separation pattern suggests a consistent spatial pattern across different analyses and datasets. It further supports the notion that there may be underlying factors or processes contributing to this spatial distribution, which result in diagonally separated zones in both observed and modelled datasets.

With some spatial variability, the authors continue to study the modelled data trends further with zone-wise diurnal temperature trends with elevation, the results of which are depicted in Figure 7.5. The number of zones, change rate and RMSE, are depicted in Table 7.3.

	Num. Zones	**Change rate (^{o}/km)**	**RMSE (^{o})**
HadCM DJF	3	-0.539	0.932
HadCM MAM	3	0.451	2.32
HadCM JJA	3	4.689	1.946
HadCM SON	2	1.737	0

Table 7.3: P-MiSTIC Seasonal Zone-wise mean DTR vs mean elevation trends for modelled Temperature

Despite the number and nature of zones identified in seasonal analysis using P-MiSTIC for modelled data, the zone-wise diurnal temperature trends with zone-wise mean elevation introduce new insights into the modelled data. The diurnal temperatures have exhibited a change rate of -0.539^o/km, 0.451^o/km, 4.689^o/km and 1.737^o/km for DJF, MAM, JJA and SON seasons respectively. The cyclic nature of this trend over the four seasons is in alignment with the cyclic nature of diurnal temperatures with elevation in observed data depicted in Figure 7.3 & Table 7.2.

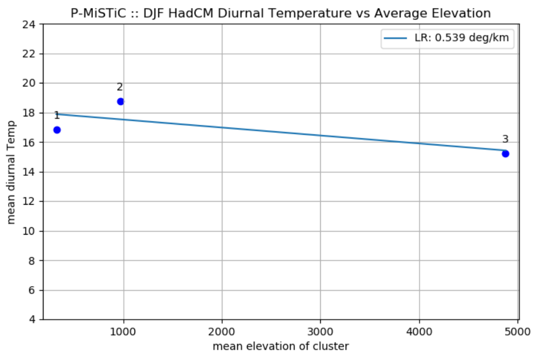

(a) DJF

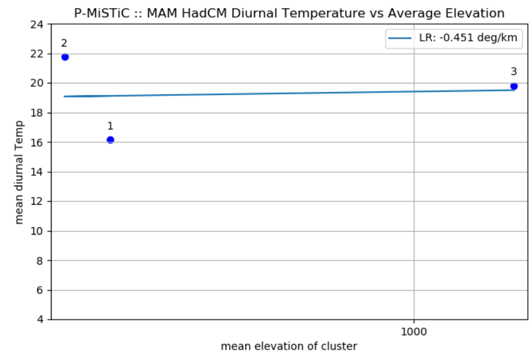

(b) MAM

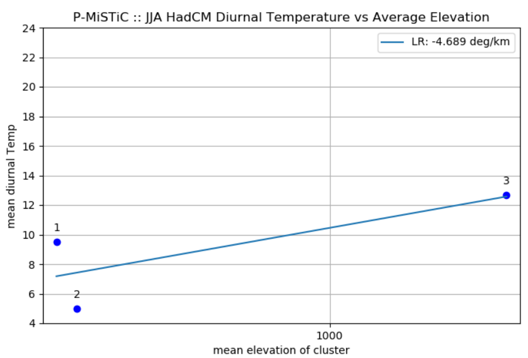

(c) JJA

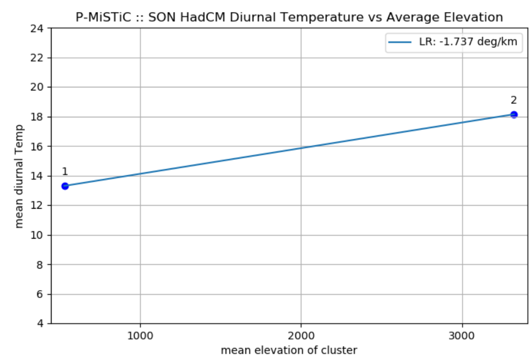

(d) SON

Figure 7.5: P-MiSTIC Seasonal zone-wise DTR trends with Elevation for Modelled Data

The analysis of zone-wise diurnal temperature trends with zone-wise mean elevation in the seasonal analysis using P-MiSTIC for the modelled data has revealed intriguing insight. In the DJF season, there is a notable decrease in diurnal temperatures with increasing elevation, with a change rate of -0.539°/km. This suggests a cooling effect as elevation increases during this season. In contrast, during the MAM season, there is an increasing trend in diurnal temperatures with elevation, with a change rate of 0.451°/km. This indicates a warming effect as elevation increases in this season. The JJA season exhibits the most significant increase in diurnal temperatures with elevation, with a change rate of 4.689°/km. This suggests a strong warming effect associated with higher elevations during this season. Lastly, the SON season shows a moderate increase in diurnal temperatures with elevation, with a change rate of 1.737°/km. This indicates a less pronounced but still noticeable warming effect with increasing elevation during this season.

Notably, the cyclic nature observed in the diurnal temperature trends with elevation for the modelled data across the four seasons aligns with the cyclic nature observed in the diurnal temperatures with elevation for the observed data, as depicted in Figure 7.2 and Table 7.1. This consistency reinforces the patterns observed in the observed data and suggests that the modelled data is capturing similar temperature dynamics.

To investigate whether the season-wise alignment observed in the cyclic diurnal temperature trends with elevation continues to the zone-wise temporal trends of the modelled data, the authors conducted a zone-wise temporal trend analysis on the identified zones for each of the four seasons. This analysis aimed to assess if the cyclic patterns observed in the observed data, as depicted in Figure 7.3 and Table 7.2, extend to the temporal trends of the modelled data within each zone.

By analyzing the zone-wise temporal trends, the study sought to examine whether the cyclic nature observed in the diurnal temperature trends of the observed data is also present in the modelled data and whether it persists across the different identified zones for each season. The results of this zone-wise temporal trend analysis, along with corresponding statistics, are presented in Figure 7.6 & Table 7.5.

	DJF		**MAM**		**JJA**		**SON**	
	Change rate (^{o}/decade)	**RMSE (^{o})**	**Change rate (^{o}/decade)**	**RMSE (^{o})**	**Change rate (^{o}/decade)**	**RMSE (^{o})**	**Change rate (^{o}/decade)**	**RMSE (^{o})**
Zone 1	-0.04	0.103	0.02	0.055	0	0.077	0.01	0.117
Zone 2	-0.04	0.152	0.05	0.11	-0.13	0.192	0.14	0.7
Zone 3	-0.07	0.497	0.01	0.09	0.02	0.16	-	-

Table 7.4: P-MiSTIC Seasonal zone-wise change rate of DTR per decade for modelled Temperature

In the zone-wise temporal trends of the seasonal modelled data, a cyclic pattern similar to the observed data is observed, as depicted in Figure 7.6. However, due to the lack of similarity between the identified zones for the observed and modelled data, it is not possible to directly correlate the zone-wise trends.

The zone-wise temporal trends in the modelled data show generally insignificant change rates ranging from -0.07^o/decade to 0.05^o/decade. These minute changes indicate minimal or

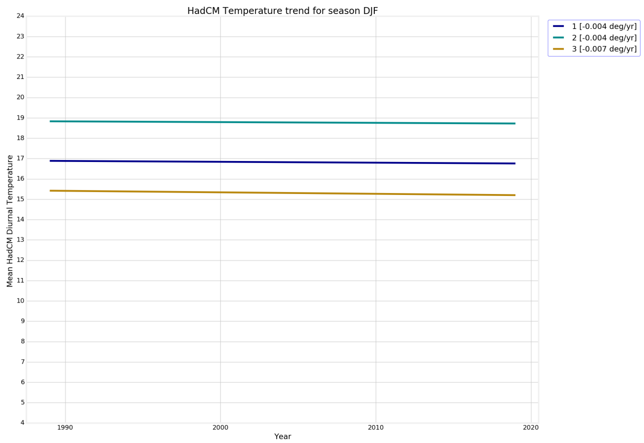

(a) DJF

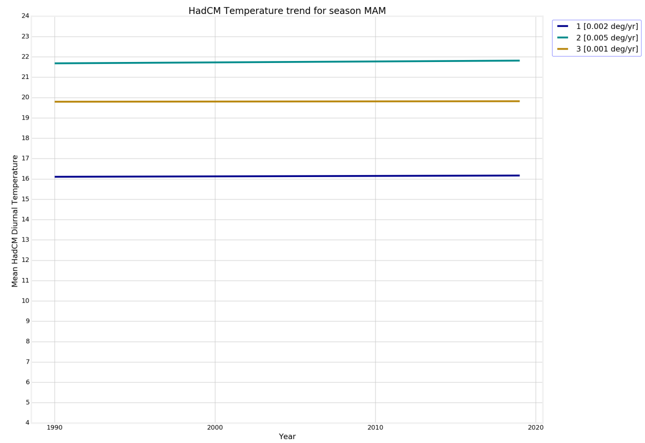

(b) MAM

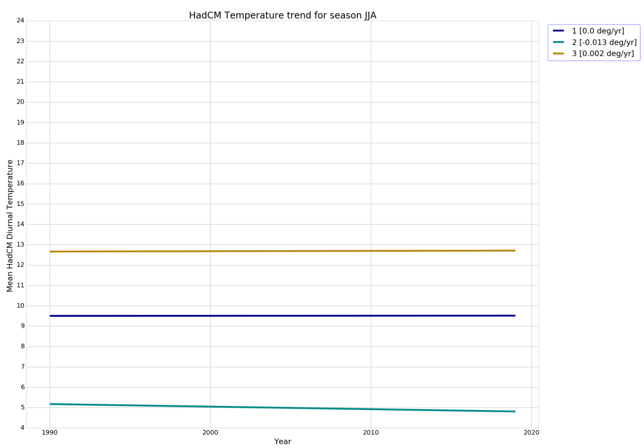

(c) JJA

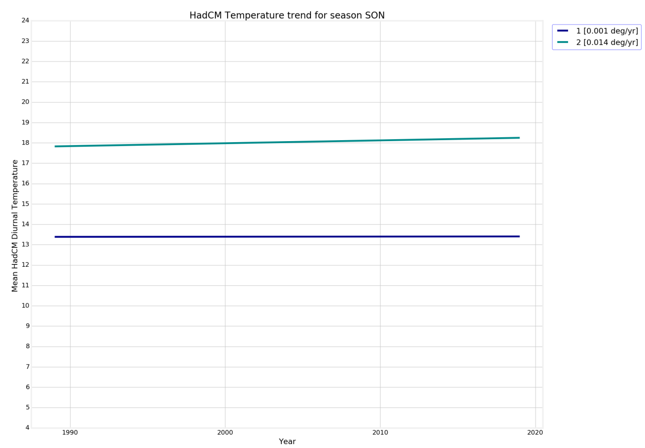

(d) SON

Figure 7.6: P-MiSTIC Seasonal zone-wise Temporal Trends for Modelled Data

negligible changes in diurnal temperature patterns within each zone over time.

However, in the SON season, where a part of the Himalayan region has been identified as a zone, there is an increasing temporal trend of 0.14^{o}/decade. This suggests that the modelled data partially captures the high elevation characteristics during the SON season. However, it should be noted that this consistency in trends is not carried on to the other seasons, where the overall change rates remain relatively small and insignificant.

The findings indicate that while the modelled data exhibit some degree of alignment with the observed cyclic patterns and trends in diurnal temperatures, especially during the SON season, it does not consistently capture the same trends across all seasons or over the study period. This may suggest that there are certain limitations or discrepancies in the model's representation of the temporal dynamics within the identified zones for different seasons.

7.3 Seasonal Analysis of Decade 3 Observed Data using P-MiSTIC

The authors further delve into the dataset to analyze the seasonal trends of decade-3 observed temperature data since decade-3 has exhibited a significant shift in trends, as explained in Chapter 6. The zones identified for the four seasons are presented in Figure 7.7. For seasons DJF, MAM, JJA, and SON, P-MiSTIC identified 10, 10, 10 and 9 zones, respectively.

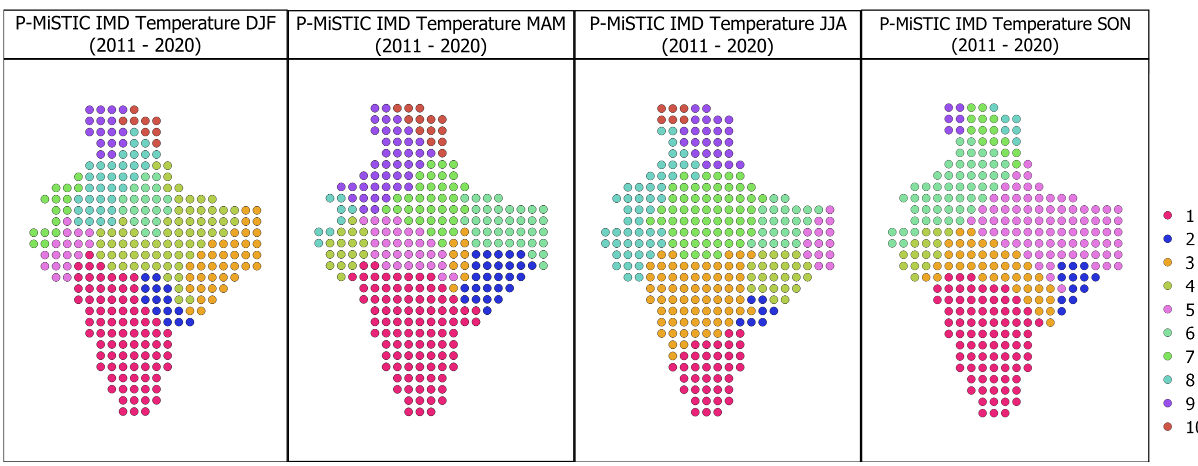

Figure 7.7: P-MiSTIC Zones identified for seasons a) DJF b) MAM c) JJA & d) SON of Decade-3 Observed Temperature dataset

A considerable shift in the zonal boundaries is observed between seasons, with some zones of one season merging into a single zone in another season. The Himalayan zones are identified in all the seasons. However, in MAM, the Western Himalayas and part of the desert are identified as a single zone. In JJA, the central highlands of Gujarat join the desert, while the Himalayan regions are identified distinctly. In SON, fragmented zones are found in the Himalayan region, whereas larger zones are found in the rest of the study region, hinting that the Himalayan region could be experiencing different dynamics and respond differently to temperature variations. It has been observed in some zones that the zonal boundaries are more or less similar in 3 out of 4 seasons. For example, the southern Peninsula and the central highlands of Gujarat are similar in DJF, MAM and SON but distinct in JJA. This strongly indicates that the temperature-based regions vary significantly over seasons, which can be identified only through data-driven zoning analysis without any external zone information to avoid bias.

The study delves deeper into the season-wise zones and their associated temperature trends by examining the change rate of the zone-wise mean Diurnal Temperature Range (DTR) with the zone-wise mean elevation for each dataset. This analysis provides insights into how the DTR varies with changes in elevation within specific zones over various seasons over the study period.

Figure 7.8 visually represents the trends of the zone-wise mean DTR with respect to the zone-wise mean elevation for each dataset. Table 7.5 presents the numerical values of the change rates, providing quantitative information on how the DTR changes with elevation for the respective seasons.

	Num. zones	**Change rate (^{o}/km)**	**RMSE**
IMD DJF	10	0.196	0.85
IMD MAM	10	0.172	0.82
IMD JJA	10	0.478	1.25
IMD SON	9	0.185	0.80

Table 7.5: P-MiSTIC Seasonal Zone-wise mean DTR vs mean elevation trends for observed Temperature

The DJF, MAM, and SON seasons present nearly the same rate of increase in DTR with elevation at 0.196^o/yr, 0.172^o/yr and 0.185^o/km. Although, season JJA exhibits a significant increasing trend of DTR with elevation at 0.478^o/km. But this does not subvert that the observed diurnal temperature is increasing with elevation in all the seasons of decade 3, implying that the difference between minimum and maximum temperatures is widening significantly. This highlights the intricate nature of localized temperature patterns and re-iterates that the DTR trends with elevation vary at the seasonal scale.

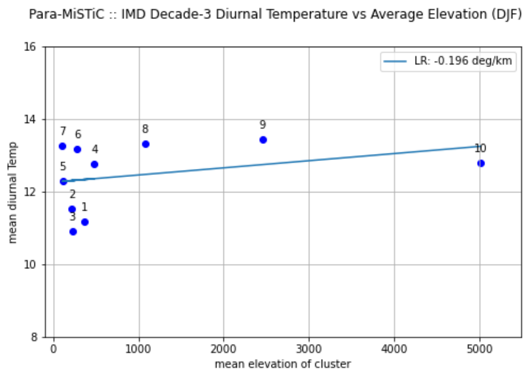

(a) DJF

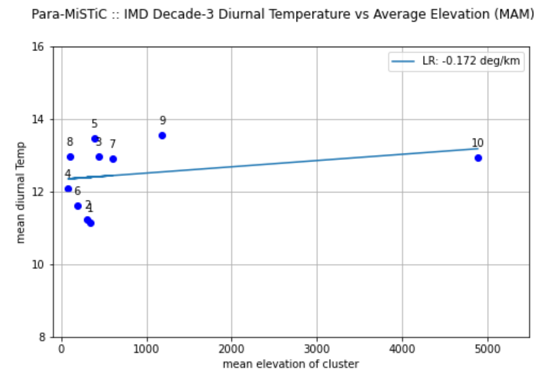

(b) MAM

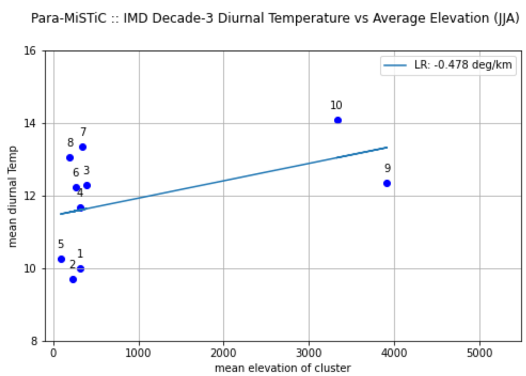

(c) JJA

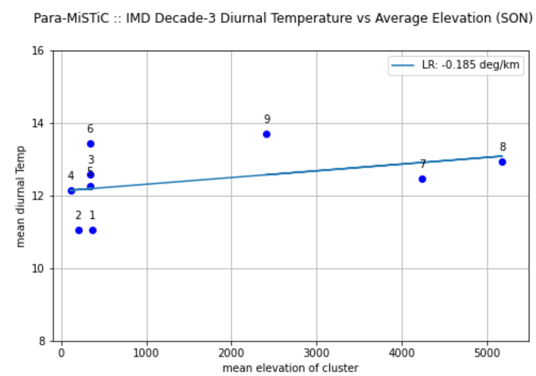

(d) SON

Figure 7.8: P-MiSTIC Seasonal zone-wise DTR trends with Elevation for Decade-3 Observed Data

By analyzing the temporal trends within each zone, the study aims to delve deeper into the underlying mechanisms that drive the observed patterns in diurnal temperature variations with elevation. It allows for the identification of zone-specific temperature dynamics, such as areas experiencing amplified temperature changes during specific seasons, providing valuable insights into the micro-scale temperature patterns. The zone-wise temporal trends for four seasons have been depicted in Figure 7.9 & Table 7.6.

The analysis of the decade-3 seasonal mean Diurnal Temperature Range (DTR) temporal trends, as depicted in Figure 7.10, reveals interesting patterns for different zones, particularly in the JJA and SON seasons. Although all the seasons exhibit an increasing DTR with eleva-

	DJF			MAM			JJA			SON		
	Change rate (o/decade)	**RMSE (o)**	**Tmin-Tmax (C)**	**Change rate (o/decade)**	**RMSE (o)**	**Tmin-Tmax (C)**	**Change rate (o/decade)**	**RMSE (o)**	**Tmin-Tmax (C)**	**Change rate (o/decade)**	**RMSE (o)**	**Tmin-Tmax (C)**
Zone 1	-0.054	0.297	7.157 - 19.121	-0.015	0.103	8.198 - 18.076	-0.004	0.119	5.584 - 10.854	-0.056	0.211	7.18 - 14.62
Zone 2	-0.099	0.634	9.26 - 17.842	0.015	0.236	9.136 - 16.708	-0.011	0.213	4.626 - 10.705	0.001	0.431	7.396 - 14.935
Zone 3	-0.021	0.323	9.415 - 16.832	0.063	0.189	13.789 - 17.435	-0.055	0.193	6.578 - 9.641	-0.034	0.383	7.736 - 12.463
Zone 4	-0.012	0.425	8.969 - 18.662	-0.028	0.145	10.619 - 16.126	-0.017	0.174	7.141 - 10.365	0.012	0.131	6.759 - 15.2
Zone 5	-0.008	0.296	12.194 - 17.621	0.011	0.097	13.998 - 18.092	0.005	0.122	5.655 - 12.18	0.038	0.353	8.352 - 15.109
Zone 6	0.007	0.34	12.402 - 17.606	-0.004	0.248	8.215 - 17.45	0.012	0.114	5.479 - 9.067	0.019	0.252	8.489 - 15.937
Zone 7	-0.014	0.538	9.527 - 18.036	-0.036	0.136	10.927 - 16.132	0.027	0.284	6.612 - 11.682	-0.097	3.3	9.849 - 91.258
Zone 8	0.008	0.357	8.599 - 17.99	0.012	0.2	11.942 - 17.747	-0.008	0.264	6.513 - 10.058	0.16	5.235	9.664 - 91.579
Zone 9	-0.144	6.849	6.864 - 100.425	0.013	1.252	10.964 - 91.463	0.032	1.862	7.304 - 82.646	0.062	8.203	11.886 - 90.558
Zone 10	0.02	4.568	8.309 - 100.463	-0.048	5.68	10.988 - 92.372	-0.083	10.885	9.914 - 81.83	-	-	-

Table 7.6: P-MiSTIC Seasonal zone-wise change rate of DTR per decade for Decade-3 observed Temperature

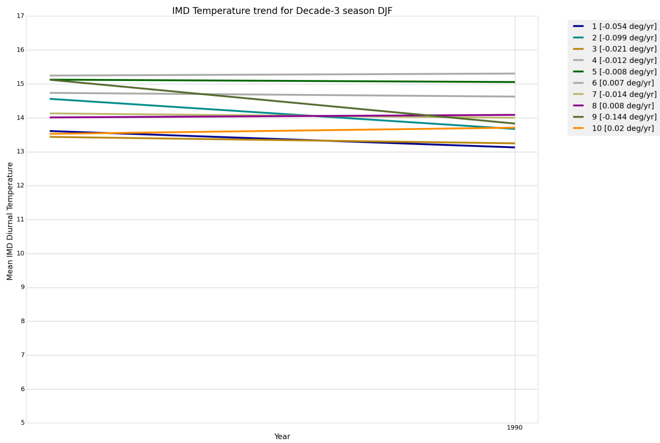

(a) DJF

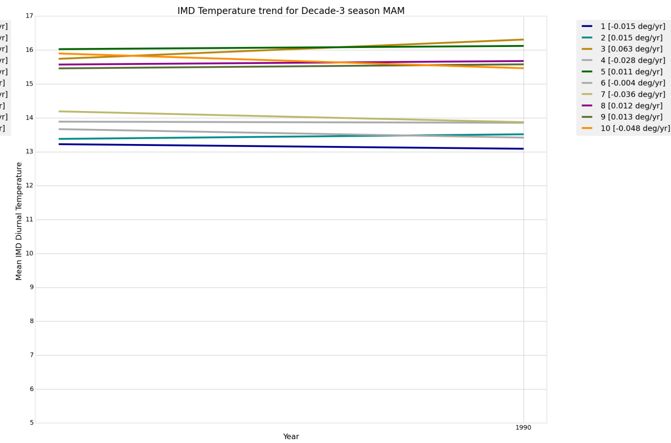

(b) MAM

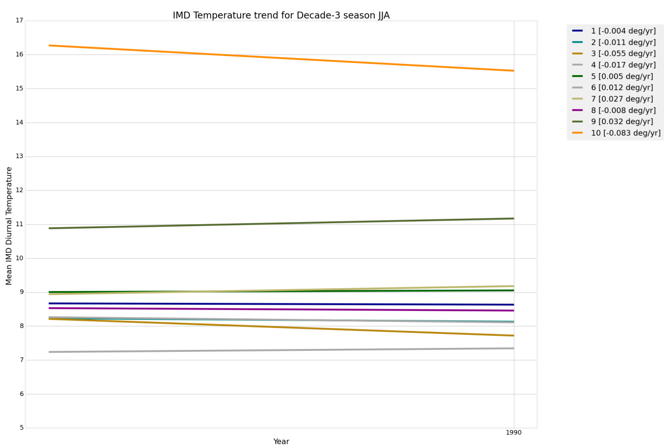

(c) JJA

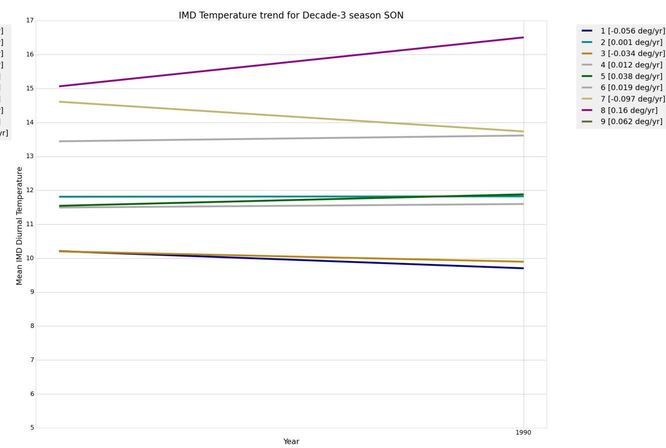

(d) SON

Figure 7.9: P-MiSTIC Seasonal zone-wise Temporal Trends for Decade-3 Observed Data

tion, the zones of each season exhibit both increasing and decreasing trends with time. The zone-wise DTR ranges lie within a small window in DJF and MAM, while the DTR range is spread over a longer window in seasons JJA and SON. Many zones in DJF present a decreasing DTR trend with time, indicating the rise of minimum temperatures at a higher rate than the rise of maximum temperatures in this season. A similar trend is observed in MAM, but the magnitude of change is relatively less compared to DJF. A transition of DTR is observed from DJF to MAM, specifically for zones 3, 5, 8, 9, and 10, which present an elevated DTR in MAM. JJA exhibits a mixed trend, with some zones having an increasing trend and some having a decreasing trend, while two zones have a relatively insignificant rate of change ($\leq 0.005^{o}$/yr). JJA also presents a clear distinction between the Himalayan zones (Zone 9 and 10) and the other zones in Figure 7.10(c), demonstrating the elevated DTR in these zones during JJA. Apart from these two zones, the other zones experience lower DTR ranges during the JJA season. One of the Himalayan zones experienced an increasing trend (0.032^{o}/yr) while the other presented a decreasing trend (0.083^{o}/yr). Season SON witnessed a higher number of zones with increasing DTR. The elevated DTR in zones 7 and 8, which correspond to the Himalayan regions, is also exhibited during this season, similar to JJA.

The decade-3 seasonal temperatures present distinct trends compared to the 30-year seasonal temperatures. This demonstrates that from decades 1 and 2 to decade 3, the temperature patterns of the study region have changed significantly, which, if ignored, can enter a feedback loop and impact the climate of the study region, in turn impacting the global scale.

Chapter 8

Discussion

The utilization of data-driven zoning analysis provides a comprehensive understanding of the temporal variations in zonal boundaries and temperatures. These zones facilitate the examination of divergent patterns within a study region, which can be difficult to generalize across extensive geographical areas. The observed data zones provide evidence of a decrease in zonal variability over the past three decades, indicating the possibility of a similar trend occurring in regions beyond the study area. The analysis also highlighted the shifting zonal boundaries in different decades and seasons, suggesting shifting patterns in the study area. This observation emphasizes the temporal variability of climatic zones in the study region, which can be attributed to its dynamic nature. The modelled data revealed low spatiotemporal heterogeneity, with a single zone throughout the study and decade-wise datasets. The identification of diagonal zone separation in the seasonal analysis highlights the presence of inherent discrepancies within the model, potentially stemming from parameterizations and systematic errors.

8.1 Data and inherent characteristics: Observed Data vs Modelled Data

A preliminary temporal analysis on observed and modelled data to examine the change rates of temperature with time (Figure 3.2 & 3.3). For the observed data, the change rate of minimum temperature was found to be 0.13^{o}/decade, while the change rate of maximum temperature was 0.17^{o}/decade. The diurnal temperature exhibited an overall increasing trend with a change rate of 0.03^{o}/decade. This indicates that over the study period, the observed minimum, maximum, and diurnal temperatures have been gradually increasing.

In contrast, the modelled data displayed slightly different trends. The change rate of minimum temperature was estimated to be 0.43°/decade, while the change rate of maximum temperature was 0.45°/decade. The diurnal temperature exhibited a slightly increasing trend with a change rate of 0.02°/decade. Over the study period, the observed minimum, maximum, and diurnal temperatures have been gradually increasing.

These contrasting trends in the observed and modelled data suggest that the model overestimates the rate of warming in the study region. The study also evaluates the lapse rates of actual data using linear regression. The lapse rate, which indicates the rate of temperature change with elevation, plays a crucial role in understanding temperature variations in both observed and modelled data. The analysis of the lapse rate provides insights into the vertical temperature distribution and its relationship with elevation.

The observed lapse rates for minimum, maximum, and diurnal temperatures are 2.38°/km, 2.34°/km, and -0.19°/km, respectively. In the observed data, these lapse rates indicate that there is a decreasing trend in temperature as elevation increases for minimum and maximum temperatures, while there is an increasing trend for diurnal temperatures.

The lapse rates estimated for the modelled data are 6.34°/km, 5.95°/km, and -0.39°/km for minimum, maximum, and diurnal temperatures, respectively. These lapse rates in the modelled data suggest a steeper decrease in temperature with elevation for both minimum and maximum temperatures compared to the observed data. Additionally, the modelled diurnal temperature lapse rate indicates an increasing trend with elevation. Some interesting observations can be made comparing the lapse rate values of observed and modelled data with the global average environmental lapse rate of 6.5°/km [60]. Firstly, the modelled data appears to align closely with the global average lapse rate, indicating that the model incorporates a standard lapse rate assumption in its calculations. This assumption may overlook the intricate complexities of the study region's local topography and specific temperature patterns.

In contrast, the observed data exhibits a significantly lower lapse rate compared to the global average. This suggests that the study region experiences unique characteristics, where temperature changes with elevation differ from the global average. The complex topography and localized temperature patterns within the study region contribute to this deviation, resulting in a lower observed lapse rate.

The discrepancy in the lapse rates between the observed and modelled data underscores the need for improved modelling techniques that account for local complexities and temperature patterns. These findings highlight the importance of considering a study region's specific characteristics and complexities when modelling temperature variations and underscore the limitations of using global average values in complex topographical areas. Using a global average lapse rate may oversimplify the temperature patterns and fail to capture the unique dynamics of the study area. Incorporating more localized and region-specific lapse rates in the model can lead to more accurate temperature simulations and improve the predictions of temperature trends within the study region.

The impact of these lapse rates in both observed and modelled data is significant. The decreasing lapse rates for minimum and maximum temperatures in the observed data suggest that minimum and maximum temperatures decrease at higher elevations. This finding is consistent with the general understanding that as one moves to higher altitudes, temperatures tend to decrease due to the decrease in atmospheric pressure and adiabatic cooling. But the observed and modelled data's diurnal temperature lapse rate implies an increasing trend of temperature with elevation, indicating that as one moves higher in altitude, temperatures tend to rise. This aligns with the understanding that high-elevation regions experience a more pronounced warming effect.

In order to gain a deeper understanding of the temperature patterns and trends, the study employs a spatio-temporal analysis approach to identify zones within the study region that exhibit unique characteristics. This analysis utilizes the MiSTIC (Mining Spatio-Temporally Invariant Cores) method to identify zones based on minimum and maximum temperatures. To further enhance the analysis and capture more comprehensive insights, the study introduces the P-MiSTIC method, which is a multi-variate extension of MiSTIC. P-MiSTIC considers multiple variables and parameters to identify spatio-temporal zones with distinct diurnal temperature trends. This method is implemented on both observed and modelled data, allowing for a comparison between the two datasets.

8.2 Spatio-Temporal zoning & the regulating behaviour of identified zones

8.2.1 Spatio-Temporal Analysis of the complete datasets

MiSTIC has identified 12 zones for observed minimum temperatures, 9 zones for observed maximum temperatures, 8 for modelled minimum temperatures, and 4 for modelled maximum temperatures, as depicted in Figure 5.1. The relationships between diurnal temperature and elevation within these zones resulted in change rates at which diurnal temperatures change with increasing elevation. Using linear regression, the change rates were estimated as -2.57^o/km for observed minimum temperatures, -2.19^o/km for observed maximum temperatures, -7.48^o/km for modelled minimum temperatures, and -6.67^o/km for modelled maximum temperatures.

Notably, these change rates closely align with the actual lapse rates calculated from the data, indicating the effectiveness of the MiSTIC method in capturing temperature patterns and trends. This consistency between the estimated change rates and the actual lapse rates adds confidence to the analysis's accuracy and validates the results' reliability.

P-MiSTIC has identified 11 zones in the study region for observed data and 1 zone (entire study region) for modelled data, presented in Figure 5.3. This discrepancy in the number of zones between the observed and modelled data signifies notable differences in the spatial patterns and characteristics. The presence of multiple zones in the observed data suggests that there are diverse and localized temperature patterns and behaviours across the study region. These zones likely correspond to specific geographical features, climate variations, or other factors that influence temperature distributions. The identification of multiple zones provides a more detailed and nuanced understanding of the spatial dynamics of temperature.

In contrast, the modelled data exhibits a single zone, indicating a more uniform and homogeneous temperature modelled across the study region. This suggests that the model fails to capture the localized variations and distinct temperature patterns observed in the real-world data. The limited number of zones in the modelled data implies a lack of spatial heterogeneity and a simplified representation of the temperature dynamics. It underscores the challenges in accurately simulating and reproducing the complex spatio-temporal patterns of temperature in climate models. It also underscores the importance of using analysis techniques like P-MiSTIC to uncover and understand the spatio-temporal dynamics of temperature in observational and modelled data, which can aid in model evaluation and improvement.

The observed data exhibits a lapse rate of -0.133^{o}/km, indicating an increase in diurnal temperature with increasing elevation. This implies that higher elevations experience higher diurnal temperatures compared to lower elevations. This negative lapse rate hints at the Elevation Dependent Warming phenomenon in the study region.

The zone-wise temporal trends of the P-MiSTIC zones, as depicted in Figure 5.5 and Tables 5.5 and 5.6, have revealed valuable insights regarding the observed and modelled data. The overall temporal change rate of both observed and modelled data is estimated to be 0.02^{o}/decade, indicating that the model captures the general trend of temporal change in the study region. The positive change rates for the observed data indicate an overall increasing trend of diurnal temperatures with time. This suggests a general pattern of widening diurnal temperature ranges over the study period.

Additionally, the analysis highlights the distinct trends exhibited by two specific clusters within the dataset, which correspond to the high-elevation Himalayan zones, namely the Western Himalayan region and the Karakoram region. These high-elevation Himalayan zones exhibit noteworthy increasing trends, with the Western Himalayan region showing an increase of 0.19^{o}/decade and the Karakoram region exhibiting a higher rate of increase at 0.28^{o}/decade. Identifying these specific high-elevation zones with pronounced increasing trends highlights the significance of elevation in driving temperature variations within the study region, suggesting that the high-elevation Himalayan zones are experiencing a more pronounced warming effect than other regions. The observed increasing trends in these zones may be influenced by various factors such as local topography, atmospheric conditions, and climate dynamics specific to high-elevation areas.

The ability of P-MiSTIC to identify these distinct trends in high-elevation Himalayan zones reaffirms its effectiveness in capturing spatio-temporal patterns and providing valuable insights into temperature variations.

8.2.2 Spatio-Temporal Analysis of the decadal datasets

The decadal analysis using P-MiSTIC analyses the three decade-wise observed and modelled datasets. The identified zones for each decade offer a deeper understanding of the localized behaviours and trends exhibited by the data.

In the observed data, the decadal analysis has resulted in varying numbers of zones for each decade while still exhibiting similarities across the datasets. The presence of similar zones in different decades indicates consistent spatial characteristics and behaviours of temperature over time. This suggests the existence of specific geographical features, climatic patterns, or other factors that influence temperature distributions and remain relatively stable over the study period.

In contrast, the modelled data has resulted in a single zone for all the decade-wise datasets. This suggests a lack of spatial heterogeneity and a more homogeneous temperature distribution in the model output. The absence of multiple zones implies that the model fails to capture the localized variations and distinct temperature patterns observed in the observed data.

Analyzing the change rates of the Diurnal Temperature Range (diurnal temperature) with elevation provides valuable insights into the relationships between temperature and elevation. In the observed data, the change rates of diurnal temperatures with elevation exhibit both positive and negative values. Positive change rates represent an increasing trend, while negative change rates indicate a decreasing trend of diurnal temperatures with elevation. These contrasting trends reflect the complex interactions between temperature and elevation in different regions.

The observed change rates of diurnal temperatures with elevation in the three decades reveal interesting trends. Decades 1 and 2 exhibit decreasing diurnal temperatures change rates of -0.012^o/km and -0.028^o/km, respectively, implying a decrease in the diurnal temperature with elevation. However, a sharp shift is observed in decade 3, where the diurnal temperatures change rate significantly increases to 0.533^o/km. This shift indicates a reversal in the temperature trend, with diurnal temperature increasing with elevation.

The shift in trends from decades 1 and 2 to decade 3 suggests a significant change in temperature dynamics over time. It may be indicative of various factors, such as shifts in climate patterns, changes in atmospheric circulation, or alterations in local environmental conditions.

The observed increasing diurnal temperature change rate in decade 3 highlights a potential intensification of temperature gradients with elevation during this period.

They provide insights into the complex interactions between elevation, time, and temperature patterns, which can have significant implications for understanding climate change impacts, ecosystem dynamics, and regional weather patterns.

The specific characteristics of zones 8 and 9 in the observed decade 3 dataset, which corresponds to the Western Himalayan region and the Karakoram region, play a crucial role in driving the increasing trend of diurnal temperature with elevation during this period (Figure 6.2(c)). The zone-wise temporal trend analysis further provides insights into the behaviour of these zones across all the decades.

The Western Himalayan region shows a decreasing trend in diurnal temperature change rates over decades 1, 2 and 3, with rates of -0.14°/decade, -0.29°/decade and -0.41°/decade, respectively. Similarly, the Karakoram region exhibits a distinct pattern in the zone-wise temporal trends. It shows a relatively stable diurnal temperature change rate over decades 1 and 2 (0.11°/decade and 0.13°/decade, respectively). However, in decade 3, there is a substantial increase in the diurnal temperature change rate to 2.46°/decade. These findings highlight the unique characteristics of the Karakoram region, where the diurnal temperature exhibits a significant increasing trend with elevation, suggesting elevation-dependent warming in this region.

8.2.3 Spatio-Temporal Analysis of the seasonal datasets

The seasonal analysis of observed data reveals distinct zones for each season, with 11, 10, 7, and 8 zones identified for DJF, MAM, JJA, and SON, respectively. Each season exhibits its own unique set of zones, indicating the presence of season-specific temperature patterns. Notably, two zones within the high-elevation Himalayan region are consistently identified in all seasons using P-MiSTIC. This reiterates that the high-elevation regions experience significant and distinct temperature variations compared to other areas.

On the other hand, the modelled data results in a consistent number of zones (3, 3, 3, and 2) for DJF, MAM, JJA, and SON, respectively. These zones are diagonally separated, suggesting discrepancies or limitations in the model's ability to capture the true spatial variability of temperature patterns. The differences in zone identification between observed and modelled data indicate the challenges in accurately representing the complex temperature dynamics in the study region.

The diurnal temperature change rates with elevation further provide insights into the temperature variations within each season. For observed data, the diurnal temperature change rates with elevation are estimated as -0.518°/km, -0.089°/km, 0.668°/km, and 0.453°/km for DJF, MAM, JJA, and SON, respectively. These rates highlight the contrasting temperature trends with elevation across the seasons with an inversion in winter. The negative rates in DJF and MAM indicate a decrease in diurnal temperature with increasing elevation, while the positive rates in JJA and SON suggest an increase in diurnal temperature with elevation.

In contrast, the modelled data's diurnal temperature change rates with elevation exhibit different patterns. The rates are estimated as -0.539°/km, 0.451°/km, 4.689°/km, and 1.737°/km for DJF, MAM, JJA, and SON, respectively. These rates indicate significant variations in diurnal temperature with elevation, particularly in JJA and SON, where the rates are notably higher. This reiterates that the model possibly incorporates the average environmental lapse rate of 6.5°/km. The presence of a zone in the high-elevation Himalayan region in the SON season for modelled data suggests that the model might have partially captured the unique temperature variations associated with this region during that season.

Furthermore, a cyclic pattern is observed in the mean diurnal temperature of identified zones in both observed and modelled data, with minimum ranges in the JJA (summer) season followed by a gradual increase in the SON season, providing additional insights into the seasonal temperature dynamics. The cyclic pattern with a minimum in the JJA (summer) season and a gradual increase in the SON season indicates that the nighttime temperatures are warmer during the summer season, resulting in a reduced diurnal temperature range. As the seasons transition to SON, the decrease in warmer nighttime temperatures leads to a broader diurnal temperature range. Various factors, including solar radiation, humidity, atmospheric conditions and local climate dynamics, can influence this cyclic pattern. However, the study reveals that JJA experienced the most remarkable rate of increase in diurnal temperature with elevation among the four seasons.

The findings highlight the presence of spatial variability at the seasonal scale in the modelled data, which is not evident when all seasons are analyzed together. The diagonal separation of the zones in both the seasonal and previous analyses highlights the nature of the climate model, whose specific characteristics and inherent spatial and elevational gradients affect its representation of spatial and temporal variability. These observations emphasize the importance of considering both spatial and temporal aspects in studying climate patterns and the benefits of using methods like P-MiSTIC to uncover and analyze such spatial and spatio-temporal patterns.

P-MiSTIC consistently identifies zones that exhibit consistent behaviours over time, supporting its effectiveness in analyzing spatio-temporal trends.

Further, the seasonal analysis of decade-3 seasonal data identified 10, 10, 10 and 9 zones in seasons DJF, MAM, JJA and SON. A considerable shift in zonal boundaries was observed, indicating the complex pattern shifts of temperature through seasons. All the seasons of decade 3 exhibited warming with elevation, with maximum warming occurring in the summer (JJA). This implies that with elevation, the maximum temperatures are rising at a higher rate than minimum temperatures. Further, the analysis of zone-wise temporal trends highlights the distinct trends during all the seasons of decade 3 compared to the 30-year seasonal analysis. This is an indication of a significant shift in temperature patterns from decades 1 & 2 to decade 3. These warming trends can continue in a feedback loop, causing further warming, which in turn can trigger disasters and have a global-scale impact.

8.3 Spatio-Temporal analysis and its application for enhanced comprehension of climate aspects

The Spatio-Temporal analysis is a powerful approach that combines both spatial and temporal dimensions to explore and understand complex patterns and dynamics in various fields, including climate science. In the context of this study, spatio-temporal analysis is conducted using two methods: MiSTIC (Chapter 5, section 1) and P-MiSTIC (Chapters 5, 6 & 7).

MiSTIC (Mining Spatio-Temporal Invariant Cores) is a method employed in this study to identify invariant cores in observed and modelled spatio-temporal temperature data. It focuses on mining patterns that exhibit consistent behaviours across space and time. By analyzing the minimum and maximum temperatures, MiSTIC identifies zones that share similar temperature characteristics over the study period. This method helps uncover areas with distinct temperature patterns and provides insights into regional variations and trends.

Building upon MiSTIC, P-MiSTIC (Parametric MiSTIC) is introduced in this study as a modified version that incorporates multiple input variables or parameters. P-MiSTIC aims to capture the spatial and temporal dependencies of multiple variables simultaneously, allowing for a more comprehensive analysis of complex spatio-temporal patterns. In the case of this study, P-MiSTIC considers the minimum and maximum temperatures, assigning them specific weights based on their relevance. By evaluating the weighted average at each point in space and time, P-MiSTIC identifies combined focal points and delineates zones with consistent behaviours across different variables.

The usage of P-MiSTIC in this study provides several benefits for understanding climate aspects. Firstly, it allows for a comprehensive analysis by considering multiple variables simultaneously. This is particularly important in climate studies, where various factors, such as temperatures, precipitation, and atmospheric conditions, interact to shape climate patterns. By incorporating these variables, P-MiSTIC enables a holistic understanding of the interplay between different climate factors and their spatial and temporal variations.

Furthermore, P-MiSTIC facilitates the identification of spatio-temporal zones that exhibit unique characteristics. These zones represent regions with distinct climate behaviours, such as specific temperature patterns or trends. By analyzing these zones, researchers can gain insights into the underlying mechanisms and drivers of climate variations. For example, in this study, the identification of high-elevation Himalayan zones with increasing diurnal temperature trends highlights the critical role of elevation in influencing temperature patterns and warming trends.

The identified spatial and temporal patterns stem from complex interactions between various climatic factors, geographical features, and human activities. Spatial heterogeneity is influenced by diverse topographies, land use, land cover type, and localized climatic influences. Temporal trends reflect the interplay of natural climate variability and anthropogenic influences like greenhouse gas emissions and land-use changes, accelerating warming trends with time. The specific reasoning for the identified spatial and temporal patterns requires focused research into possible factors and their scale of influence at different zones. Changing zonal boundaries also indicate shifting patterns at different scales.

The influence of India's agro-ecological zones on temperature dynamics is demonstrated by a comparison of P-MiSTIC identified zones with these zones (described in chapters 5, 6, and 7). However, it's also clear that the effect has varied with each decade and season, indicating that other elements of the environment have a bearing on the dynamics of temperature.

The observed rise in precipitation levels in the Thar desert until 2015 [62] suggests that the desert area is undergoing a gradual and incremental change in climate, potentially affecting its arid conditions. This observation is consistent with the delineations generated during the third decade, wherein a portion of the Thar desert depicts patterns that resemble those observed in the neighbouring semi-arid regions.

Despite its data-driven nature, the approach exhibits a correlation with natural patterns, effectively demonstrating the influence of specific environmental and ecological conditions on climate dynamics within the studied region. The study area exhibits localized temperature patterns, with variations in temperature observed across different regions. Therefore, it is imperative to employ data-driven models in order to comprehend the environmental and ecological ramifications effectively.

By analyzing the change rates of diurnal temperatures with elevation and over time, the authors have quantified the dynamics of temperature variations based on the zones identified across the study region for complete, decadal, and seasonal datasets. These trends can provide valuable information about climate change, regional climate characteristics, and the potential impacts on ecosystems and human activities.

Climate processes and phenomena are inherently dynamic and exhibit variations across space and time. By incorporating both spatial and temporal aspects, P-MiSTIC provides a more comprehensive understanding of climate dynamics. One of the critical advantages of P-MiSTIC is its ability to capture the heterogeneity and variability of climate patterns at different scales.

The results of the spatio-temporal analysis can also have implications for climate change research. Climate change is expected to impact regional climate patterns, and understanding these changes at different spatial and temporal scales is crucial for adaptation and mitigation strategies. P-MiSTIC can help identify areas that are more susceptible to climate change effects, such as regions experiencing amplified warming trends or exhibiting unique temperature patterns. This information can inform decision-making processes related to land-use planning, infrastructure development, and climate resilience.

Furthermore, the ability of P-MiSTIC to integrate observed and modelled data provides an opportunity to assess the performance of climate models and validate their ability to capture spatio-temporal climate variations. By comparing the identified zones and their characteristics between observed and modelled data, the authors evaluate the model's ability to reproduce the observed climate patterns. Discrepancies or mismatches between observed and modelled results can offer insights into areas for model improvement and refinement.

In conclusion, the spatio-temporal analysis using methods like P-MiSTIC is a valuable tool for understanding climate aspects by integrating spatial and temporal dimensions. It facilitates the identification of zones with unique climate characteristics, the analysis of multi-variable interactions, and the assessment of spatial and temporal trends. Through its application in climate studies, P-MiSTIC contributes to our understanding of climate dynamics, climate change impacts, and the development of effective climate adaptation and mitigation strategies.

8.4 Elevation Dependent Warming

This thesis focuses on investigating elevation-dependent warming in the study region. The study utilizes a combination of data mining techniques, including MiSTIC and P-MiSTIC, to identify spatio-temporally consistent zones and analyze spatio-temporal climate data and uncover the relationships between temperature, elevation, and time.

The analysis begins by identifying zones based on minimum and maximum temperatures using the MiSTIC method. This initial step helps delineate regions with similar temperature characteristics and behaviours and understand the spatial heterogeneity in observed and modelled data. Subsequently, the P-MiSTIC method is employed to perform a more comprehensive analysis of the identified zones, considering minimum and maximum temperatures and their spatial and temporal dependencies.

By implementing P-MiSTIC on observed and modelled data, the study explores the spatio-temporal patterns and trends of diurnal temperature range (DTR) across the study region. Statistical values, such as change rates and lapse rates, are calculated to quantify the relationships between temperature, elevation, and time.

The results reveal several key findings. Firstly, the study finds overall increasing trends of 0.133^o/km and 0.02^o/km for observed and modelled data. Further, the study identifies two distinct high-elevation zones within the study region, the Western Himalayan region and the Karakoram region. These zones exhibit unique characteristics, including significantly increas-

	Western Himalayan region		Karakoram region	
	Change rate (°/decade)	RMSE (°)	Change rate (°/decade)	RMSE (°)
30-years	0.19	2.606	0.28	1.848
Decade 1	-0.14	0.092	0.11	0.114
Decade 2	-0.29	0.192	0.13	0.116
Decade 3	-0.41	2.562	2.46	3.17
Season DJF	0.28	2.652	0.26	2.383
Season MAM	0.34	2.63	0.26	1.668
Season JJA	0.22	2.607	0.27	1.403
Season SON	0.21	2.062	0.25	2.048

Table 8.1: Temporal trends of the Western Himalayan region and the Karakoram region for all the datasets using P-MiSTIC

ing trends in diurnal temperature with elevation.

The consolidated temporal trends exhibited by the Western Himalayan region and the Karakoram region are depicted in Table 8.1. The critical influence of elevation on warming trends is evident from the change rates of DTR with elevation presented in this study, including the zone-specific trends of the high-elevation Himalayan zones presented in Table 8.1.

Furthermore, the statistical values, such as lapse rates, help evaluate the performance of the model and compare it with observed data. The modelled data generally aligns with the global average lapse rate, which is higher than the lower lapse rate observed data exhibits in the study region. This discrepancy highlights the influence of complex topographies and localized temperature patterns, underscoring the importance of capturing regional characteristics in climate modelling.

By utilizing data mining techniques and statistical analyses, the study uncovers the unique characteristics of high-elevation zones, the changing trends over time, and the influence of elevation on temperature patterns. These findings establish the emergence & existence of Elevation Dependent Warming (EDW) in the study region with quantitative analysis.

The findings of the analysis carry significant implications for climate change research. Further, understanding temperature patterns and improving predictions further enhances the prediction capability of various models using climate data. The enhanced information has an impact over various sectors like water management (predicting shifts in precipitation patterns and snowmelt timing impacting water availability and quality), ecology (understanding habitat suitability, species distributions, and explaining phenological events affecting biodiversity and ecosystems), agriculture (crop yield estimation, understanding pest infestations, identifying optimal planting time), land-use planning (for sustainable development and conservation policies) and disaster management (planning, mitigation and reducing vulnerability to extreme weather events).

Chapter 9

Conclusions

- The study unravelled the inherent difference in observed and modelled data, highlighting the lack of spatio-temporal heterogeneity and underlying biases in the modelled data.
- The method proposed in the thesis, P-MiSTIC, has effectively identified spatio-temporal zones with specific temperature characteristics and successfully captured the varying temperature trends within the high-elevation Himalayan region by consistently identifying the Western Himalayan region and the Karakoram region.
- The analysis has demonstrated the emergence and evident presence of elevation-dependent warming (+0.133^o/km) in the study region while establishing a clear trend of accelerated warming from 2010 (+0.533^o/km).
- The Karakoram region has exhibited higher warming trends (0.28^o/decade) than the Western Himalayan region (0.19^o/decade) over the study period, reaffirming the profound impact of elevation on warming trends.
- Data-driven zonal analysis presented a decrease in zonal variability over the three decades.
- The study has demonstrated seasonal variations in DTR through the identification of cyclic seasonal trends of DTR in observed and modelled data. Seasons JJA and SON exhibited warming with elevation.
- The thesis unveils the elevated warming trends in JJA when the DTR values are at the minimum.
- Seasonal analysis of decade-3 data highlighted the presence of elevation-dependent warming in all the seasons.
- Himalayan zones have consistently exhibited higher rates of warming in the analysis.

- The analysis of seasonal and decadal temperature trends in the study region revealed distinct variations in temperature trends, highlighting the intricate dynamics of temperature variations.
- These findings emphasize the vitality of Spatio-Temporal variations and Elevation-Dependent Warming (EDW) in climate studies of complex topographies
- These findings have implications for climate modelling, mitigation efforts, and conservation strategies in the study region.
- Refining climate models, performing long-term monitoring, and investigating the underlying mechanisms driving spatio-temporal temperature variations are potential areas of further research to enhance the understanding of local-scale temperature patterns and assess the persistence and magnitude of observed trends.

Related Publications

1. E Ankitha Reddy, K. S. Rajan, *Decadal Analysis of Observed Temperature using P-MiSTIC*, accepted for presentation at the I-GUIDE Forum 2023.
2. E Ankitha Reddy, K. S. Rajan, *Seasonal Analysis Of Observed Temperature in contiguous Peninsular India Using P-MiSTIC*, accepted for presentation at the Asian Conference on Remote Sensing - ACRS 2023.

Bibliography

[1] IPCC. Summary for policymakers. In: Climate Change 2021: The Physical Science Basis. Contribution of Working Group I to the Sixth Assessment Report of the Intergovernmental Panel on Climate Change (eds, Masson-Delmotte, V., Zhai, P., Pirani, A., Connors, S. L., Péan, C., Berger, S., Caud, N., Chen, Y., Goldfarb, L., Gomis, M. I., Huang, M., Leitzell, K., Lonnoy, E., Matthews, J.B.R., Maycock, T. K., Waterfield, T., Yelekçi, O., Yu, R. & Zhou, B.) (IPCC, 2021).

[2] Global Temperature - Climate Change: Vital Signs of the Planet. https://climate.nasa.gov/vital-signs/global-temperature/. Accessed 05 July 2023.

[3] Ross, R.S., Krishnamurti, T.N., Pattnaik, S. et al. Decadal surface temperature trends in India based on a new high-resolution data set. Sci Rep 8, 7452 (2018). https://doi.org/10.1038/s41598-018-25347-2

[4] Sanjay, J. et al. (2020). Temperature Changes in India. In: Krishnan, R., Sanjay, J., Gnanaseelan, C., Mujumdar, M., Kulkarni, A., Chakraborty, S. (eds) Assessment of Climate Change over the Indian Region. Springer, Singapore. https://doi.org/10.1007/978-981-15-4327-2_2

[5] Sun, Q., Miao, C., Duan, Q., Ashouri, H., Sorooshian, S., & Hsu, L. (2018). A Review of Global Precipitation Data Sets: Data Sources, Estimation, and Intercomparisons. Reviews of Geophysics, 56(1), 79-107. https://doi.org/10.1002/2017RG000574

[6] Hofstra, N., Haylock, M., New, M., Jones, P., and Frei, C. (2008), Comparison of six methods for the interpolation of daily, European climate data, J. Geophys. Res., 113, D21110, doi:10.1029/2008JD010100.

[7] IPCC, 2013: Climate Change 2013: The Physical Science Basis. Contribution of Working Group I to the Fifth Assessment Report of the Intergovernmental Panel on Climate Change [Stocker, T.F., D. Qin, G.-K. Plattner, M. Tignor, S.K. Allen, J. Boschung, A. Nauels, Y.

Xia, V. Bex and P.M. Midgley (eds.)]. Cambridge University Press, Cambridge, United Kingdom and New York, NY, USA, 1535 pp.

[8] Wikipedia contributors. HadCM3. Wikipedia, The Free Encyclopedia. July 12, 2023, 04:39 UTC.

[9] Met Office Hadley Centre (2012): WCRP CMIP5: Met Office Hadley Centre (MOHC) HadCM3 model output collection. Centre for Environmental Data Analysis, Accessed 12 July 2023. http://catalogue.ceda.ac.uk/uuid/2e0bf0c18b7e44ba8815bc0b455ab959

[10] Shukla, Rituraj & Khare, Deepak & Dwivedi, Anuj & Rudra, Ramesh & Palmate, Santosh S. & Ojha, Chandra & Singh, Vijay. (2023). Evaluation of statistical downscaling model's performance in projecting future climate change scenarios. Journal of Water and Climate Change. 14. 10.2166/wcc.2023.207.

[11] Mountain Research Initiative EDW Working Group. Elevation-dependent warming in mountain regions of the world. Nature Clim Change 5, 424–430 (2015). https://doi.org/10.1038/nclimate2563

[12] Zhang, Y.; Shen, X.; Fan, G. Elevation-Dependent Trend in Diurnal Temperature Range in the Northeast China during 1961–2015. Atmosphere 2021, 12, 319. https://doi.org/10.3390/atmos12030319

[13] Palazzi, E., Mortarini, L., Terzago, S. et al. Elevation-dependent warming in global climate model simulations at high spatial resolution. Clim Dyn 52, 2685–2702 (2019). https://doi.org/10.1007/s00382-018-4287-z

[14] Körner, C. (2007). The use of 'altitude' in ecological research. Trends in Ecology & Evolution, 22(11), 569-574.

[15] Yadav, J.S., Tiwari, S.K., Misra, A. et al. High-altitude meteorology of Indian Himalayan Region: complexities, effects, and resolutions. Environ Monit Assess 193, 654 (2021). https://doi.org/10.1007/s10661-021-09418-y

[16] Hengl, T., Heuvelink, G. B., & Rossiter, D. G. (2007). About regression-kriging: from equations to case studies. Computers & Geosciences, 33(10), 1301-1315.

[17] Fotheringham, A. S., Brunsdon, C., & Charlton, M. (2002). Geographically Weighted Regression: The Analysis of Spatially Varying Relationships. John Wiley & Sons.

[18] Ansari, M.Y., Ahmad, A., Khan, S.S. et al. Spatiotemporal clustering: a review. Artif Intell Rev 53, 2381–2423 (2020). https://doi.org/10.1007/s10462-019-09736-1

[19] Shi, Z.; Pun-Cheng, L.S.C. Spatiotemporal Data Clustering: A Survey of Methods. ISPRS Int. J. Geo-Inf. 2019, 8, 112. https://doi.org/10.3390/ijgi8030112

[20] Kisilevich, S., Mansmann, F., Nanni, M., Rinzivillo, S. (2009). Spatio-temporal clustering. In: Maimon, O., Rokach, L. (eds) Data Mining and Knowledge Discovery Handbook. Springer, Boston, MA. https://doi.org/10.1007/978-0-387-09823-4_44

[21] Mishra, A. K. (2019). Quantifying the impact of global warming on precipitation patterns in India. Meteorological Applications, 26(1), 153-160. https://doi.org/10.1002/met.1749

[22] Sun, Q., Miao, C., Duan, Q., Ashouri, H., Sorooshian, S., & Hsu, L. (2018). A Review of Global Precipitation Data Sets: Data Sources, Estimation, and Intercomparisons. Reviews of Geophysics, 56(1), 79-107. https://doi.org/10.1002/2017RG000574

[23] Hofstra, N., Haylock, M., New, M., Jones, P., and Frei, C. (2008), Comparison of six methods for the interpolation of daily, European climate data, J. Geophys. Res., 113, D21110, doi:10.1029/2008JD010100.

[24] Kilibarda, M., T. Hengl, G. B. M. Heuvelink, B. Graler, E. Pebesma, M. Percec Tadi C, and B. Bajat (2014), Spatio-temporal interpolation of daily temperatures for global land areas at 1 km resolution, J. Geophys. Res. Atmos. 119, 2294–2313, DOI:10.1002/2013JD020803.

[25] McIntosh, J., & Yuan, M. (2005). Assessing Similarity of Geographic Processes and Events. Transactions in GIS, 9(2), 223-245. https://doi.org/10.1111/j.1467-9671.2005.00214.x

[26] T. V. Ramachandra, Uttam Kumar, "Geographic Resources Decision Support System for land use, landcover dynamics analysis", proceedings of the FOSS/GRASS Users Conference - Bangkok, Thailand, 12-14 September 2004.

[27] Max J. Pfeffer, John W. Schlelhas, Stephen D. DeGloria, Jorge Gomez, Population, conservation, and land use change in Honduras, Agriculture, Ecosystems & Environment, Volume 110, Issues 1–2, 2005, Pages 14-28, ISSN 0167-8809, https://doi.org/10.1016/j.agee.2005.05.003.

[28] Christine Noe, “The Dynamics of Land Use Changes and their Impacts on the Wildlife Corridor between Mt. Kilimanjaro and Amboseli National Park, Tanzania”, LUCID Working Paper Number: 31 - LUCID’s Land Use Change Analysis as an Approach for Investigating Biodiversity Loss and Land Degradation Project, March 2003.

[29] Sa’adi, Z., Shahid, S. & Shiru, M.S. Defining climate zone of Borneo based on cluster analysis. Theor Appl Climatol 145, 1467–1484 (2021). https://doi.org/10.1007/s00704-021-03701-1.

[30] Summers, T., Mackie, E., Ueno, R., Simpson, C., Hosking, J.S., Suciu, T. et al. (2022) Localized impacts and economic implications from high temperature disruption days under climate change. Climate Resilience and Sustainability, 1, e35. https://doi.org/10.1002/cli2.35.

[31] Kollukuduru Sravanthi, K.S. Rajan, ”Spatio-Temporal Mining of Core Regions: Study of Rainfall Patterns in Monsoonal India,” 2010 IEEE International Conference on Data Mining Workshops, pp. 30- 37, 2011 IEEE 11th International Conference on Data Mining Workshops, 2011.

[32] Kallio, A., Tuimala, J. (2013). Data Mining. In: Dubitzky, W., Wolkenhauer, O., Cho, KH., Yokota, H. (eds) Encyclopedia of Systems Biology. Springer, New York, NY. https://doi.org/10.1007/978-1-4419-9863-7_599.

[33] M. Ramzan and M. Ahmad, ”Evolution of data mining: An overview,” 2014 Conference on IT in Business, Industry and Government (CSIBIG), Indore, India, 2014, pp. 1-4, doi: 10.1109/CSIBIG.2014.7056947.

[34] Plotnikova V, Dumas M, Milani F. Adaptations of data mining methodologies: a systematic literature review. PeerJ Comput Sci. 2020 May 25;6:e267. doi: 10.7717/peerj-cs.267. PMID: 33816918; PMCID: PMC7924527.

[35] Bracco, A., Falasca, F., Nenes, A. et al. Advancing climate science with knowledge-discovery through data mining. npj Clim Atmos Sci 1, 20174 (2018). https://doi.org/10.1038/s41612-017-0006-4.

[36] V. Bogorny and S. Shekhar, ”Spatial and Spatio-temporal Data Mining,” 2010 IEEE International Conference on Data Mining, Sydney, NSW, Australia, 2010, pp. 1217-1217, doi: 10.1109/ICDM.2010.166.

[37] Gowtham Atluri, Anuj Karpatne, and Vipin Kumar. 2018. Spatio-Temporal Data Mining: A Survey of Problems and Methods. ACM Comput. Surv. 51, 4, Article 83 (July 2019), 41 pages. https://doi.org/10.1145/3161602

[38] Kotawadekar, R. (2021). Satellite data: Big data extraction and analysis. Artificial Intelligence in Data Mining, 177-197. https://doi.org/10.1016/B978-0-12-820601-0.00008-2

[39] Shekhar, S., Huang, Y., Wu, W., Lu, C.T., Chawla, S. (2001). What's Spatial About Spatial Data Mining: Three Case Studies. In: Grossman, R.L., Kamath, C., Kegelmeyer, P., Kumar, V., Namburu, R.R. (eds) Data Mining for Scientific and Engineering Applications. Massive Computing, vol 2. Springer, Boston, MA. https://doi.org/10.1007/978-1-4615-1733-7_26

[40] Spatial Analysis: A Guide for Ecologists by Fortin & Dale, 2005.

[41] G. Christodoulou, E. G. M. Petrakis and S. Batsakis, "Qualitative Spatial Reasoning Using Topological and Directional Information in OWL," 2012 IEEE 24th International Conference on Tools with Artificial Intelligence, Athens, Greece, 2012, pp. 596-602, doi: 10.1109/ICTAI.2012.86.

[42] Shekhar, S., & Vatsavai, R. R. (2008). Spatial Data Mining: Progress and Challenges. Communications of the ACM, 51(11), 115-119.

[43] Stein, M. L. (2020). Spatial and Spatio-Temporal Statistics: Recent Developments and Future Challenges. Annual Review of Statistics and Its Application, 7, 373-396.

[44] John F. Roddick, Myra Spiliopoulou, "A Bibliography of Temporal, Spatial and SpatioTemporalData Mining Research", ACM SIGKDD Explorations, Vol1, 34-38, June 1999

[45] Alam, M. M., Torgo, L., & Bifet, A. (2021). A Survey on Spatio-temporal Data Analytics Systems. ArXiv. /abs/2103.09883

[46] Collins, M., Knutti, R., Arblaster, J., Dufresne, J. L., Fichefet, T., Friedlingstein, P., ... & Wehner, M. (2013). Long-term climate change: Projections, commitments and irreversibility. In Climate Change 2013: The Physical Science Basis. Contribution of Working Group I to the Fifth Assessment Report of the Intergovernmental Panel on Climate Change.

[47] Wilby, R. L., Dawson, C. W., & Barrow, E. M. (2002). SDSM—a decision support tool for the assessment of regional climate change impacts. Environmental Modelling & Software, 17(2), 147-159.

[48] Tebaldi, C., & Knutti, R. (2007). The use of the multi-model ensemble in probabilistic climate projections. Philosophical Transactions of the Royal Society A: Mathematical, Physical and Engineering Sciences, 365(1857), 2053-2075.

[49] Stainforth, D. A., Aina, T., Christensen, C., Collins, M., Faull, N., Frame, D. J., ... & Smith, L. A. (2005). Uncertainty in predictions of the climate response to rising levels of greenhouse gases. Nature, 433(7024), 403-406.

[50] Marty, C. and Meister, R. (2012). Long-term snow and weather observations at Weissfluhjoch and its relation to other high-altitude observatories in the Alps. Theoretical and Applied Climatology 110, 573–583.

[51] Cai, D., You, Q., Fraedrich, K., & Guan, Y. (2017). Spatiotemporal Temperature Variability over the Tibetan Plateau: Altitudinal Dependence Associated with the Global Warming Hiatus. Journal of Climate, 30(3), 969-984. https://doi.org/10.1175/JCLI-D-16-0343.1.

[52] Qinglong You, Deliang Chen, Fangying Wu, Nick Pepin, Ziyi Cai, Bodo Ahrens, Zhihong Jiang, Zhiwei Wu, Shichang Kang, Amir AghaKouchak, Elevation dependent warming over the Tibetan Plateau: Patterns, mechanisms and perspectives, Earth-Science Reviews, Volume 210, 2020, 103349, ISSN 0012-8252, https://doi.org/10.1016/j.earscirev.2020.103349

[53] Shukla, R., Chakraborty, A. & Joshi, P.K. Vulnerability of agro-ecological zones in India under the earth system climate model scenarios. Mitig Adapt Strateg Glob Change 22, 399–425 (2017). https://doi.org/10.1007/s11027-015-9677-5

[54] Srivastava, A. K., Rajeevan, M., & Kshirsagar, S. R. (2009). Development of a high resolution daily gridded temperature data set (1969–2005) for the Indian region. Atmospheric Science Letters, 10(4), 249-254. https://doi.org/10.1002/asl.232

[55] Randall, D. A., Wood, R. A., Bony, S., Colman, R., Fichefet, T., Fyfe, J., ... & Zhang, M. (2007). Climate models and their evaluation. In Climate change 2007: The physical science basis. Contribution of Working Group I to the Fourth Assessment Report of the Intergovernmental Panel on Climate Change.

[56] de Ferranti J (2014a) Digital Elevation Data—with SRTM voids filled using accurate topographic mapping. http://www.viewfinderpanoramas.org/dem3.html. Accessed July 13, 2023.

[57] Han, J. & Kamber, M. (2000) Data Mining: Concepts and Techniques, 8 ed., The Morgan Kaufmann Series in Data Management Systems, Jim Gray, Series Editor, Morgan Kaufmann Publishers.

[58] MiSTIC: Mining Spatio-Temporally Invariant Cores, Sravanthi Kollukuduru, June 2013. Advisor: K S Rajan. Report no: IIIT/TH/2013/19.

[59] Did global warming stop in 1998? - NOAA Climate.gov. https://www.climate.gov/news-features/climate-qa/did-global-warming-stop-1998 (Accessed on 14 July 2023)

[60] Barry, R. G., and R. J. Chorley, 1987: Atmosphere, Weather, and Climate. 5th ed. Methuen, 460 pp.

[61] E Ankitha Reddy, KS Rajan, Spatiotemporal Cluster Analysis of Gridded Temperature Data - A Comparison Between K-means and MiSTIC, IJSRED 6(1):585-590, Jan-Feb 2023.

[62] Rajesh, P. V., & Goswami, B. N. (2023). Climate change and potential demise of the Indian deserts. Earth's Future, 11, e2022EF003459. https://doi.org/10.1029/2022EF003459